

**COMPARISON OF SHELF LIFE OF PACKED FOODSTUFFS IN USE OF
POLYETHYLENE AND POLYETHYLENE NANOCOMPOSITES**

**M.Sc. Thesis by
Büşra BÜYÜKSAKALLI**

Department : Polymer Science and Technology

Programme : Polymer Science and Technology

**Thesis Supervisor: Prof. Dr. Nurseli UYANIK
Co-Supervisor: Prof. Dr. Onur DEVRES**

JUNE 2011

**COMPARISON OF SHELF LIFE OF PACKED FOODSTUFFS IN USE OF
POLYETHYLENE AND POLYETHYLENE NANOCOMPOSITE FILMS**

**M.Sc. Thesis by
Büşra BÜYÜKSAKALLI
(515091024)**

**Date of submission : 05 May 2011
Date of defence examination: 07 June 2011**

**Supervisor (Chairman) : Prof. Dr. Nurseli UYANIK (ITU)
Co-Supervisor : Prof. Dr. Onur DEVRES (ITU)
Members of the Examining Committee : Prof. Dr. Ahmet AKAR (ITU)
Prof. Dr. Candan ERBİL (ITU)
Asist. Prof. Dr. Filiz ALTAY (ITU)**

JUNE 2011

İSTANBUL TEKNİK ÜNİVERSİTESİ ★ FEN BİLİMLERİ ENSTİTÜSÜ

**POLİETİLEN VE POLİETİLEN NANOKOMPOZİT FİLMLERDE
AMBALAJLANAN GIDALARIN RAF ÖMRÜNÜN KARŞILAŞTIRILMASI**

**YÜKSEK LİSANS TEZİ
Büşra BÜYÜKSAKALLI
(515091024)**

Tezin Enstitüye Verildiği Tarih : 05 Mayıs 2011

Tezin Savunulduğu Tarih : 07 Haziran 2011

**Tez Danışmanı : Prof. Dr. Nurseli UYANIK (İTÜ)
Eş Danışmanı : Prof. Dr. Onur DEVRES (İTÜ)
Diğer Jüri Üyeleri : Prof. Dr. Ahmet AKAR (İTÜ)
Prof. Dr. Candan ERBİL (İTÜ)
Yrd. Doç. Dr. Filiz ALTAY (İTÜ)**

HAZİRAN 2011

ACKNOWLEDGEMENT

First and foremost i would like to express my indebtedness to my advisor Prof. Dr. Nurseli UYANIK who has supported and encouraged me from the beginning of this study and shared her deep knowledge and experience.

I would like to thank to my co-advisor Prof Dr. Onur DEVRES for his invaluable advice and guidance.

I would like to thank to Tolga GÖKKURT who shared his knowledge and experience generously during this study.

I am very grateful to Assoc. Prof. Dr. Hüseyin GÜN for his help, guidance, sharing knowledge and supplying me foodstuffs.

I would like to acknowledge Aksoy Plastik A.Ş. for their support, material supplying and contributions to my study.

Finally, I would like to thank my father Bekir BÜYÜKSAKALLI, my mother Seyhan BÜYÜKSAKALLI, my brother Burak BÜYÜKSAKALLI and my fiance Ozan KAYA. Their endless love, understanding and support were the main motivation of this study. Therefore this thesis is dedicated to them.

June 2011

Büşra BÜYÜKSAKALLI
(Chemist)

TABLE OF CONTENTS

	<u>Page</u>
ACKNOWLEDGEMENT.....	v
TABLE OF CONTENTS	vii
ABBREVIATIONS	xi
LIST OF SYMBOLS	xiii
LIST OF TABLES	xv
LIST OF FIGURES	xvii
SUMMARY	xxi
ÖZET	xxv
1. INTRODUCTION.....	1
2. THEORETICAL PART	3
2.1 Nanocomposites	3
2.1.1 Polymer nanocomposites components.....	3
2.1.1.1 Polymer..	4
2.1.1.2 Nanoclay	7
2.1.1.3 Compatibilizer.....	9
2.1.1.4 The other additives.....	10
2.1.2 Polymer nanocomposites production.....	12
2.1.3 Polymer nanocomposites features.....	14
2.1.3.1 Micro structure.....	14
2.1.3.2 Mechanical properties	16
2.1.3.3 Gas barrier properties.....	18
2.1.3.4 Thermal stability properties	20
2.1.3.5 Optical and surface properties of packaging films	21
2.2 Polyolefin nanocomposites packaging application.....	22
2.2.1 Need for packaging	22
2.2.2 Packaging materials	22
2.2.3 Production of packaging	24
2.2.4 Active packaging technologies	24
2.2.5 Ethylene removing packaging.....	28
2.2.5.1 The chemistry of ethylene.....	28
2.2.5.2 Synthesis of ethylene	28
2.2.5.3 Adsorption and absorption.....	29
2.2.5.4 Deleterious effects of ethylene.....	30
2.2.5.5 New and novel approaches to ethylene-removing packaging...	31
3. EXPERIMENTAL PART	33
3.1 Chemicals Used	33
3.1.1 Low density polyethylene	33
3.1.2 Nanoclay	33
3.1.3 Maleic anhydride grafted polyethylene	34
3.1.4 Ethylene absorber.....	34

3.2 Instrument and characterization methods for nanocomposite materials	34
3.2.1 Twin screw extruder.....	34
3.2.2 Cast film line.....	36
3.2.3 XRD Analysis	36
3.2.4 FTIR Analysis	37
3.2.5 Thermal Analysis with DSC	37
3.2.6 Thermal Gravimetric Analysis.....	38
3.2.7 Melt Viscosity Measurement with MFI.....	38
3.2.8 Polarized microscopy.....	39
3.2.9 Mechanical analysis	39
3.2.10 Colour measurement of nanocomposite films	40
3.2.11 Oxygen and carbon dioxide gas permeability analysis.....	41
3.3 Instrument and characterization method for food packaging..	41
3.3.1 Storage conditions.....	41
3.3.2 Oxygen, carbon dioxide, ethylene changes in package versus time	42
3.3.3 Weight lose analysis	42
3.3.4 pH analysis.....	43
3.3.5 Taste and general quality evaluation.....	43
3.3.6 Sugar amount analysis	44
4. RESULTS AND DISCUSSION	45
4.1 Characterization Results	46
4.1.1 XRD results.....	46
4.1.2 FTIR results	47
4.1.3 DSC results	47
4.1.4 TGA results	48
4.1.5 MFI results	48
4.1.6 POM results	50
4.1.7 Mechanical analysis results.....	50
4.1.8 Colour measurement of nanocomposite films	50
4.1.9 Oxygen and carbon dioxide gas permeability results	52
4.2 Analysis results for food packaging.....	52
4.2.1 Analysis results of strawberry.....	53
4.2.1.1 Gas composition changes versus time	53
4.2.1.2 Weight lose analysis results	53
4.2.1.3 pH changes results	54
4.2.1.4 Sugar amount analysis results of strawberry	54
4.2.1.5 Taste and general quality evaluation results	54
4.2.1.6 Shelf life analysis results	54
4.2.2 Analysis results of parsley	55
4.2.2.1 Gas composition changes versus time	55
4.2.2.2 Weight lose analysis results	55
4.2.2.3 pH changes.....	56
4.2.2.4 Taste and general quality evaluation results	56
4.2.2.5 Shelf life analysis results	56
4.2.3 Analysis results of iceberg lettuce	56
4.2.3.1 Gas composition changes versus time	56
4.2.3.2 Weight lose analysis results	57
4.2.3.3 pH changes.....	57
4.2.3.4 Taste and general quality evaluation results	57
4.2.3.5 Shelf life analysis results	57

5. CONCLUSION	59
APPENDICES	61
REFERENCES.....	95
CURRICULUM VITAE.....	107

ABBREVIATIONS

LDPE	: Low Density Polyethylene
LDPE-g-MA	: Maleic Anhydride Grafted Polyethylene
XRD	: X-Ray Diffraction
FTIR	: Fourier Transform Infrared
DSC	: Differential Scanning Calorimeter
TGA	: Thermal Gravimetric Analysis
PNC	: Polymer Nanocomposites
PA	: Polyamide
PS	: Polystyrene
PMMA	: Poly Methyl Metacrylate
PET	: Poly Ethylene Terephthalate
PEN	: Poly Ethylene Naphthalate
PBT	: Poly Buthylene Terephthalate
PEO	: Polyethylene Oxide
PLA	: Polylactic Acid
PVC	: Polyvinyl Chloride
EVA	: Ethylene-Acetate Copolymers
EVOH	: Ethyl-Vinyl Alcohol
PU	: Polyurethanes
PI	: Polyimides
PVP	: Polyvinyl Pyrolidon
HDPE	: High Density Polyethylene
UHMWPE	: Ultra High Molecular Weight Polyethylene
LLDPE	: Linear Low Density Polyethylene
MDPE	: Medium Density Polyethylene
MMT	: Montmorillonite
LSNC	: Layered Silicate Nanocomposites
CO₂	: Carbon Dioxide
O₂	: Oxygen
C₂O₄	: Ethylene

LIST OF SYMBOLS

nm	: Nanometer
g	: Gram
cm³	: Cubic centimeter
MPa	: Mega Pascal
KCal	: Kilocalorie
g	: Gram
cm³	: Cubic centimeter
λ	: Wavelength
d_{001}	: Layer distance of clay platelets
θ	: Diffraction angle
ΔH	: Enthalpy

LIST OF TABLES

	<u>Page</u>
Table 2.1: Types of polyethylene	6
Table 2.2: Processing techniques for layered silicate/polymer nanocomposites.	15
Table 4.1: Properties of PETILEN F2-12 LDPE	33
Table 4.2: Sample Number and Their Compositions.....	46
Table 4.3: DSC test results of samples.....	48
Table 4.4: TGA Analysis results of film samples.	49
Table 4.5: MFI and n-MFI Results of LDPE samples.	49
Table 4.6: Mechanical analysis test results	51
Table 4.7: Colour, opacity and transparency measurements of LDPE film samples	51
Table 4.8: Oxygen and carbondioxide gas permeability results ..	52

LIST OF FIGURES

	<u>Page</u>
Figure 2.1 : Schematic drawing of polymerization of polyethylene.....	5
Figure 2.2 : Molecules of LDPE, LLDPE and HDPE.....	5
Figure 2.3 : Shematic represantation of structure of montmorillonite being a 2:1 clay mineral	8
Figure 2.4 : Structure of 2:1 phyllosilicates.	9
Figure 2.5 : The chemical structure of MAH monomer.....	10
Figure 2.6 : Flowchart of solution approach to synthesis nanocomposites.....	13
Figure 2.7 : Flowchart of in-situ polymerization method to prepare nanocomposite	13
Figure 2.8 : Flowchart of melt intercalation method to synthesis nanocomposite	14
Figure 2.9 : Schematically illustration of three different types of thermodynamically achievable polymer/layered silicate nanocomposites	16
Figure 2.10 : Reinforcement mechanism in composite materials	17
Figure 2.11 : Schematic illustration of formation of highly tortuous path in nanocomposite.....	19
Figure 4.1 : The chemical structure of PE-g-MA.....	34
Figure 4.2 : Schematic drawing of a melt flow indexer..	39
Figure 4.3 : Typical tensile test curve	40
Figure 4.4 : OxyBABY oxygen and carbon dioxide analyser instrument	42
Figure 4.5 : ICA56 Smart Fresh ethylene analyser instrument.....	42
Figure 4.6 : Orion 3-star pH meter instrument	43
Figure 4.7 : Brix refractometer	44
Figure A.1 : XRD result of I44 nanoclay	61
Figure A.2 : XRD result of DK4 nanoclay	61
Figure A.3 : XRD result of Active ingredient of N10774	62
Figure A.4 : XRD result of 5% DK4 nanoclay containing LDPE.....	62
Figure A.5 : XRD result of 5% I44 nanoclay+ 4% N10774 ethylene absorber containing LDPE	62
Figure A.6 : XRD result of 5% DK4 nanoclay+ 4% N10774 ethylene absorber containing LDPE	63
Figure A.7 : FTIR spectrum of LDPE	63
Figure A.8 : FTIR spectrum of 5% I44 nanoclay LDPE	63
Figure A.9 : FTIR spectrum of 5% DK4 nanoclay LDPE.....	64
Figure A.10 : FTIR spectrum of 4% N10774 LDPE.....	64
Figure A.11 : FTIR spectrum of 4% N10776 LDPE.....	64
Figure A.12 : FTIR spectrum of 5% I44 nanoclay + 4% N10774 LDPE.....	65
Figure A.13 : FTIR spectrum of 5% DK4 nanoclay + 4% N10774 LDPE	65
Figure A.14 : DSC graphs of LDPE (heating and cooling relatively).....	66

Figure A.15 : DSC graph of 5% I44 nanoclay LDPE (heating and cooling relatively).....	67
Figure A.16 : DSC graph of 5% DK4 nanoclay LDPE (heating and cooling relatively)	68
Figure A.17 : DSC graph of 4% N10774 LDPE (heating and cooling relatively) ...	69
Figure A.18 : DSC graph of 4% N10776 LDPE (heating and cooling relatively) ...	70
Figure A.19 : DSC graph of 5% I44 nanoclay + 4% N10774 LDPE (heating and cooling relatively)	71
Figure A.2 : DSC graph of 5% DK4 nanoclay + 4% N10774 LDPE (heating and cooling relatively)	72
Figure A.21 : TGA graph of I44 nanoclay	72
Figure A.22 : TGA graph of DK4 nanoclay	73
Figure A.23 : TGA graph of N10774 ethylene absorber	73
Figure A.24 : TGA graph of LDPE	73
Figure A.25 : TGA graph of 5% I44 nanoclay LDPE	74
Figure A.26 : TGA graph of 5% DK4 nanoclay LDPE.....	74
Figure A.27 : TGA graph of 4% N10774 LDPE	74
Figure A.28 : TGA graph of 4% N10776 LDPE	74
Figure A.29 : TGA graph of 5% I44 nanoclay + 4% N10774 LDPE.....	75
Figure A.30 : TGA graph of 5% DK4 nanoclay + 4% N10774 LDPE	75
Figure A.31 : POM image of 5% I44 nanoclay LDPE film	76
Figure A.32 : POM image of 5% DK4 nanoclay LDPE film	76
Figure A.33 : POM image of 4% N10774 LDPE film	76
Figure A.34 : POM image of 5% I44 nanoclay + 4% N10774 LDPE.....	77
Figure A.35 : POM image of 5% DK4 nanoclay + 4% N10774 LDPE	77
Figure A.36 : Gas composition changes versus time of LDPE package for strawberry (Sample no:1)	77
Figure A.37 : Gas composition changes versus time of 5% I44 nanoclay LDPE package for strawberry (Sample no:2)	78
Figure A.38 : Gas composition changes versus time of 5% DK4 nanoclay LDPE package for strawberry (Sample no:3).....	78
Figure A.39 : Gas composition changes versus time of 4% N10774 LDPE package for strawberry (Sample no:4)	78
Figure A.40 : Gas composition changes versus time of 4% N10776 package for strawberry (Sample no:5)	79
Figure A.41 : Gas composition changes versus time of 5% I44 nanoclay + 4% N10774 package for strawberry (Sample no:6)	79
Figure A.42 : Gas composition changes versus time of 5% DK4 nanoclay + 4% N10774 LDPE package for strawberry (Sample no:7)	79
Figure A.43 : The graph of weight lose changes of strawberries during 10 days storage versus time	80
Figure A.44 : The graph of pH changes of strawberries during 10 days storage versus time.....	80
Figure A.45 : The graph of brix changes of strawberries during 10 days storage versus time.....	80
Figure A.46 : The graph of general quality changes of strawberries during 10 days storage versus time	81
Figure A.47 : The strawberry pictures stored in LDPE packages at 3 th , 5 th , 8 th , 10 th days (Sample no:1).....	81

Figure A.48 : The strawberry pictures stored in 5% I44 LDPE packages at 3 th , 5 th , 8 th , 10 th days (Sample no:2).....	81
Figure A.49 : The strawberry pictures stored in 5% DK4 LDPE packages at 3 th , 5 th , 8 th , 10 th days (Sample no:3).....	82
Figure A.50 : The strawberry pictures stored in 4% N10774 LDPE packages at 3 th , 5 th , 8 th , 10 th days (Sample no:4).....	82
Figure A.51 : The strawberry pictures stored in 4% N10776 LDPE packages at 3 th , 5 th , 8 th , 10 th days (Sample no:5).....	82
Figure A.52 : The strawberry pictures stored in 5% I44 + 4% N10774 LDPE packages at 3 th , 5 th , 8 th , 10 th days (Sample no:6).....	82
Figure A.53 : The strawberry pictures stored in 5% DK4 + 4% N10774 LDPE packages at 3 th , 5 th , 8 th , 10 th days (Sample no:7).....	83
Figure A.54 : Gas composition changes versus time of LDPE package for parsley (Sample no:1).....	83
Figure A.55 : Gas composition changes versus time of 5% I44 LDPE package for parsley (Sample no:2).....	83
Figure A.56 : Gas composition changes versus time of 5% DK4 LDPE package for parsley (Sample no:3).....	84
Figure A.57 : Gas composition changes versus time of 4% N10774 LDPE package for parsley (Sample no:4).....	84
Figure A.58 : Gas composition changes versus time of 4% N10776 LDPE package for parsley (Sample no:5).....	84
Figure A.59 : Gas composition changes versus time of 5% I44 + 4% N10774 LDPE package for parsley (Sample no:6).....	85
Figure A.60 : Gas composition changes versus time of 5% DK4 + 4% N10774 LDPE package for parsley (Sample no:7).....	85
Figure A.61 : The graph of weight lose changes of parsley during 17 days storage versus time.....	85
Figure A.62 : The graph of pH changes of parsley during 17 days storage versus time.....	86
Figure A.63 : The graph of general quality changes of parsley during 17 days storage versus time.....	86
Figure A.64 : The parsley pictures stored in LDPE packages at 5 th , 12 th , 15 th , 17 th days (Sample no:1).....	86
Figure A.65 : The parsley pictures stored in 5% I44 LDPE packages at 5 th , 12 th , 15 th , 17 th days (Sample no:2).....	87
Figure A.66 : The parsley pictures stored in 5% DK4 LDPE packages at 5 th , 12 th , 15 th , 17 th days (Sample no:3).....	87
Figure A.67 : The parsley pictures stored in 4% N10774 LDPE packages at 5 th , 12 th , 15 th , 17 th days (Sample no:4).....	87
Figure A.68 : The parsley pictures stored in 4% N10776 LDPE packages at 5 th , 12 th , 15 th , 17 th days (Sample no:5).....	87
Figure A.69 : The parsley pictures stored in 5% I44 + 4% N10774 LDPE packages at 5 th , 12 th , 15 th , 17 th days (Sample no:6).....	88
Figure A.70 : The parsley pictures stored in 5% DK4 + 4% N10774 LDPE packages at 5 th , 12 th , 15 th , 17 th days (Sample no:7).....	88
Figure A.71 : Gas composition changes versus time of LDPE package for iceberg lettuce (Sample no:1).....	88
Figure A.72 : Gas composition changes versus time of 5% I44 LDPE package for iceberg lettuce (Sample no:2).....	89

Figure A.73 : Gas composition changes versus time of 5% DK4 LDPE package for iceberg lettuce (Sample no:3).....	89
Figure A.74 : Gas composition changes versus time of 4% N10774 LDPE package for iceberg lettuce (Sample no:4).....	89
Figure A.75 : Gas composition changes versus time of 4% N10776 LDPE package for iceberg lettuce (Sample no:5).....	90
Figure A.76 : Gas composition changes versus time of 5% I44 + 4% N10774 LDPE package for iceberg lettuce (Sample no:6).....	90
Figure A.77 : Gas composition changes versus time of 5% DK4 + 4% N10774 LDPE package for iceberg lettuce (Sample no:7).....	90
Figure A.78 : The graph of weight lose changes of iceberg lettuce during 22 days storage versus time	91
Figure A.79 : The graph of pH changes of iceberg lettuce during 22 days storage versus time.....	91
Figure A.80 : The graph of general quality changes of iceberg lettuce during 22 days storage versus time.....	91
Figure A.81 : The iceberg lettuce pictures stored in LDPE packages at 7 th , 9 th ,18 th , 22 th days (Sample no:1).....	92
Figure A.82 : The iceberg lettuce pictures stored in 5% I44 LDPE packages at 7 th , 9 th ,18 th , 22 th days (Sample no:2).....	92
Figure A.83 : The iceberg lettuce pictures stored in 5% DK4 LDPE packages at 7 th , 9 th ,18 th , 22 th days (Sample no:3).....	92
Figure A.84 : The iceberg lettuce pictures stored in 4% N10774 LDPE packages at 7 th , 9 th ,18 th , 22 th days (Sample no:4).....	92
Figure A.85 : The iceberg lettuce pictures stored in 4% N10776 LDPE packages at 7 th , 9 th ,18 th , 22 th days (Sample no:5).....	93
Figure A.86 : The iceberg lettuce pictures stored in 5% I44 + 4% N10774 LDPE packages at 7 th , 9 th ,18 th , 22 th days (Sample no:6).....	93
Figure A.87 : The iceberg lettuce pictures stored in 5% DK4 + 4% N10774 LDPE packages at 7 th , 9 th ,18 th , 22 th days (Sample no:7).....	93

COMPARISON OF SHELF LIFE OF PACKED FOODSTUFFS IN USE OF POLYETHYLENE AND POLYETHYLENE NANOCOMPOSITES FILMS

SUMMARY

In this study, it was aimed to enhance shelf lives of foodstuffs by using special packaging materials. For this purpose, firstly the penetration of the oxygen should be prevented by packaging. Secondly, the ethylene gas released by the foodstuff must be kept in the material. Within the scope of work, the special film samples used for this purpose were prepared by melt mixing of polyethylene with nanoclay as oxygen barrier and ethylene absorber additives.

For this purpose, low density polyethylene (LDPE) nanocomposite masterbatches were prepared by using LDPE, nanoclay, compatibilizer with/without ethylene absorber with determined proportions by melt compounding in a counter-rotating twin screw extruder, firstly. Nanocomposites pellets were prepared by mixing of 25% the named masterbatch with 75% LDPE and these nanocomposites were used in cast-film line to obtain thin films having 100 micron thickness. The final compositions of these films were defined as 85% LDPE, 10% compatibilizer, and 5% nanoclay or 82.5% LDPE, 9% compatibilizer, 4.5 % nanoclay, and 4% ethylene absorber. 2 kinds of nanoclay and 2 kinds of ethylene absorber were used in this study. 100% LDPE film and 4% both types of ethylene absorber containing films were also prepared for the comparison purposes.

It must be pointed here that this study consists of two parts: one of them is production and characterization of film samples, the other one is food application of these film samples.

The characterization of these seven different films were performed by using Fourier Transform Infrared (FTIR), X-Ray Diffraction (XRD), Differential Scanning Calorimeter (DSC), Thermogravimetric Analysis (TGA), Polarized Optical Microscopy (POM), oxygen (O₂) and carbondioxide (CO₂) gas permeability test, Melt Flow Index (MFI) apparatus with mechanical analysis and colour measurements tests. FTIR peaks were used to see characteristic peaks of additives in polymer matrix. According to XRD graphs, exfoliation/intercalated morphological structure was obtained in nanocomposites with organoclay. Melting temperature was increased as crystallization increases for all

nanocomposite samples. It was observed that contribution of these additives to polymer matrix, starting temperature of degradation was decreased from the TGA graphs. TGA results of all samples were obtained. It was found that the inorganic contents of samples were consistent with the assigned initial values. POM images showed that the achievement of homogenous dispersion of additives in polymer matrix was provided in all samples. MFI values were measured and the normalized values were calculated of the nanocomposite samples. The addition of DK4 nanoclay increased the processability, while I44 nanoclay decreased since their different intercalation structure in polymer matrix since their different chemistry and modification method. These results were confirmed on the Samples No.2; 3 and 6; 7 (See the formulation table 4.2 given below). Tensile tests measurements of film samples from main and cross directions were made by using universal testing machine. Mechanical properties of the nanocomposite (Sample no 2,3,6 and 7) and composite (4 and 5) films were better than those of standart polyethylene. The 3% secant modulus of nanocomposite films increased with increasing the strain at break. Colour measurement showed that, polymer nanocomposite films take the colour of additives depending on their percentage. On the other hand, opacities of films increased while transparencies decreased.

Table 4.2: Sample number and their compositions.

SAMPLE NO	FINAL FORMULA
1	LDPE
2	85% LDPE + 10% PE-g-MA + 5% I44
3	85% LDPE + 10% PE-g-MA + 5% DK4
4	92% LDPE + 8% N10774
5	92% LDPE + 8% N10776
6	82.5% LDPE + 9% PE-g-MA + 4.5 % I44 + 4% N10774
7	82.5% LDPE + 9% PE-g-MA + 4.5 % DK4 + 4% N10774

The prepared films were used in foodstuff tests. 15x25 nanocomposite films were handled as packages to store strawberry, parsley and iceberg lettuce. 4-6 parallel studies were started. Every two days, one of parallel series consisting of six different nanocomposite packages and one LDPE control packages were opened and weight loose, sugar amount, pH changes, texture, taste, colour tests were conducted.

Strawberry, parsley and iceberg lettuce were chosen for the foodstuffs experiments, due to their low respiration. The changes of concentration of ethylene, oxygen and carbon dioxide

gases in packages were measured everyday. The acidity changes, sugar amount changes (only for strawberry), weight lost changes, taste evaluations, appearance changes and texture were also determined in every two days. The odour, taste, texture and general quality of foods were determined over the storage time by a 4 membered of panel. The foodstuffs stored in PNC film were compared with foodstuffs stored in standard polyethylene film.

It was observed that organoclay even at low level had significant effect on barrier properties of the nanocomposites. On the other hand, using ethylene absorber compositions, ethylene amount in the package ambient was decreased demonstrably. The nanocomposite packaging film which include both nanoclay and ethylene absorber showed better results. The gas changes effects on perishability of foodstuffs could be clearly seen. High amount of oxygen and ethylene gas allow fast spoilage.

Weight loose of foodstuffs are crucial, due to every loss in weight being translated into an economical loss. During respiration, strawberries lose water so much. Ten days later, weight loose in LDPE packages reached to 6,41% while in the other packages around 1-2%. Especially in the sample no 6 and 7 (which have both barrier and ethylene absorber additive), the weight loose was around 0,400-0,100%.

pH changes and sugar amount changes did not give an idea to monitor spoilage. Because these two parameters are directly related to maturity of product and choosing the products having same maturity and same properties is difficult. Besides, changes in brix percentage does not changes dramatically like weight loose.

Taste and general quality changes were enrolled. According to results; after 5 days, strawberries stored in LDPE decreased down to acceptable limit while the other all packages are fresh and eatable. In parsleys, after 12 days parsleys stored in LDPE started to turn yellow, the other all packages are still green. At the end of the storage period (10 days for strawberries, 17 days for parsleys and 22 days for iceberg lettuces), the foods in standard polyethylene film were not proper even to eat and taste, while the foods in polymer nanocomposite films were tasteful, eatable and buyable.

Every two days also photographs of 2 standard series were taken and all period were observed on these series. In this way, the conducted study was proved with photographs.

As a result of this study, it was obtained that, there is big difference between LDPE films and LDPE composite films used in packaging from the point of shelf-life analysis. The packages including both barrier (nanoclay) and ethylene absorber additives were best packages since these additives provide desired gas configuration in packages.

POLİETİLEN VE POLİETİLEN NANOKOMPOZİT FİMLERDE AMBALAJLANAN GIDALARIN RAF ÖMRÜNÜN KARŞILAŞTIRILMASI

ÖZET

Bu çalışmada, özel ambalaj malzemeleri kullanılarak, gıdaların raf ömrünün uzatılması amaçlanmıştır. Bu kapsamda ilk olarak, oksijenin ambalaj içine girişinin ambalaj tarafından engellenmesi gerekir. İkinci olarak, gıda tarafından salınan etilen gazı, ambalaj malzemesi tarafından tutulmalıdır. Çalışma kapsamında, bunları sağlamak için hazırlanan özel ambalaj numuneleri, oksijen bariyeri özelliğine sahip olan nanokilin, polietilen ve etilen absorban katkı ile karıştırılması ile hazırlanır.

Bu amaçla önce alçak yoğunluklu polietilen (LDPE) nanokompozit “masterbatch”ler belli miktarlarda LDPE, nanokil, uyumlaştırıcı, etilen absorbanla beraber ya da ayrı, ters-dönüştürülmüş çift vidalı ekstrüderde karıştırılarak hazırlanmıştır. Nanokompozit granüller, %25 oranında “masterbatch”in %75 LDPE ile karıştırılmasıyla hazırlanmış ve bu nanokompozitler 100 mikron kalınlığına sahip filmlerin elde edilmesi için “cast film” hattında kullanılmıştır. Bu filmlerin nihai bileşimi, %85 LDPE, %10 uyumlaştırıcı ve %5 nanokil veya %82,5 LDPE, %9 uyumlaştırıcı, %4,5 nanokil ve %4 etilen absorban olarak belirlenmiştir. Bu çalışmada 2 tip nanokil ve 2 tip etilen absorban kullanılmıştır. Karşılaştırma amaçlı ayrıca %100 LDPE film ve %4 oranında 2 etilen absorban tipini içeren filmler hazırlanmıştır.

Bu çalışma iki kısımdan oluşmuştur. Bunlardan ilki film numunelerinin üretimi ve karakterizasyonu, diğeri ise gıda saklama uygulama kısmıdır.

Bu yedi farklı film numunelerinin karakterizasyonları; Fourier Dönüşümlü Infrared (FTIR), X Işınları Kırınımı (XRD), Diferansiyel Kalorimetre Taraması (DSC), Termogravimetrik analiz (TGA), Polarize Optik Mikroskop (POM), oksijen ve karbondioksit gaz geçirgenlik testi, Eriyik Akış İndeksi (MFI) teçhizatlarının yanı sıra mekanik analiz, renk ölçüm testleri ile yapılmıştır. FTIR pikleri, polimer matriks içerisinde bulunan katkının karakteristik piklerini görmek amaçlı kullanılmıştır. XRD grafiklerine göre, kil içeren nanokompozitlerde

“exfoliated/intercalated” morfolojik yapısı gözlenmiştir. DSC grafiklerinden, bu katkıların polimer matrikse eklenmesiyle başlangıç bozunma sıcaklığının düşürüldüğü gözlenmiştir. Erime sıcaklığı, tüm nanokompozit örneklerinde kristalizasyon arttıkça artmıştır. Tüm numunelerin TGA sonuçları alınmıştır. Numunelerin inorganik içeriğinin, belirtilen başlangıç değerleriyle tutarlı olduğu gözlenmiştir. POM resimleri, polimer matriks içerisinde katkının homojen dağılımının başarılı olduğunu göstermiştir. Numunelerin MFI değerleri ölçülmüş ve nanokompozit örneklerin normalize edilmiş MFI değerleri hesaplanmıştır. Farklı kimyaları ve modifikasyon metodlarından ötürü, DK4 kilinin polimer matrise eklenmesi polimerin işlenebilirliğini artırırken, I44 nanokil azaltmıştır. Bu sonuçlar, numune 2;3 ve 6;7 üzerinde onaylandı (Aşağıda verilen formülasyon tablosu 4.2`yı inceleyiniz). Tüm örneklerin, ana ve çapraz eksenlerden çekme test analizleri yapılmıştır. Nanokompozit (Numune no 2, 3, 6 ve 7) ve kompozit (4 ve 5) filmlerin mekanik özellikleri, naturel LDPE’ye göre daha iyi çıkmıştır. Nanokompozit filmlerin %3 secant modülüs değerleri, kopmada uzama oranıyla birlikte artmıştır. Renk ölçümleri, polimer nanokompozitlerin içerdikleri katkıların yüzdesine bağlı olarak, katkıların rengini aldığını göstermiştir. Diğer taraftan filmlerin opasiteleri artırılırken, geçirgenlikleri azaltılmıştır.

Tablo 4.2: Numune numarası ve bileşimi.

NUMUNE NO	NİHAİ FORMÜL
1	LDPE
2	85% LDPE + 10% PE-g-MA + 5% I44
3	85% LDPE + 10% PE-g-MA + 5% DK4
4	92% LDPE + 8% N10774
5	92% LDPE + 8% N10776
6	82.5% LDPE + 9% PE-g-MA + 4.5 % I44 + 4% N10774
7	82.5% LDPE + 9% PE-g-MA + 4.5 % DK4 + 4% N10774

Hazırlanan filmler, gıda testlerinde kullanılmıştır. Çilek, maydanoz ve göbek marul ambalajlamak üzere, 15x25 nanokompozit filmler hazırlanmış ve 4-6 paralel çalışma başlatılmıştır. İki günde bir, altı nanokompozit ve bir LDPE kontrol ambalajdan oluşan paralellerden biri açılmış ve ağırlık kaybı, şeker miktarı, pH değişimi, doku, tat, renk testleri yapılmıştır.

Çilek, maydanoz ve göbek marul, düşük solunum hızına sahip oldukları için gıda denemelerinde kullanılmak üzere seçilmiştir. Etilen, oksijen ve karbondioksit gaz

konsatrasyonları hergün ölçülmüştür. Ayrıca asitlik değişimi, şeker miktarı değişimi (sadece çilek için), ağırlık kaybı değişimi, tat değerlendirmesi, görünüm değişimi ve doku değişimi iki günde bir incelenmiştir. Koku, tat, doku ve genel kalite bakımından, açılmış ambalajdaki gıdalar, 4 kişiden oluşan duyusal analiz grubu tarafından yapılmıştır. PNC içerisinde ambalajlanan gıdalar, normal polietilen ambalajlarda bulunan gıdalarla karşılaştırılmıştır.

Düşük miktarlardaki organokil ilavesinin bile, nanokompozitlerde önemli derecede bariyer etkisi sağladığı gözlenmiştir. Diğer taraftan, etilen absorban bileşimlerini kullanarak, ambalaj içerisindeki etilen miktarı, bariz bir biçimde azaltılmıştır. Nanokil ve etilen absorban içeren nanokompozit ambalaj filmleri, daha iyi sonuçlar vermiştir. Gıdaların bozunmasına gaz değişiminin etkisi açıkça görülmüştür. Yüksek miktarlardaki oksijen ve etilen gazı, gıdaların hızlı bozunmasına sebep olmaktadır.

Gıdaların ağırlık kaybı, her ağırlık kaybının ekonomik bir kayıba dönüşmesinden ötürü çok önemlidir. Solunum sırasında, çilekler çok fazla su kaybeder. 10 gün sonra, LDPE ambalajlarda ağırlık kaybı %6.41'e ulaşırken, diğer ambalajlarda %1-2 arasındaydı. Özellikle 6 ve 7 numaralı ambalajlarda (bariyer ve etilen absorban katkıların ikisini de içeren) kütle kaybı %0.40-0.10 civarındaydı.

Ürünlerdeki pH ve şeker miktarı değişimi, bozunma ile ilgili olmasına rağmen, çalışmada açık bir ayrım ortaya koymamıştır. Bu iki parametre direkt olarak ürünün olgunluk derecesiyle alakalı olup, olgunluğa bağlı olarak çilekten çileğe değişim gösterebilmektedir. Bunun yanı sıra brix değeri, kütle kaybı gibi büyük değişimler göstermemektedir.

Çalışmada, tat ve genel kalite değişimleri de incelenmiştir. Sonuçlara göre; 5 gün sonra standart bir LDPE ambalaj içerisinde saklanan çilekler kabul edilebilir limitin altına düşerken, diğer bütün ambalajlardaki çilekler hala taze ve yenilebilir durumda kalmışlardır. Maydanozlarda, 12 gün sonra, LDPE ambalaj içerisindeki ambalajlardaki maydanozlar sarıya dönerken, aynı sürede diğer tüm ambalajlardaki maydanozlar iyi durumdaydı. Göbek marullarda ise, 18 gün sonra ambalaj içerisinde su miktarının artmasının etkisiyle, LDPE film ambalajlardaki göbek marullar, yumuşamaya ve kabul edilebilir limitin altına düşmüştür. Saklama sürecinin sonunda (çilekler için 10 gün, maydanozlar için 17 gün, göbek marullar için 22 gün), naturel LDPE filmlerdeki gıdalar tatmak ve yemek için uygun değil iken, polimer nanokompozit ambalajlardaki gıdalar hala taze ve satın alınabilir durumdaydı.

İki günde bir, iki standart serinin fotoğrafları alınmış ve tüm periyot, bu seriler üzerinden gözlemlenmiştir. Böylelikle yapılan çalışmalar, fotoğraflarla kanıtlanmıştır.

Bu çalışmanın sonucu olarak, LDPE ve LDPE nanokompozit ambalajlar arasında raf ömrü analizi bakımından büyük bir farklılık olduğu gözlenmiştir. Bariyer katkı (nanokil) ve etilen

absorban katkıların ikisini de içeren ambalajlar, ambalajın içerisinde istenilen gaz bileşimini sağladığı için en iyi bileşim olarak belirlenmiştir. Ambalajların hem mekanik özellikleri hem de raf ömrü analizleri göz önünde bulundurulduğunda, en iyi ambalaj katkı formülasyonunun I44 nanokil ve N10774 etilen absorbanı içeren 6 numune numaralı ambalaj ile sağlanmış olduğu görülmektedir.

1. INTRODUCTION

Polymers have become one of the most important materials in our daily life. Increasing demand for using them forced the scientists to improve their properties. Therefore, in recent years, inorganic nanoparticle filled polymer composites have received increasing research interest, mainly due to their ability to improve properties of polymers.

In general, when composites are formed two or more physically and chemically distinct phases (usually polymer matrix and reinforcing element) are joined and the properties of the resulting product differ from and are superior to those of the individual components. The structures and properties of the composite materials are greatly influenced by the component phase morphologies and interfacial properties.

Nanocomposites are based on the same principle and are formed when phase mixing occurs at a nanometer dimensional scale. As a result, nanocomposites show superior properties over their micro counterparts or conventionally filled polymers.

Polyethylene has the biggest portion in polymer nanocomposite area and especially in packaging. There are a lot of packaging system to preserve foods properly and keep longer time fresh. Among the chemical, biological and physical methods of preservation, physical methods are the most convenient due to causing least change in the properties of produce. This complies with the recent studies in food science which aimed to minimize the processing so that the food resembles its natural features to the maximum extent. In this aspect, for food processing modified atmosphere and controlled atmosphere storage and packaging gain importance for fresh produce.

But in this study, it was aimed to solve the problems which cannot be solved by current preservation techniques like “controlled atmosphere storage” and “active packaging system”. Most schemes for improving polyolefins gas barrier property involve either addition of higher barrier plastics via multilayer structure or high barrier surface coatings, however, these approaches are not cost effective. The properties supplied by additives to the packaging materials were investigated by using nanoclays and ethylene absorbers especially from the point of increased shelf-life.

In order to preserve foods properly and increase their shelf-lives, firstly the degradation mechanisms of foods must be understood clearly. As we know, after harvesting, fresh fruits

and vegetables keep their respiration process. In this process, the sugar existing in the bodies of food products is broken through oxygen and afterwards some gases like carbon dioxide, water vapour, aromatic materials, and ethylene gas are released. Presence of oxygen and ethylene gases accelerates the respiration and maturation process. So, we must prevent oxygen entrance to the packaging ambient and ethylene gas which is produced by foodstuffs must be absorbed.

For this purpose, in the first stage, masterbatches containing nanoclay with/without organoclay were prepared in twin screw extruder. In the second stage, by adding these masterbatches to the Low Density Polyethylene (LDPE) in different proportions, films of 100 microns thickness on the cast-film line. The physical and chemical properties of these films were determined by FTIR, XRD, DSC, TGA, MFI, oxygen and carbondioxide gas permeabilities, visual analysis and tensile test of the films were evaluated. Afterwards, these films were used for food packaging and effects on food quality were discussed. With this purpose; oxygen, carbon dioxide and ethylene amount in packaging were measured everyday, pH values of foodstuffs, sugar amount, weight loose, taste evaluations, external appearance, texture and shelf-life analysis were performed on these film. Here, our reference was the standart polyethylene packaging films which are used in our daily lives.

As a result of these tests and evaluations, it was proved that by using the nanocomposite films having nanoparticle, the shelf life of foodstuffs could be increased effectively.

2. THEORETICAL PART

In this study, LDPE Nanocomposite (NC) films were prepared and these films were used to package foodstuffs. So, theoretical part consist of two main subjects: Nanocomposites and polyolefin nanocomposites packaging application.

2.1. Nanocomposites

The benefits of using nanomaterials, which always existed in nature, have been widely studied since the early 1990's with the Toyota's first use of clay/nylon-6 nanocomposite in production of timing belt covers [1]. The nanoscale should be defined by the "nano" term that refers to a size scale measured in nanometers (nm), which is 10^{-9} m. Nanocomposites are a subset of nanotechnology with filler loading often less than 5% by weight as compared to 20-40% loading of conventional materials [2]. To be defined as a nanocomposite, the loaded fillers must have at least one dimension at the range of 1-100 nm. Nanotechnology has wide effects in many industrial sectors, including; packaging, wire and cable, automotive, pipes and tubing and construction [3].

In recent years, inorganic nanoparticle filled polymer composites have received increasing research interest, since they exhibit larger filler/matrix interface and small interparticle distance which affect the composites' properties to a much greater extent at rather low filler concentration as compared to conventional micro-particulate composites [2,4]. For example, tensile strengths of the nanocomposites of PE are higher than that of neat polymer. This is different from what is observed in conventional micrometer particles/polymer composites, i.e., tensile strength of the composites remarkably decreases with the addition of the particulate fillers due to the poor bonding at the interface [5,6].

2.1.1 Polymer Nanocomposite Components

The polymer nanocomposites, which have been prepared by mixing with nano fillers, consist of three main components. These are; polymer that is the main matrix part, nano-sized additive and compatibilizers which provide interface interaction between polymer phase and nanofiller or increase these interactions. The interface interactions and compatibility within

the polymer nanocomposite components are directly related to forming and performances of these materials. The interactions between “polymer-nanofiller”, “polymer-compatible”, “compatible-nanofiller” and “nanofiller-nanofiller” carry importance since total interactions determine the micro structure of polymer nanocomposites.

2.1.1.1. Polymer

Many of polymers belonging to thermoset and thermoplastic classes are possible to use for preparing polymer nanocomposites. In the literature, there are a lot of studies in this area and the features of nanocomposites have been investigated by preparing these with different proportions of various nanofiller. Especially, it has been studied about nanocomposite preparation by mixing polymers having polar groups on the main chain or side chain with various nanoclays and investigation of physical properties. The polymers used in these studies; polyamides (PA) [7-11], polystyrene (PS) [12-16], polymethyl metacrylate (PMMA) [17-19], epoxy resins [20-22], various polyesters (polyethylene terephthalate (PET) [23-27], polyethylene naphthalate (PEN) [28, 29], polybutylene terephthalate (PBT) [30-32], vs.), polyethylene oxide (PEO) [33-35], biodegradable polymers like polylactide and polylactic acid (PLA) [36-38], polyvinyl chloride (PVC) [39, 40], polyvinyl alcohol (PVA) [41, 42], ethylene-vinyl acetate copolymers (EVA) [43-45], ethylene-vinyl alcohol copolymers (EVOH) [46-48], thermoplastic polyurethanes (PU) [49, 50], polyimides (PI) [51-53], different type rubbers [54-56], polyaniline [57], polyvinyl pyrrolidone (PVP) [58] and copolymers. There are limited studies about preparation of nanocomposites of polymers which does not have any polar groups compared to polymers having polar groups. Although challenges in the preparation of polyolefin nanocomposites; the consumption ratio in total plastic consumption (approximately 45-50%) and need for polyolefin nanocomposites having superior physical properties trigger development of these nanocomposites.

Polyethylene

Polyethylene (PE), being the major group of polyolefins, is the most popular plastic in the world. As well as being so versatile, it has the simplest structure among all commercial plastics. Schematic drawing of polymerization of polyethylene from ethylene monomer is given in Figure 2.1.

Polyethylene is popular since it is inexpensive, light, flexible and resistant to most solvents and has good toughness at low temperatures. Since the processing temperatures for many additives are limited to temperatures below 200°C, the use of polyethylene is preferable over

many other thermoplastics due to its lower melting point. It is mostly used in films, moulding, insulation, cable and pipe.

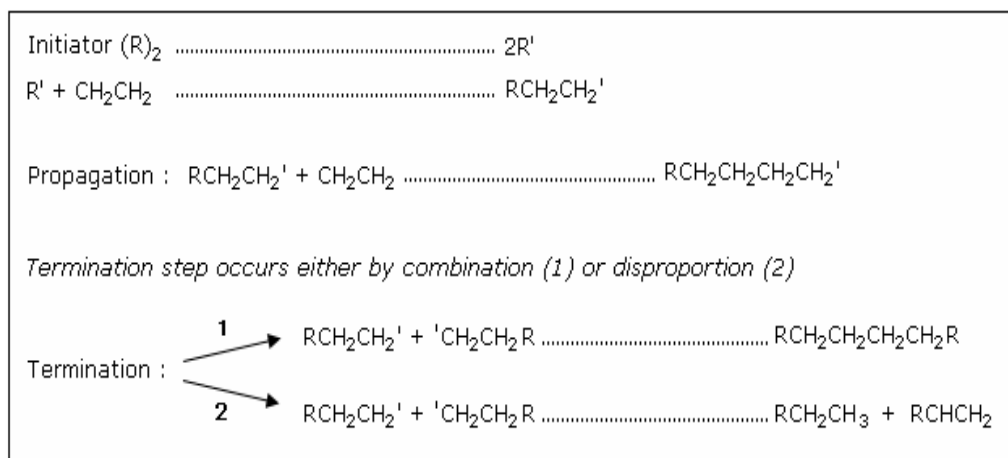


Figure 2.1: Schematic drawing of polymerization of polyethylene [59].

Polyethylene is classified into several different categories based mostly on its density and branching. Its simple basic structure, of ethylene monomers, can be linear as in high-density (HDPE) and ultrahigh-molecular-weight polyethylenes (UHMWPE); or branched to a greater or lesser degree as in low-density (LDPE), linear low-density (LLDPE) and medium density polyethylenes (MDPE) as shown in general form Figure 2.2.



Figure 2.2: Molecules of LDPE, LLDPE and HDPE.

The branched polyethylenes have similar structural characteristics, properties and uses such as low crystalline content, high flexibility and use in packaging film, plastic bags, insulation, squeeze bottles, toys, and house wares. HDPE has a dense, highly crystalline structure of high strength and moderate stiffness; uses include bottles, boxes, barrels, and luggage. UHMWPE is made in molecular weights above 2×10^6 [60].

The most common types of polyethylene, their densities and branching properties are listed in Table 2.1. These different types are produced at high pressures and temperatures in the presence of any of several catalysts, depending on the desired properties for the finished product. The mechanical properties of polyethylene significantly depend on variables such as the extent and type of branching, the crystal structure, and the molecular weight.

Table 2.1: Types of polyethylene [61-62].

Name	Density Range (g/cm³)	Degree of Branching
Low Density PE (LDPE)	0.910-0.940	high degree of short and long chain
Linear Low Density PE (LLDPE)	0.915-0.925	significant numbers of short branches
Medium Density PE (MDPE)	0.926-0.940	relatively low branching
High Density PE (HDPE)	>0.940	no branching

Low Density Polyethylene (LDPE) is defined by a density range of 0.910 - 0.940 g/cm³. LDPE has a high degree of short and long chain branching, which means that the chains do not pack into the crystal structure as well. This results in a lower tensile strength and increased ductility. LDPE is produced by free radical polymerization. The high degree of branches with long chains gives molten LDPE unique and desirable flow properties. LDPE is used for both rigid containers and plastic film applications such as plastic bags and film wrap [63].

LDPE is produced by a free-radical initiated reaction using oxygen or other free radical initiators such as organic peroxides or azo compounds. Synthesis conditions are usually 250–300 °C outlet temperature, 81-276 MPa pressure. Heat of polymerization is about 800 KCal/g.m, which must be removed during the short residence time available. Only a small part of this heat can be removed through the reactor walls because of their comparatively limited area and necessary thickness. In addition, the polymer tends to deposit on cool surfaces. In practice, heat is removed by recirculating excess cool monomer and the system operates essentially adiabatically. Therefore, production rates vary directly with the ethylene recirculation rate and the allowable temperature rises through the reactor. Heat balance limits conversion to 15– 20% on each pass. Reactors are of two general types, autoclaves and high

pressure tubes. Each of these types produces slightly different polymers, primarily because of differing temperature profiles through the reactors [63-65].

2.1.1.2. Nanoclay

Nanoclays are nanoparticles of layered mineral silicates. Depending on chemical composition and nanoparticle morphology, nanoclays are organized into several classes such as montmorillonite, bentonite, kaolinite, hectorite, and halloysite. Organically-modified nanoclays (organoclays) are an attractive class of hybrid organic-inorganic nanomaterials with potential uses in polymer nanocomposites, as rheological modifiers, gas absorbents and drug delivery carriers.

There are 4 types of clay minerals which are classified by their chemical formula; caolinite, smectide, illite and clorite.

Caolinit group contains caolinit, dicit and nacrit. The general formula of the caolinit group is $\text{Al}_2\text{O}_3 \cdot 2\text{SiO}_2 \cdot 2\text{H}_2\text{O}$. There is no pure caolinit source in nature and generally they contain iron oxide, silica, silica types components. They are used as filler in ceramics paint, plastics and rubber and they are widely used in paper industry to product bright paper.

Illit groups differ from smectite group clays by including potassium and can called as mica group. They are water included microscobic muscovit minerals and they are formation minerals which can be seperated to layers. The general formula of illit group is $(\text{K}, \text{H}) \text{Al}_2 (\text{Si}, \text{Al})_4 \text{O}_{10} (\text{OH})_2 \cdot x\text{H}_2\text{O}$. The stucture of this group is the same with slicate layered montmorillonite group. It can be used as filler material and in driling mud.

Clorit group clays have slim grain structure and green colour. This group clay includes a great deal of magnesium, Fe (II), Fe (III) and alumina. Clorit group minerals are generally known as fillosilicate group and they are not accepted as one of clay group. This group has got a lot of members like amesite, nimite, dafnite, panantite and peninite. General formula of Clorit group is $\text{X}_4 \cdot 6 \text{Y}_4 \text{O}_{10} (\text{OH}, \text{O})_8$. In this formula, X shows Al, Fe, Li, Mg, Mn, Ni, Zn and rarely Cr elements, and Y shows Al, Si, B, Fe elements. They are not used in industry [66,67].

The smectite minerals are classified according to the nature of the octahedral sheet (dioctahedral versus trioctahedral), by the chemistry of the layer and by the site of the charge (tetrahedral versus octahedral). The smectite minerals are very complex group, frequently having both octahedral and tetrahedral substitutions each contributing to the overall layer charge.

Montmorillonite structure

General formula of montmorillonite (MMT) is $\text{Na}_{0.2}\text{Ca}_{0.1}\text{Al}_2\text{Si}_4\text{O}_{10}(\text{OH})_2(\text{H}_2\text{O})_{10}$. Montmorillonite is a fine powder which has monoclinic-pyramidal crystal structure (Figure 2.3), a colour from white to brown-green and yellow, average density of 2.35 g/cm^3 , molecular weight of 549.07 g/mol and hardness of 1.5–2. Single montmorillonite crystals are quite fine, granulated and they got random outer lines. In general a montmorillonite crystal consists of 15–20 silicate units. This property is so useful for engineering projects. There are two different swelling types of montmorillonite according to expansion size of the basal space as crystallized and osmotic swelling. Crystallized swelling occurs when the water molecules enter in to the unit layers. First layer of the water molecules which are adsorbed occurs when they bind with hydrogen bonds to hexagonal oxygen atoms. Montmorillonites whose cations are exchangeable hydrates as Na^+ , Li^+ can swell to 30–40 Å. Moreover, sometimes this swelling level increases up to hundred. This type distance is called as osmotic swelling. Montmorillonites do not swell much when they got high valenced cations as exchangeable cations [68-72].

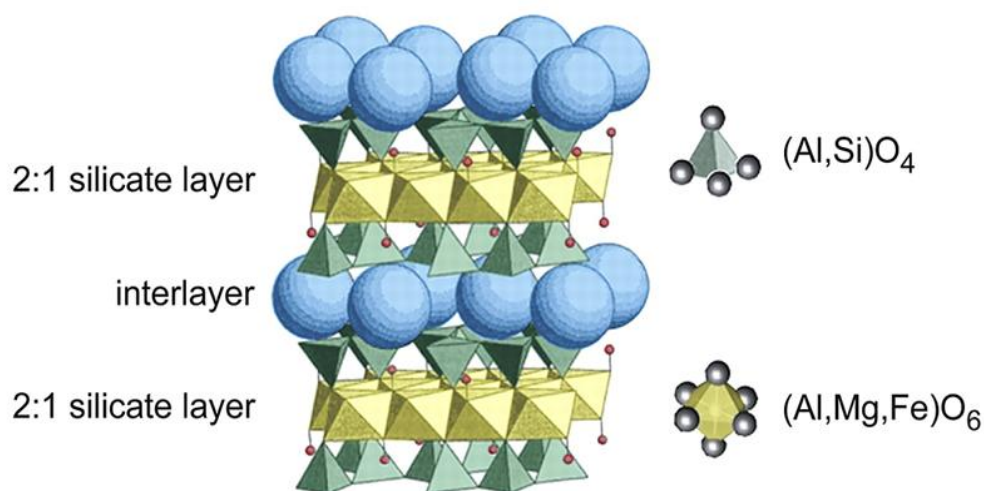


Figure 2.3: Schematic representation of structure of montmorillonite being a 2:1 clay mineral.

The reason of this situation is that gravitational forces between silicate and cation layers are higher than ion hydration thrust force [73]. Montmorillonites enable polar or ionic organic molecules to penetrate between the layers. Adsorption of organic mixtures causes to formation of organo-complex montmorillonites. Penetrating of big molecules into layers of clay mineral could be determined by using XRD measurements. Montmorillonites have 2:1

type layered structure. Crystal-like structure of the montmorillonite occurs from, silicon-oxygen (Si-O) tetrahedral layer with (Al-OOH) octahedral layer which is between two Si-O layers. Silicon atoms are bonded with 4 oxygen atoms in (Si-O) layers. Oxygen atoms are placed regularly as one in centre of silicon atom and the other 4 atoms are on the corners of the tetrahedron (Figure 2.4). Layers are divided between every third neighbour tetrahedral layer structure from 4 oxygen atoms of tetrahedron layer. All of the fourth oxygen atom of the tetrahedron has condition as oriented to lower side of structure which can be seen in Figure 2.4 and they are at the same plane with the -OH groups of alumina octahedral layers [74,75].

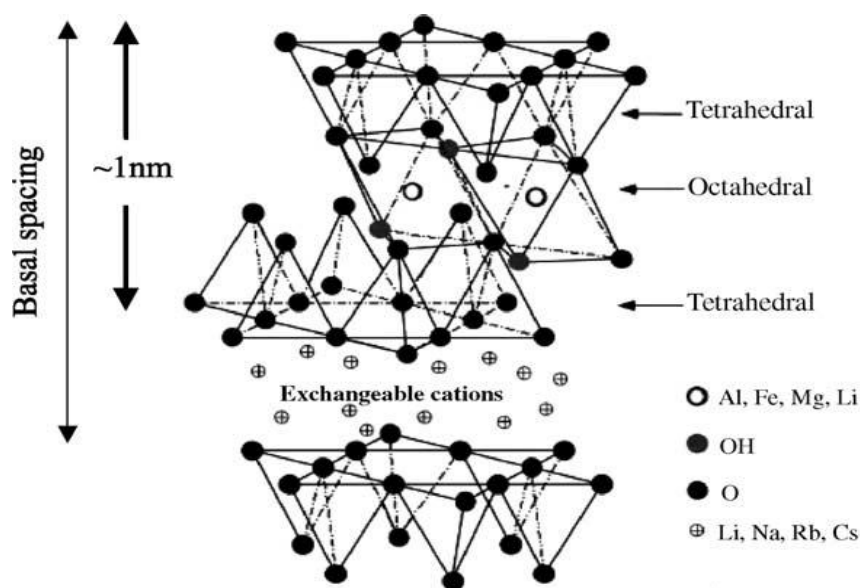


Figure 2.4: Structure of 2:1 phyllosilicates.

Properties of montmorillonite

The essential nanoclay raw material is montmorillonite, a 2:1 layered smectite clay mineral with a platelet structure. Individual platelet thicknesses are just one nanometer (one-billionth of a meter), but surface dimensions are generally 300 to more than 600 nanometers, resulting in an unusually high aspect ratio. Naturally occurring montmorillonite is hydrophilic. Since polymers are generally organophilic, unmodified nanoclay disperses in polymers with great difficulty. Through clay surface modification, montmorillonite can be made organophilic and, therefore, compatible with conventional organic polymers. Surface compatibilization is also known as “intercalation”. Compatibilized nanoclays disperse readily in polymers.

2.1.1.3. Compatibilizer

Compatibilizer is a polymeric additive that bonds the two phases to each other more tightly and modifies their interphases. It is used to increase the toughness of engineering plastics and

compatibility of the fillers. A strong filler-matrix adhesion leads to enhanced strength of particulate composites and this can be provided by a suitable compatibilizer.

Since polyolefins are widely used economical thermoplastic polymers, it is beneficial to upgrade the properties of polyolefins by using some additives. However, because of their hydrophobic nonpolar structures, polyolefins are not able to make strong connections with polar hydrophilic fillers. In such cases, surface modification of the filler increases the miscibility, but the modification process requires the usage of some solvents which are not so advantageous economically and for the environment. Using compatibilizer shows the same effect as surface modification, without the disadvantages of using solvents.

Maleic anhydride (MAH) is non-corrosive, highly polar, active group and has a decreasing effect on crystallinity and also has excellent heat stability allowing high processing temperatures. Copolymerization with MAH improves the physicochemical properties of polymers by providing increased polarity, rigidity, T_g and functionality. MAH based functionality promotes hydrophilicity, adhesion, compatibility and provides a reactive group for possible reactions.

MAH increases adhesion to polar substrates and allows the creation of chemical bonds by introducing reactivity with $-NH_2$, $-OH$ and epoxy groups of the polymer, substrate or filler. The cyclic structure of MAH is given in Figure 2.5.

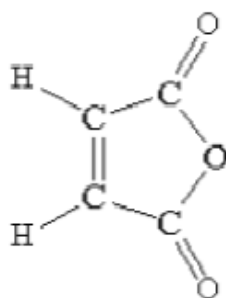


Figure 2.5: The chemical structure of MAH monomer.

2.1.1.4. The other additives

It is useful at this point to consider the definition of an additive as given by the European Commission: an additive is a substance which is incorporated into plastics to achieve a technical effect in the finished product, and is intended to be an essential part of the finished article. Some examples of additives are antioxidants, antistatic agents, antifogging agents, emulsifiers, fillers, impact modifiers, lubricants, plasticisers, release agents, solvents,

stabilisers, thickeners, UV absorbers and ethylene absorbers. Additives may be either organic (e.g. alkyl phenols, hydroxybenzophenones), inorganic (e.g. oxides, salts, fillers) or organometallic (e.g. metallocarboxylates, Ni complexes, Zn accelerators) [76].

Since the very early stages of the development of the polymer industry it was realised that useful materials could only be obtained if certain additives were incorporated into the polymer matrix, in a process normally known as ‘compounding’. Additives confer on plastics significant extensions of properties in one or more directions, such as general durability, stiffness and strength, impact resistance, thermal resistance, resistance to flexure and wear, acoustic isolation, etc. The steady increase in demand for plastic products by industry and consumers shows that plastic materials are becoming more performing and are capturing the classical fields of other materials. This evolution is also reflected in higher service temperature, dynamic and mechanical strength, stronger resistance against chemicals or radiation, and odourless formulations. Consequently, a modern plastic part often represents a high technology product of material science with the material’s properties being not in the least part attributable to additives. Additives (and fillers), in the broadest sense, are essential ingredients of a manufactured polymeric material. An additive can be a primary ingredient that forms an integral part of the end product’s basic characteristics, or a secondary ingredient which functions to improve performance and/or durability. Polypropylene is an outstanding example showing how polymer additives can change a vulnerable and unstable macromolecular material into a high-volume market product. The expansion of polyolefin applications into various areas of industrial and every-day use was in most cases achieved due to the employment of such speciality chemicals.

Additives are needed not only to make resins processable and to improve the properties of the moulded product during use. As the scope of plastics has increased, so has the range of additives: for better mechanical properties, resistance to heat, light and weathering, flame retardancy, electrical conductivity, etc. The demands of packaging have produced additive systems to aid the efficient production of film, and have developed the general need for additives which are safe for use in packaging and other applications where there is direct contact with food or drink. Especially in foodstuff applications, improvement of ethylene absorption and oxygen barrier properties of packaging films gained much more importance than before [77].

Ethylene Absorber

Ethylene gas ($\text{CH}_2=\text{CH}_2$) is a harmless odourless, colourless, gas that is produced from both natural and man-made sources, and that has a profound effect on the freshness of produce.

It was discovered that fruits and vegetables actually produce ethylene as they ripen. The ethylene acts as a signal to other plants to synchronize ripening to maximize their appeal to their seed disseminators (e.g. birds), thus assuring the dispersal of their seeds. Scientists have since studied the effects of ethylene on produce and found that the effects are widespread. Other plant tissues can produce this gas, as well. Even after harvest, fruits, vegetables and flowers are still alive, continuing their biochemical processes, including ripening and the generation of ethylene. Bruising or cutting some fruits and vegetables can even cause them to increase their ethylene production.

Since the discovery of the relationship between ethylene gas and the ripening process, industry has developed technology to manage the amount of ethylene gas in order to accelerate or slow down ripening and spoilage. Commercial warehouses, ships and trucks are nearly all fitted either with ethylene absorption technology or ethylene generation machines. However, when you buy fruits and vegetables and bring them home they sit on your counter or in your refrigerator where ethylene gas accumulates and accelerates the ripening process.

In this study, two kinds of ethylene absorber types were used. These absorbers absorb ethylene gas which is the main catalyst gas in the ripening process of foodstuffs. By controlling ethylene amount in packaging ambient we are able to slow down the ripening process and so shelf life is able to be increased.

2.1.2. Polymer Nanocomposites Production

There are four general approaches for the synthesis of layered silicate/polymer nanocomposites as listed below. Each polymer system requires a special set of processing conditions to be formed, based on the processing efficiency and desired product properties as seen in Table 2.2.

• *Solution approach*

This is based on a solvent system in which the polymer or pre-polymer is soluble and the silicate layers are swellable. The layered silicate is first swollen in a solvent, such as water, chloroform, or toluene. When the polymer and layered silicate solutions are mixed, the polymer chains intercalate and displace the solvent within the interlayer of the silicate. Upon

solvent removal, the intercalated structure remains, resulting in layered silicate/polymer nanocomposite, as shown in Figure 2.6 [78].

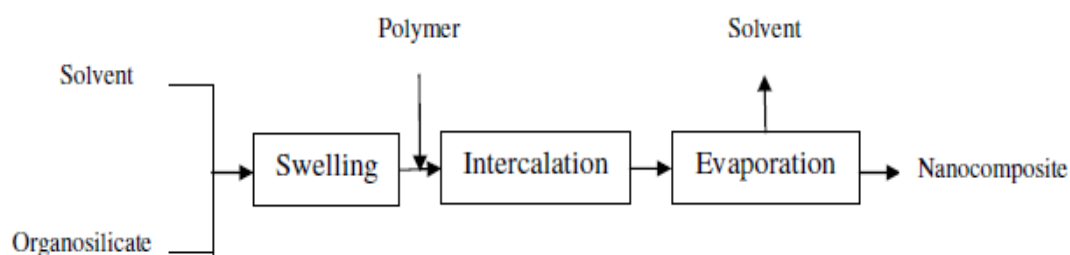


Figure 2.6: Flowchart of solution approach to synthesis nanocomposites

- ***In-situ polymerization***

The in-situ polymerization approach was the first strategy used to synthesize polymer-silicate nanocomposites and it is a convenient method for layered silicate/thermoset nanocomposites. This method is capable of producing well-exfoliated nanocomposites and has been applied to a wide range of polymer systems [79]. Once the organosilicate has been swollen in the liquid monomer or a monomer solution, the curing agent is added to the system, as shown in Figure 2.7. Upon polymerization, the silicate nanolayers are forced apart and no longer interact through the surfactant chains. Thus, highly exfoliated nanocomposites are formed [80].

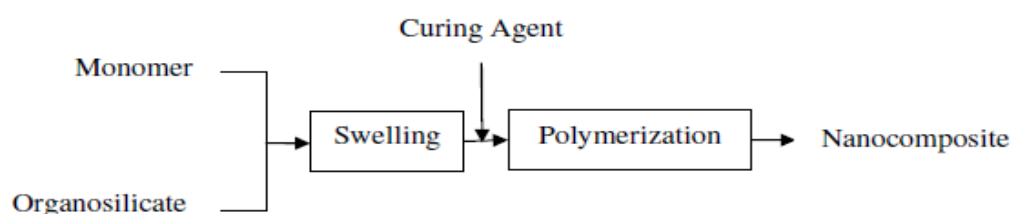


Figure 2.7: Flowchart of in-situ polymerization method to prepare nanocomposite [81].

- ***Melt intercalation***

The melt blending process involves mixing the layered silicate under shear, with the polymer while heating the mixture above the softening point of the polymer as shown in Figure 2.8 [82]. During this process, the polymer chains diffuse from the bulk polymer melt into the galleries between the silicate layers.

In some cases the polymer-silicate mixture can be extruded by using (a) static melt intercalation: by mixing and grinding dried powders of polymer and organic silicate in a pestle and mortar and then heating the mixture in vacuum, and (b) extrusion melt

intercalation: by extruding the mixture with twin screw extruder to produce a polymer nanocomposite from the polymer and modified clay.

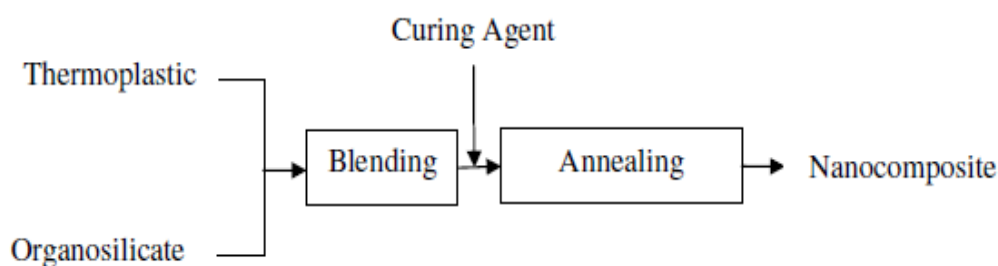


Figure 2.8. Flowchart of melt intercalation method to synthesis nanocomposite.

- ***Sol-gel technology***

It consists in a direct crystallization of the silicates by hydrothermal treatment of a gel containing organics and organometallics, including polymer. As the precursor for the silicate silica sol, magnesium hydroxide sol and lithium fluoride are used. This method has the potential of promoting the high dispersion of the silicate layers in a one-step process, without the presence of the onium ions [83].

2.1.3. Polymer Nanocomposites Features

Nanocomposites consisting of a polymer and layered silicate (modified or not) frequently exhibit remarkably improved mechanical and materials properties as compared to those of pristine polymers containing a small amount (<5 wt.%) of layered silicate. Improvements include a higher modulus, increased strength and heat resistance, decreased gas permeability and flammability, and increased biodegradability of biodegradable polymers [84]. The main reason for these improved properties in nanocomposites is the stronger interfacial interaction between the matrix and layered silicate, as compared with conventional filler-reinforced systems.

2.1.3.1. Micro structure

It is not always possible to end with a nanocomposite when the organoclay is mixed with a polymer. Unseparated montmorillonite layers are called as tactoids after they are introduced into the polymer [85]. The dispersion of the inorganic compound must be at the nanometer level that is down to elementary clay platelet [86]. The layer thickness of the layered silicates is on the order of 1 nm and they have a very high aspect ratio (10-10000). Compared to conventional composites, a few weight percent of layered silicates create much higher surface area for polymer-filler interaction [87]. Three types of nanocomposites that are called

intercalated, exfoliated and flocculated can be obtained depending on the nature of the components used and the method of preparation [88]. The types of polymer-layered silicate nanocomposites are given in Figure 2.3.

Table 2.2: Processing techniques for layered silicate/polymer nanocomposites.

Processing	Drive Force	Advantages	Disadvantages	Examples
<i>In-situ polymerization</i>	Interaction strength between monomer and silicate surface: enthalpy evolution during the interlayer polymerization.	Suitable for low or non-soluble polymers: a conventional process for thermoset nanocomposites.	Silicate exfoliation depends on the extent of silicate swelling and diffusion rate of monomers in the gallery: oligomer may be formed upon incompletely polymerization.	Nylon 6, epoxy, polyurethane, polystyrene, polyethylene oxide, unsaturated polyesters, polyethylene terephthalate.
<i>Solution Approach</i>	Entropy gained by desorption of solvent, which compensates for the decrease in conformational entropy of intercalated polymers.	Prefer to water-soluble polymers.	Compatible polymer-silicate solvent system is not always available; use of large quantities of solvent; co-intercalation may occur for solvent and polymer.	Epoxy, polyimide, polyethylene, polymethyl methacrylate
<i>Melt Intercalation</i>	Enthalpic contribution of the polymer-organosilicate interactions.	Environmental benign approach: no solvent required.	Slow penetration of polymer within the confined gallery.	Nylon 6, polystyrene, polyethylene terephthalate

• *Intercalated nanocomposites*

In intercalated nanocomposites, the insertion of a polymer matrix into the layered silicate structure occurs in a crystallographically regular fashion, regardless of the clay to polymer ratio. Intercalated nanocomposites are normally interlayer by a few molecular layers of polymer. Properties of the composites typically resemble those of ceramic materials [87].

• *Flocculated nanocomposites*

Conceptually this is same as intercalated nanocomposites. However, silicate layers are sometimes flocculated due to hydroxylated edge-edge interaction of the silicate layers [87].

• *Exfoliated nanocomposites*

In an exfoliated nanocomposite, the individual clay layers are separated in a continuous polymer matrix by an average distances that depends on clay loading. Usually, the clay content of an exfoliated nanocomposite is much lower than that of an intercalated nanocomposite.

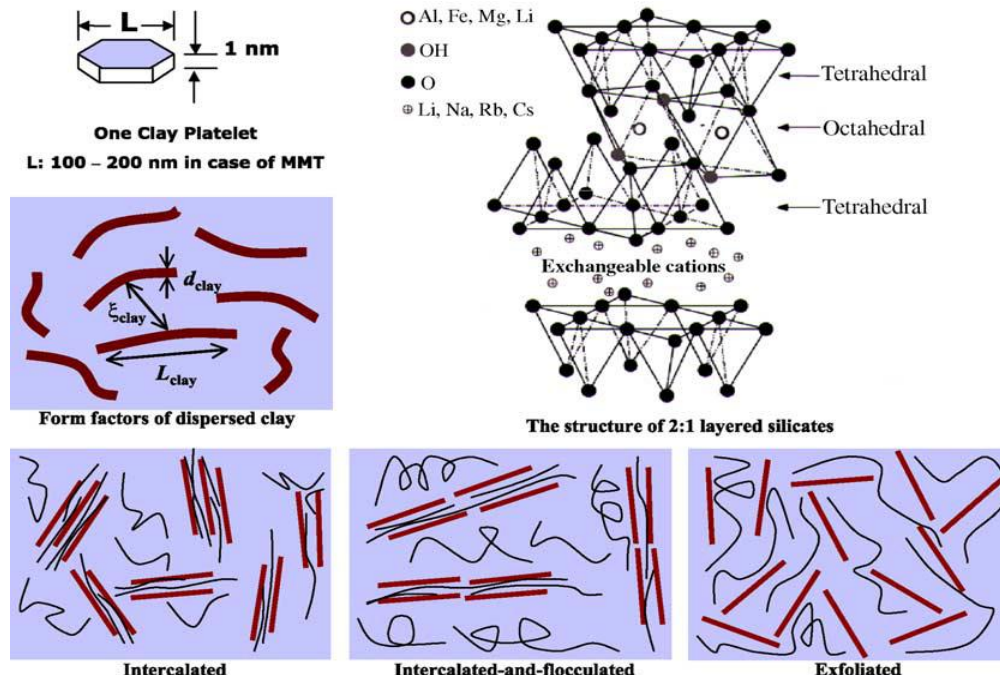


Figure 2.9: Schematically illustration of three different types of thermodynamically achievable polymer/layered silicate nanocomposites. Reproduced from Sinha Ray, Okamoto and Okamoto by permission of American Chemical Society, USA [89].

2.1.3.2. Mechanical properties

Mechanical properties are critical as barrier properties for a packaging material. Along the travel of the packaged food, packaging must be durable and free from minor defects to ensure the safety of food. Sufficient mechanical strength of packaging material is critical in terms of preventing food to be effected from physical impacts and also to satisfy the barrier properties required [90].

The potential of polymeric layered silicate nanocomposites in materials science was first evidenced by the effective reinforcing capability of exfoliated layered silicate nanoclays in polymer matrix. Improvements in mechanical properties of polymers could be achieved in a larger extend by employing nanocomposites compared to conventional composites prepared by using micro size fillers. As in the case of barrier improvements of layered silicate

nanocomposites, several factors were proposed for the performance of LSNC (Layered Silicate Nanocomposites). These factors can be sum up in two headings; factors that can be explained by composite theory and nano-effects occurred in polymer structure due to efficient distribution of nanofillers in the polymer matrix [92, 95].

Reinforcing mechanism of fillers such as fibers can be put in use to understand the effect of LSNC on mechanical properties. High moduli rigid fillers within the relatively soft polymer matrix create a mechanically restrained area of polymer, particularly adjacent to filler. Reinforcing mechanism of fillers was given in the Figure 2.10 below. As long as adequate bonding between polymer and filler phases exists, the structure would tend to act as a stronger material than the pristine polymer. At this point, the enormous surface area (characterized in several hundred meter squares) benefited due to effective distribution of layered silicate platelets can be used to explain the more expressed improvements in a LSNC than a conventional composite [91-93].

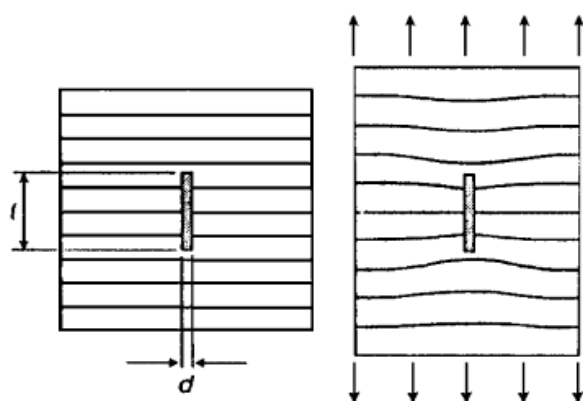


Figure 2.10: Reinforcement mechanism in composite materials [91].

Several reviews and studies discussed the successful stiffening of polymers by LSNC with less filler content compared to conventional composites to achieve the same degree of improvement. Paul and Robeson (2008) reviewed comparison of PE/MMT nanocomposites with PE/Talc composites and Nylon6/MMT nanocomposites with Nylon6/glass fiber composites. The required amount of MMT to double elastic modulus of neat polymers was reported to be 4 and 3 times lower than talc and glass fibers; indicating a significant weight reduction for the same performance [92]. Petersson and Oksman (2006) studied PLA nanocomposites prepared by bentonite LS and PLA microcomposites prepared by microcrystalline cellulose. Concentration of both fillers was 1 wt% with respect to polymer. Authors reported 50% increase in elastic modulus and yield strength for LSNC of PLA while

cellulose composites slightly reduced the modulus of films without significantly improving the yield strength.

Beside improvements in stiffness, the addition of LSNC increased the maximum tensile strength of polymers. While elastic modulus increase in LSNC was mainly attributed to existence of stiffer layered silicates platelets, improvements in tensile strength of LSNC were attributed to degree of bonding between nanoclay and polymer matrix [91, 93]. Dean and coworkers (2008) improved the tensile strength of PVOH/Starch blends by using MMT. Higher increase in tensile strength in PVOH blends compared to single starch films were attributed to enhanced bonding between PVOH and MMT as evidenced by FTIR. Many reviews concerning the mechanical properties of LSNC reported that tensile strength improvements in LSNC are more sensitive to nanoclay content than modulus changes due to level of interactions between nanofiller and polymer [91, 94, 95]. Maximum elongation of polymeric films under tensile load is another important mechanical aspect of nanocomposites. It is well known that polymeric composites improve modulus and tensile strength at the expense of flexibility of the material. Decreased flexibility is generally observed in nanocomposites as well. Nanocomposites are thought to alter flexibility of polymers in lesser extent than conventional composite systems that results in better interactions between filler and polymer matrix due to higher surface area available for bonding [92-94].

2.1.3.3. Gas barrier properties

Among several interesting properties of polymer layered silicate nanocomposites (LSNC), the most attractive one from food packaging aspect is the availability of nanocomposites for unique improvements in gas and water vapour barrier of packaging films. Compositing inorganic fillers with polymers is a common application in the industry to improve barrier properties of packaging materials. Micro size filler content required for adequate improvements is generally high, and may lead to deteriorations in mechanical strength and optical properties of produced films [96]. Besides, possible problems such as higher processing temperature and poor melt rheology may occur. In the case of nanocomposites, level of barrier improvement is higher and such adverse effects are less likely to occur.

Improvements in barrier properties by the introduction of fillers in the polymer matrix are primarily attributed to the tortuous path formed for the permeating molecules. A diffusing molecule tends to travel in the path where it will face with least resistance. Any source of resistance, such as crystalline domains within the structure or irregularities in the sequence of the polymer molecules results in longer path that a permanent must travel reducing the

permeability as discussed in the previous chapters. Tortuosity concept where the inorganic fillers are assumed to be impermeable for gas and liquid molecules is analogous to above mentioned transport properties of molecules [97].

Basically, nanocomposites also improve barrier of polymers by creating more tortuous path for diffusing molecules due to incomparably higher aspect (length to width) ratio of nanofillers. While conventional composites are accepted to improve the barrier properties of polymers due to increased tortuosity; several additional factors were also proposed for nanocomposites. Small particle size and enormous surface area offered by layered silicates (LS) reported to alter matrix structure and change the permeation properties. Restrained polymer chain mobility resulted in decrease of free volume fraction of rubber/hectorite nanocomposites due to interactions in LS-polymer matrix and decrease in gas permeability [98]. Nanoscale dimensions of nanocomposites may act as seeds for the creation of crystalline domains in the structure. MMT exfoliation within Nylon 6 increased matrix crystallinity and improved barrier properties [93].

LSNCs offer unique improvements in barrier properties of polymers due to their special geometry and properties. Polymer chains can be inserted between the LS stackings by several preparation methods and LS surface can be modified to enhance compatibility with the polymer matrix. Fine distribution of LS platelets, defined as exfoliation, may give aspect ratios in the range of several hundreds [95, 99, 100]. Schematic explanation of more effective tortuous path formation in LSNC in comparison to conventional composites was given in Figure 2.11.



Figure 2.11: Schematic illustration of formation of highly tortuous path in nanocomposite. Conventional filler reinforced composites at left and, polymer/layered silicate nanocomposites at right.

Petersson and Oksman (2006) compared bentonite/PLA LSNC and microcrystalline cellulose (MCC)/PLA microcomposite by fixing the weight percent of filler. Results showed very significant differences in oxygen permeability values approving the effect of aspect ratio.

Oxygen permeability of bentonite LSNC decreased while MCC composites destructed polymer structure and resulted in high permeability to O₂; even three times higher than the value for neat PLA. The most important feature of LSNC is the availability to achieve the same level of barrier improvement with small concentrations of nanofiller around 1-5 wt% without altering the mechanical strength of polymeric films due to high length to width ratio of LS compared to conventional fillers.

In the literature, barrier property improvements obtained by LSNC were mostly interpreted by the extensive tortuosity formed due to exfoliation of LS. Changes in polymer structure such as crystallinity, directed by LS platelets are hard to follow, and some polymer classes such as protein based biopolymers are amorphous. Several models based on tortuosity exist in the literature proposed to explain the effect of dispersed LS within the polymer matrix. Most of the permeability models applicable to LS systems were generally constructed by ignoring any possible structure change in the polymer as a result of nanocomposite formation [91, 93, 96].

2.1.3.4. Thermal stability

Since processing of most polymer-clay nanocomposites need high temperatures irrespective of the fabrication route, thermal stability of organoclay has a significant role on the performance and application of nanocomposites. In general, nanoclay layers possess substantial barrier properties (including thermal and mass transport) that protect the polymer from fire and make it difficult for the degraded products to leave. Molecular dynamics simulation of thermal degradation of nano-confined polyethylene also supports this mechanistic hypothesis [101]. The presence of alkyl ammonium cations on the clay surface (organoclay) may result in decomposition following Hofmann's elimination reaction that depends on the basicity of the anion, the steric environment around the ammonium, temperature, and its product, in addition to clay itself, which can catalyze the degradation of the polymer matrix [102,103]. The multiple pathways are attributed to a fraction of excess (un-exchanged) surfactant and the chemically heterogeneous morphology of the layered silicate. This will reduce the thermal stability of the polymer-clay nanocomposites. It has been shown that with the addition of low fractions of nano-clay that is well-dispersed into fine layers in the polymer, the barrier effect is predominant. But with increasing clay loading, the catalyzing effect rapidly increases so that the thermal stability of the nanocomposites decreases [104].

In contrast, many previous studies also showed that organoclay filled polymer nanocomposites could enhance thermal stability compared to the pristine polymer. The

improved thermal stability observed in these nanocomposites was generally attributed to the hindered diffusion of volatile decomposition products (such as small cyclic siloxanes for polydimethylsiloxane decomposition) as a direct result of their decreased permeability. Hence, the improvement in thermal stability is related to barrier properties and the radical-trapping effect of clay platelets. Clays can act as free radical scavengers and traps by reacting with the propagating or initiating radicals [105].

In summary, the role of clay in the nanocomposite structure and the type of surfactant used may be the main reasons responsible for the difference in thermal stability of different polymer-clay nanocomposite systems. Clay can act as a heat barrier (that enhances the overall thermal stability of the system) and to assist the char formation after thermal decomposition. That is, in the initial stages of thermal decomposition, clay would shift the decomposition to higher temperature. After that, this heat barrier effect would result in a reverse thermal stability. Therefore, the stacked silicate layers could hold up the accumulated heat that might be used as a heat source to accelerate the decomposition process, in concert with the heat flow supplied by the outside heat source [106]. In addition, the variation of the surface polarity of clay and host polymer at their interface owing to the use of different compatibilizers and the radical-trapping effect of clay platelets also affect the thermal stability of polymer-layered silicate nanocomposites.

2.1.3.5. Optical and surface properties of packaging films

Food packaging has also communication aspect additional to barrier and mechanical properties required to ensure the quality of food until final consumer use. In terms of marketing purposes, the appearance and design of the packaging is very important. The name, properties or trademark of the product must always be printed on the packaging. In some cases, food packaging is better to be transparent in order to directly present the food inside.

Surface properties of the films, surface energy or surface tension are critical for food packaging films. Surface energy of the films depends on variations on the homogeneity and roughness of the surface as well as composition and crystal orientation of the packaging material [107]. Surface energy of the films cannot be measured directly. Surface energy parameters are obtained from contact angle analysis of several probe liquids such as water. Contact angle measurements can give an idea about the surface characteristics such as hydrophobicity. Level of surface hydrophobicity is important since interactions with other layers such as printing ink applied on packaging films or coatings require compatibility with

the surface for good adhesion. Besides, surface characteristics are also important in production processes such as blending or co-extrusion applications.

Another feature of packaging films is their optical properties. Transparency, ability of a material to let light through a film is important. Transparency of packaging films are required in applications which product visibility from outside is desired. Consumer surveys showed better acceptance of products are obtained by transparent packaging of fresh vegetables and fruits and also for snacks [108]. Most of the synthetic polymers like PET, PP, PE are well known transparent materials. Beside transparency, appearance of the films is important. Haze; simply scattering of light which results into cloudy appearance, is not desired in food packaging [109]. Colour of the films is also important since details of the product may deteriorate when deviances to more yellow or green colours exists in packaging. Colour of the pristine film is also important in terms of printing applications.

2.2. Polyolefin Nanocomposites Packaging Application

2.2.1. Need For Packaging

Most food is consumed far removed in time and space from the point of its production and hence proper packaging is a necessary aid for the storage and distribution of the food. There serve as a material handling tool and a processing aid as well as a convenience item for the consumer and marketing. Further, when properly used they are cost saving devices [110]. A food product is packaged for prevention of possible kinds of degradation that may render it unsuitable for consumption or impart a lower sensorial value [111]. In this aspect, it is important that the food should be fresh, intact and suitable for being packaged. That is, a package can function to preserve an existing quality at the state of wrapping.

In the economical aspect of packaging instead of maximum protections against all sources of degradations, it is proposed that the packaging material should only possess protection efficiency in relation with the chosen shelf life.

2.2.2. Packaging Materials

There are various types of packaging materials according to the need as; metals, metal foils, paper, plastic films, wood, edible films and some combinations of them. In choosing a packaging material to protect a food product during the storage, primarily the physical and chemical properties of the packaged food are considered [111].

Plastic films have become the mostly used material for packaging during the last century due to their advantages and the resulting wide application areas. There are various polymeric

materials with densities in the range 900 to 1400 kg/m³ for most of them. The ability of a plastic to provide lightweight packages, which is an important parameter for consumer convenience and a way for processors to reduce shipping costs, is one of the largest driving forces behind the well acceptance of plastics in the market for food containers that were once the exclusive province of metal and glass.

The necessity that nearly all packages must be closed in some way, to protect its contents from environmental factors renders plastics an advantage as vast majority of such materials can be closed by heat sealing. Polymer coatings and adhesives are universally used to perform this function. No other packaging material can match the ability of plastics to create strong, hermetic sealed at low temperatures (35-125 °C). Many plastic film substrates can be heat sealed to them without an additional adhesive coating. This greatly increases the productivity of the machines since mechanisms for adhesives can be eliminated.

All common plastic can readily convert into thin, strong and clear films. This means that for thousands of flexible packaging applications metal and glass cannot be used and only paper, glassine and cellophane can compete. In addition, plastics are unsurpassed in the ease with which special shapes can be readily created particularly important for rigid containers.

Unmodified plastic films and sheets in appearance from crystal clear to hazy. Pigments or soluble dyes can be added to produce total opacity in virtually any colour or to produce transparent coloured films and sheets. For example, if the food being packaged is sensitive to light catalyzed oxidation, as many foods are, pigmentation or metallization can be used to screen out light. No other packaging material offers the package designer such a wide range of choices.

Tear and puncture resistance gives plastics a major edge over paper, cellophane and aluminium foil in flexible packages.

Many food products are sensitive to attack by water vapour and oxygen. Glass, metal and pinhole-free aluminium foils are totally impermeable to these two gases which damage so many food products. Plastics rank well below these materials but they are far more impermeable than uncoated paper. Even simple uncoated, homo-polymer plastics such as polyethylene exhibit sufficient barrier to moisture for many applications. Although all-plastic packages will never have the infinite oxygen barrier provided by metal and gas they are now close to providing enough oxygen barriers in order to compete for all food packaging applications.

The finite permeability of plastics to gases becomes a positive attribute in the design of packages for products such as fresh produce which continue to respire after being harvested.

2.2.3. Production of Packaging Films

In the industry, several methods have been used for the manufacture of polymer films. Most thin sheets and films are made by calendaring or extrusion.

In extrusion, the compounded material in the feed hopper is heated and forced into the die area by a screw conveyor. By the combination of the choker bar and die opening, the thickness of the sheet is controlled. After extrusion the sheet passes through oil or water cooled chromium-plated rolls before being cut to size [112].

In calendaring, the material composed of resin, plasticizer, filler and colour pigments is first compounded and heated before being fed into the calendar. The thickness of the sheet produced depends upon the clearance between the rollers the squeezing process and the speed of the finishing rollers which stretch the plastic. Before the film is wound it passes through water cooled rolls.

In manufacturing laminated products, the resin material is dissolved by a solvent to convert it into a liquid. Rolls of paper or fabric are then passed through a bath for impregnation. This is a continuous operation and as the sheet leaves the resin bath, it goes through a drier which evaporates the solvent, leaving a fairly stiff sheet impregnated with the plastic material.

2.2.4. Active Packaging Technologies

Active packaging is the term used when the packaging performs some role other than providing an inert barrier to external conditions [113].

Active packaging has developed as a series of responses to unrelated problems in maintenance of the quality and safety of foods. Accordingly, a range of types of active packaging has been developed.

In one sense active packaging is considered as a means of maintaining the optimum conditions to which a food was exposed at the immediately preceding step in its handling or processing. Passive packaging has been used in an effort to minimize the deleterious effects of a limited number of external variables such as oxygen, water, light, dust microorganisms, rodents and to some extent heat. Hence, active packaging has the potential to continue some aspects of the processing operation or to maintain chosen variables at particular levels.

Modified atmosphere packaging is the alteration of the gaseous environment produced as a result of respirations or by the addition or removal of gases from small sized food packages to manipulate the levels of O_2 , CO_2 , N_2 , and C_2H_4 in order to extend storage life of the fresh produce.

Fresh produce continue to actively metabolize during postharvest phases. After a short period of adjustment, steady-state conditions will be established inside an intact polymeric film package once the appropriate relationship among produce and package variables is achieved. Oxygen inside the package is consumed by the produce as it respire and an approximately equal amount of CO_2 is produced. The reduction in O_2 concentration and increase in CO_2 concentration create a gradient causing O_2 to enter and CO_2 to exit the package. Initially, however, the gradient is small and the flux across the package is not sufficient to replace the O_2 that was consumed or do drive out all of the CO_2 that was generated. Thus, inside the package, O_2 content decreases and CO_2 content increases. As this modified atmosphere is created inside the package, respiration rates start to fall in response to those new atmosphere concentrations. Thus, eventually new equilibrium concentrations of the gases surrounding the fruit are established. At this state, O_2 consumption equals O_2 diffusion in the package and CO_2 production equals CO_2 diffusion out of the package [114].

By this way a beneficial modified atmosphere can be passively created within a package.

In order to avoid uncontrolled levels of O_2 , CO_2 , and C_2H_4 that can be deteriorative active modification can be applied in a number of ways. It can be done by creating slight vacuum and then replacing the package atmosphere with the desired gas mixture. This mixture can be further adjusted through the use of absorbers or absorbers in the package to scavenge these gases.

Selection of a film that will result in a favourable modified atmosphere should be based on the expected respiration rate of the commodity at the transit and storage temperature to be used and the known optimum O_2 and CO_2 concentrations for the commodity.

Control of oxygen amount in a package

Fresh fruit and vegetables keep to be alive after harvesting. In this period, they takes oxygen gas from the ambient and release carbon dioxide gas to the ambient. To slower respiration of foodstuffs, the oxygen entrance to packaging environment must be prevented. Lowering the O_2 level around fresh fruits and vegetables reduces their respiration rate I proportion with the O_2 concentration. Removal of oxygen also protects the loss of any vitamins that are oxidation

sensitive. The most appropriate method of removal of oxygen from a food package depends on the nature of the food, its processing history and the packaging machinery and the way its distributed.

One major way to directly control oxygen levels in a package is the use of an oxygen scavenger system. The simplest scavenger is reduced iron and iron containing sachet that is directly put into the package. If the oxidation rate of the food and the film oxygen permeability are known, the almost of iron required for the desired shelf life can be calculated. Other chemical scavenger systems include reactive dyes, ascorbic acid and oxidizing enzymes namely glucose oxidase and alcohol oxidase. The problem is the diffusion of the reaction products from the enzymes, since if too slow, the enzyme activity will decrease. Other approaches are incorporating an organic chelator that binds oxygen into the packaging material and incorporating free radical scavengers that react with oxygen [115].

Sachets merely inserted into the food package constitute most of the present systems in commerce. Alternatively, the scavenger can be hot-melt bonded to the inner wall of the package or sachets are inserted in the form of cards, sheets or layers coated onto the inner wall of the package [113].

Control of carbon dioxide amount in a package

Carbon dioxide gas is released as a product of respiration. Increase in carbon dioxide gas allow the microbial spoilage in foodstuffs through anaerobic respiration process. A carbon dioxide generating or scavenging system is incorporated into the film or added as a sachet. Since, high CO₂ levels are desirable for some foods and plastic films are generally 3-5 times more permeable to CO₂ than O₂ a generator will be needed for some applications. On the other hand, high CO₂ levels cause fruits to enter anaerobic glycolysis which is undesirable. One commercial application is a mixed iron powder-calcium hydroxide sachet which both O₂ and CO₂ are scavenged [115].

Control of ethylene amount in a package

Ethylene has diverse and profound effects on the physiology of plants, but has been recognized as a problem in postharvest handling of horticultural products. This must be removed from the headspace otherwise the product quickly matures and shortens shelf life [115].

Most commonly used ethylene removal agents are potassium permanganate (KMnO₄) based scavengers. Typically, such products contain 4-6% KMnO₄ on an inert substrate such as

perlite, alumina, silica gel, vermiculate, activated carbon or celite. These products are available in sachet for packages and on blankets that can be placed in produce-holding rooms. Potassium permanganate is not contacted with food because of its toxicity.

Various metal catalysts on activated carbon will effectively remove ethylene from air passing over the bed of carbon. Activated charcoal impregnated with palladium catalyst and bromine-type inorganic chemicals are some examples.

In the past several years a number of packaging products have appeared based on the putative ability on certain finely dispersed minerals to absorb ethylene. Typically, these minerals are local kinds of clay that are embedded in polyethylene bags which are then used to package fresh produce.

There are many other similar bags being sold throughout the world offering improved postharvest life of fresh commodities due to the adsorption of ethylene by the minerals dispersed within the film. The evidence offered in support of this claim is generally based on the shelf life experiments comparing common polyethylene bags with mineralized bags. Such evidence generally shows an extension of shelf life and/or reduction of headspace ethylene but yet are unconvincing. Although the finely divided minerals may absorb ethylene, they will also open pores within the plastic bag and alter the gas-exchange properties of the bag. Because ethylene will diffuse much more rapidly through open pore spaces within the plastic than through the plastic itself, one would expect ethylene to diffuse out of these bags faster than through pure polyethylene bags. However, by the same phenomena exchange of CO₂ and O₂ with the ambient shall be taking place more readily than is the case for a normal polyethylene bag. These effects can improve shelf life and reduce headspace ethylene concentrations independent of any ethylene adsorption. In fact almost any powdered mineral can confer such effect without relying on expensive Oya stone or other speciality minerals [116].

Although the minerals in question may have ethylene adsorption capacity, the data supporting the commercial products incorporating these minerals fail to demonstrate such capacity. Even if they do have ethylene adsorbing capacity, it is possible that they will lack significant capacity while embedded in plastic films. The ethylene would have to diffuse through the plastic matrix before contact with the dispersed mineral, thus greatly slowing any process of adsorption. Once the ethylene has diffused half-way through the plastic film, venting to the outside may be nearly as fast and effective as adsorption on embedded minerals.

2.2.5. Ethylene Removing Packaging

Ethylene is a chemically simple, ubiquitous chemical that has diverse and profound effects on the physiology of plants. Ethylene has so many different effect on plants, is effective in such low concentrations, and its effects are so dose-dependent, that it has been identified as a plant hormone. Though many of the effects of ethylene on plants are economically positive, such as induction of flowering in pineapple, de-greening of citrus and ripening of tomatoes, often ethylene has been seen to be detrimental to the quality and longevity of many horticultural environments and in suppressing its effects.

Some of the diverse ways in which to absorb, adsorb, counteract or chemically alter ethylene have led to products designed to reduce its deleterious effects. This study will briefly review the chemistry, physiology and agricultural effects of ethylene preparatory to describing the research and commercial effort undertaken to incorporate ethylene control agents in packages for horticultural products. Some of this effort has met with commercial success, but much has not. However, with the rapid growth of packaging of fresh fruits and vegetables, particularly fresh cut salad and fruits, opportunities for such products are bound to increase. Therefore, it is timely to review the basis and activities relating to these products to better elucidate the possible forms that they can and will take and to point out some of the advantages and disadvantages of the various approaches likely to emerge.

2.2.5.1. The chemistry of ethylene

The ethylene molecule is of the alkene type, being simply two carbons linked by a double bond with two hydrogen atoms on each carbon. Such a simple molecule can be synthesized through several different pathways and is subject to many kinds of chemical reaction.

2.2.5.2. Synthesis of ethylene

Ethylene can be synthesized both biologically and non-biologically. It is a common component of smoke and can be found as a product of aerobic combustion of almost any hydrocarbon. It is thus a common air pollutant, its chief source being automobile engines.

Biological sources of ethylene include higher plant tissues, several species of bacteria and fungi, some algae, and some liverworts and mosses. The biosynthetic pathways for ethylene are diverse among these different organisms. The pathway of synthesis from methionine has been described in detail for higher plants [117]. The pathways for synthesis in bacteria appear to be diverse since any of several carbon sources other than methionine will serve as

precursors [118]. Nitrogen fixing bacteria can reduce acetylene to ethylene [119]. Appropriately 25-30% of fungal species tested produce ethylene on appropriate media [120]. The pathways of plant and fungal ethylene synthesis appear to be distinct, as the inhibitor rhizobitoxin blocks synthesis in plants but not in the fungus *Penicillium digitatum* [121]. The pathway of ethylene synthesis in non-vascular plants may be different from that in vascular plants [122].

The important point is that environmental ethylene can be biologically produced by a wide range of organisms, both visible and invisible, and such sources ought to be considered when devising strategies to reduce ambient ethylene.

2.2.5.3. Adsorption and absorption

In addition to chemical cleavage and modification, ethylene can be absorbed or adsorbed by a number of substances including activated charcoal, molecular sieves of crystalline aluminosilicates, Kieselguhr, bentonite, Fuller's earth, brick dust, silica gel [123] and aluminium oxide [124]. A number of clay materials have been reported to have ethylene adsorbing capacity. Examples include cristobalite ($>87\%$ SiO_2 , $>1\%$ Fe_2O_3) [124], Ohya-ishi (Oya stone) and zeolite [125]. Oya stone is mined from the Oya cave in Tochigi Prefecture in Japan. The cave has been used to store fresh produce and is reputed to confer added storage life. The salutary properties of the cave are thought to reside in the largely zeolitic stone interior. To improve its ethylene adsorptive capacity, the Oya stone is first finely ground with a small amount of metal oxide. The mixture is then kneaded and heated to 200-900 °C, then oxidized with ozone or electromagnetic radiation [126]. Some regenerable adsorbents have been shown to have ethylene adsorbing capacity and have the benefit of being reusable after purging. Examples of such adsorbents include propylene glycol, hexylene glycol [127], squalene, Apiezon M, phenylmethylsilicone, polyethylene and polystyrene [128]. Some adsorbents have been combined with catalysts or chemical agents that modify or destroy the ethylene after adsorption. For example, activated charcoal has been used adsorb ethylene. In some cases, the activated charcoal has been impregnated with bromine or with 15% KBrO_3 and 0.5M H_2SO_4 to eliminate the activity of the ethylene [129]. A number of catalytic oxidizers have been combined with adsorbents to remove ethylene from air. Examples include potassium dichromate, KMnO_4 , iodine pentoxide, and silver nitrate, each respectively on silica gel [130].

Electron-deficient dienes or trienes, such as benzenes, pyridines, diazines, triazines and tetrazines, having electron-withdrawing substituents such as fluorinated alkyl groups,

sulphones and aster (especially dicarboxyoctyl, dicarboxydecyl and dicarboxymethyl ester groups), will react rapidly and irreversibly with ethylene at room temperature and remove ethylene from the atmosphere. Such compounds can be embedded in permeable plastic bags or printing inks to remove ethylene from packages of plant produce [131].

Metal catalysts immobilized on absorbents, such as platinized asbestos, cupric oxide-ferric oxide pellets and powdered cupric oxide, will effectively oxidize ethylene, but in many cases the reactions require high temperatures ($>180\text{ }^{\circ}\text{C}$). Clearly such systems would be inappropriate for food packaging applications.

2.2.5.4. Deleterious effects of ethylene

Ethylene has long been recognized as a problem in postharvest handling of horticultural products. Since the discovery in 1924 that ethylene can accelerate ripening in fruit [132]. It has become clear that ethylene can be the cause of undesirable ripening of fruits and vegetables. It is now recognized that ethylene, in very low amounts, can be responsible for a wide array of undesirable effect in plants and plant parts. The physiological effects of ethylene are so important, so diverse, and are induced by such small amounts of ethylene that is considered a plant hormone. The diverse physiological effects of ethylene have been extensively reviewed elsewhere [133] so only those effects that are deleterious to packaged plant produce will be discussed here.

Respiration

Perishability of produce generally is well correlated with respiration rate. Commodities such as asparagus, broccoli and mushrooms that have very high respiration rates are very perishable, having postharvest lives measured in days. Those commodities such as nuts, dates, dried fruits, potatoes and onions that have very low respiration rates have postharvest lives measured in [134]. Reduction of respiration rate increases postharvest life and elevation of respiration rate generally decreases it. This is one of the reasons why low temperature is so important in postharvest management. Reducing the temperature rapidly reduces the respiration rate of the product.

Ethylene accelerates the respiration of fruits, vegetables and ornamental plants. In the case of climacteric fruit, ethylene can induce a rapid and irreversible elevation in respiration leading directly to maturity and senescence. In non-climacteric plant organs, ethylene induces a reversible increase in respiration in most cases, exposure to a few parts per million (ppm) of ethylene leads to increased respiration and increased perishability.

Fruit ripening and softening

Ethylene has been referred to as a ‘ripening’ hormone because it can accelerate softening and ripening of many kinds of fruit. Exposure of mature fruit to ethylene leads to increased respiration, increased production of endogenous ethylene, and softening of fruit tissues [133] this is achieved through the direct or indirect stimulation of synthesis and activity of many ripening enzymes by ethylene.

Some fruits, such as bananas and tomatoes, are often deliberately exposed to high concentrations of ethylene (~ 100 ppm) to induce rapid ripening. In most cases, for packaged fruits it would be desirable to prevent exposure to ethylene and thereby prevent rapid ripening.

Ethylene can be responsible for number of specific postharvest disorders of fruits and vegetables. Examples include russet spot (small oval brown spots, primarily on the midrib) of crisphead lettuce, formation of bitter-tasting isocoumarins in carrots, sprouting of potatoes, and toughening of asparagus [135].

Commercial applications in packaging

Various technologies have been incorporated into packaging materials that are either commercially available or are likely to become available in the near future. As is common in the commercial sector, some of the claims for ethylene ad-/absorbing capacity for these packaging materials have been poorly documented and thus the efficacy of the materials is difficult to substantiate.

Most substances designed to remove ethylene from packages are delivered either as sachets that go inside the package or are integrated into the packaging material, usually a plastic polymer film or the ink used to print on the package.

2.2.5.5. New and novel approaches to ethylene-removing packaging

There are some new and unusual approaches to developing ethylene-removing packaging that deserve mention.

Perhaps the most promising new development in ethylene-removing packaging is the use of electron-deficient dienes or trienes incorporated in ethylene-permeable packaging. The preferred diene or triene is a tetrazine. However, since tetrazine is unstable in the presence of water, it must be embedded in a hydrophobic, ethylene-permeable plastic film that does not

contain hydroxyl groups [131]. Appropriate films would include silicone polycarbonates, polystyrenes, polyethylenes and polypropylenes. Approximately 0.01-1.0 M dicarboxyoctyl ester of tetrazine incorporated in such a film was able to effect a 10-fold reduction in ethylene in sealed jars within 24 hours and a 100-fold reduction within 48 hours [131]. The tetrazine film has a characteristic pink colour when it is new and turns brown when it becomes saturated with ethylene so it is possible to know when it needs replacing.

A new product called Frisspack has been developed in Hungary for use in storage of fresh fruits and vegetables. The product consists of a chemisorbing of small particle size dispersed among the fibers in the early phase of paper production. The result is a paper sheet with putative ethylene-adsorbing capacity. The nature of the chemisorbing and data supporting the claim of ethylene adsorption are not available. No response was received from the vendor following the author's request for information.

Although there are many packaging products claiming ethylene-removing capabilities, few of the claims are backed up with reliable data. Standardized procedures for demonstrating efficacy would aid the development of this growing industry. In addition, a thorough understanding of the physiological effects of ethylene and its importance in sealed permeable packages should precede any use of these products. In many cases, the elevated carbon dioxide levels common in modified atmosphere packages may obviate the need for ethylene removal. In other cases, with very sensitive commodities such as kiwifruit and carnations, ethylene-adsorbing capability may be crucial in the maintenance of shelf-life and commercial quality.

3. EXPERIMENTAL

3.1. Chemicals Used

3.1.1. Low Density Polyethylene (LDPE)

The matrix polymer used in this study was the low density polyethylene with the commercial name of PETILEN F2-12 which is a product of PETKIM Petrokimya Holding A.S., Izmir, Turkey. Some properties of the used LDPE; PETILEN F2-12 is given in Table 4.1.

Table 4.1 Properties of PETILEN F2-12 LDPE.

PROPERTY	UNIT	VALUE	TEST METHOD
Melt Flow Rate (MFR) (2160 g, 190 °C)	g/10 min	2.0-3.5	ASTM D-1238
Density, 23 °C	g/cm ³	0,918-0,922	ASTM D-1505
Film Quality	-	A	ALKATHENE 36
<i>TYPICAL VALUES</i>			
Ash	% wt	0,14	ALKT-509
Haze	%	6,3	ASTM D-1003
Gloss	-	70	ASTM D-2457

3.1.2. Nanoclay

In this study two different organically modified montmorillonites were used as nanoclay. These organoclays whose trade names are DK4 and I44 were modified by different manufacturers with a quaternary ammonium salts.

Nanolin™ DK4 organoclay (white coloured, purity: 95–98%, and interlayer spacing: $d_{001} = 3.56$ nm), modified with octadecylammonium salt, was produced from Zhejiang Fenghong Clay Chemicals, Co. Ltd, China.

I44 named nanoclay which is based on quaternary ammonium salt was obtained from Nanocor®, Inc.

These two nanoclays are different in terms of their chemistry and modification method.

3.1.3. Maleic Anhydride Grafted Polyethylene (PE-g-MA)

The used compatibilizer is 1% maleic anhydride containing polyethylene grafted maleic anhydride (PE-g-MA) which was supplied from Clariant A.S., Istanbul, Turkey. (MFI=23 g/10 min.).

Chemical structure of the used compatibilizer is given in Figure 4.1.

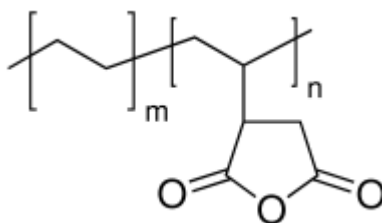


Figure 4.1: The chemical structure of PE-g-MA.

3.1.4. Ethylene Absorber

In this study, two different ethylene absorbers were used. These ethylene absorbers encoded N-10774 and N-10776 which are commercial products were obtained from Aksoy Plastik A.S. N10774 and N10776 are different only in terms of their hydrophilicity.

3.2. Instruments and Characterization Methods for Nanocomposite Materials

3.2.1. Extrusion and Twin Screw Extruder

Polymer melt intercalation is a promising method due to its high productivity, relatively lower cost and compatibility with current polymer processing techniques such as extrusion and injection molding. During extrusion in the processing device, the clay agglomerates are broken up by the external forces and the diffusion of macromolecules into the clay galleries [136].

The extrusion process is not difficult to visualize. A meat grinder is a best model for screw extrusion which is used for plastic processing. The grinder takes a large lump of meat and reduces its size by the screw, mix it all up and then extrude the result through the die. This is a simple example for extrusion process, but in fact there are several process variables that make it harder to optimize [137].

Commonly used continuous screw extruders can be classified in two groups: Single screw and twin screw extruders. The former is the most basic form of extruder that simply melts and forms the material. In contrast, twin screw extruders provide excellent melt mixing and are

widely used for polymer nanocomposite manufacturing with different types shown in Figure 4.4 [137, 138].

In addition to this, twin screw extruders are more flexible due to their modular design of screw and barrel and they have better feeding, melting, mixing and degassing properties compared to single screw extruders [138].

Twin-screw extruders are used extensively in polymer blending and also in many applications such as processing of food, essential oils, paints, and many other highly viscous materials [139, 140]. They provide high shear rate and good mixing of compounding materials at a relatively short residence time. And also temperature profile is considerably broad and can reach even up to 500 °C temperature levels depending on the melting point of polymer.

Twin screw extruders have the superior property that their screw configuration and processing conditions are exchangeable however it is not so easy to control the parameters. The main problem is obtaining the optimum screw configuration and processing conditions in terms of mixing and kneading. When the mixing function of the mixing elements is limited, it can be improved by placing some kneading elements along the screw. These mixing and kneading mechanisms changes various physical properties, such as, flow rate, pressure and shear rate distributions [141]. However, as mentioned before it is hard to measure and control these properties at desired points due to the complicated geometry of screws.

In this study the used extruder was Werner&Pfleider trademarked GmbH. Z SK 25 model (Diameter=25 mm, L/D=48) counter-rotating twin screw extruder. The temperature was adjusted between 190-210 °C depending on channel zone.

Low density polyethylene (LDPE) nanocomposite masterbatches were prepared by using LDPE, nanoclay, compatibilizer with/without ethylene absorber with determined proportions by melt compounding in a counter-rotating twin screw extruder. Nanocomposites pellets were prepared by mixing of 25% the named masterbatch with 75% LDPE.

The temperature zones and screw speeds of extruder were set in suitable conditions. Final nanocomposite compositions were designated as 85% LDPE, 10% compatibilizer, and 5% nanoclay or 82.5% LDPE, 9% compatibilizer, 4.5 % nanoclay, and 4% ethylene absorber. 2 kinds of nanoclay and 2 kinds of ethylene absorber were used in this study to prepare 4 different nanocomposite samples. 2 kinds of ethylene absorber containing 2 composite samples were also prepared by melt mixing.

3.2.2. Cast Film Line

In this study, nanocomposite films were produced by using Scientific trademarked LCR-175 Co-Ex Chill Roll model cast film line with the screw speed of 50 rpm and drawing ratio of 2.5 m/min. Thickness of final film samples were adjusted as 100-110 micron.

Film casting is an important industrial method for film production. In film casting, a polymer melt is extruded through an approximately flat die and stretched in the region between the die and a chill roll. This stretching induces some orientation in the film and causes a decrease in the width (neck-in) and the thickness of the film in the region between the die and the chill roll.

An important process parameter is the draw ratio, which is the ratio of the velocity at the chill roll to the velocity at the die exit [142]. Increasing the draw ratio increases the amount of neck-in between the die and the chill roll and also leads to a decrease in the thickness of the film. The distance between the die and the chill roll (airgap) also affects film formation since changing the air-gap length changes the flow geometry (increasing the neck-in) and the strain rate experienced by the polymer in the web. This results in variations in the width, the temperature profiles and the polymer orientation for any particular set of process conditions.

In addition to the process parameters, the characteristics of the material being processed influence the film properties. Changes in the polymer type, polymer molecular weight, and the shear and the extensional viscosity of the polymer will also affect both the film formation in the gap between the die and the chill roll and the final properties of the film.

Some problems typically encountered experimentally in film casting are edge-bead formation and draw resonance [143]. Edge-bead formation results in the edges of the final film being thicker than the central portions of the film. The film edges are usually trimmed off before further processing of the film and the material is recycled. Draw resonance is an instability whereby there is a periodic variation in the film neck-in. This occurs at high draw ratios and places a limit on the draw ratio for a particular film casting operation. The draw ratio at which this instability sets in depends on the polymer material.

Nanocomposite films were produced by using cast film line with the screw speed of 50 rpm and drawing ratio of 2.5 m/min. Thickness of final film samples were adjusted as 100-110 micron. 4 nanocomposite, 2 composite and 1 standart LDPE films were prepared to be used in experiments.

3.2.3. XRD Analysis

After incorporation of nanosized layered silicates into the polymer matrix, extend of nanofiller dispersion in the nanocomposite structure can be followed by XRD analysis by monitoring the position, shape, and intensity of the basal reflections from the distributed silicate layers [144].

The dispersion of silicate layers in the polymer matrix generally resulted in increased gallery height or d-spacing. The changes in the d-spacing can be investigated quantitatively by using the Bragg's law (Equation 3.1) where λ corresponds to the wavelength of the X-ray source used, θ is the diffraction angle measured and d is the spacing between diffractive lattice planes.

$$\lambda = 2d \sin\theta \quad (3.1)$$

As interlayer spacing between planes increases, the characteristic peak of the clay in the XRD chromatogram shifts to lower angles. Intercalated structures are identified by broader and smaller diffraction peaks in XRD. This is reflected in 2θ values observed in lower angles, since the d_{001} -spacing of silicate layers are also expected to increase. In the case of intercalation with flocculation; the new arrangement of silicate layers may lead to appearance of new basal reflections at lower angles.

As extend of intercalation increases and exfoliation of silicate layers occurs within the polymer matrix, it can be expected that all reflections disappear and the obtained XRD analysis (crystallography) of the nanocomposites is observed just like a noise. Disappearance of peaks was attributed to large gallery height; beyond the maximum d-spacing value can be determined by XRD [144]. Also exfoliation results in disordered dispersion of layered silicate stacks in several directions and lose their ordered structure that enables them to be detected [145].

In this study, the XRD measurements were conducted by using ARL trademarked 9400 Model XRD used and scattering region was 2.0000-19.9800 deg.

3.2.4. FTIR Analysis

Fourier transform infrared (FTIR) spectroscopy is a measurement technique that allows one to record infrared spectra of many chemicals.

FTIR measurements of film samples were conducted on a Spectrum 100 FTIR spectrometer to characterize the structures of polyethylene and polyethylene nanocomposites. Results gives an idea about the components of sample measured [146].

3.2.5. Thermal Analysis with DSC

Differential scanning calorimetry (DSC) is a thermo-analytical technique in which the difference in the amount of heat required to increase the temperature of a sample and reference are measured as a function of temperature [147].

When the sample undergoes a physical transformation such as phase transitions, more (or less) heat will be transferred to it, than the reference to maintain both at the same temperature. During the experiment, the instrument detects differences in the heat flow between the sample and reference and this information is sent to an output device, mostly a computer. The basic principle underlying this technique is that, this information is expressed in a plot of the differential heat flow between the reference and sample cell as a function of temperature [148].

In this study, Perkin Elmer 4000 DSC instrument was used for DSC analysis. The samples were heated at 5 °C/min. and were cooled at 5 °C/min in the range of 20-180 °C under nitrogen gas.

3.2.6. Thermal Gravimetric Analysis (TGA)

Thermogravimetric analysis or thermal gravimetric analysis (TGA) is a type of testing performed on samples that determines changes in weight in relation to change in temperature.

TGA is commonly employed in research and testing to determine characteristics of polymers, to determine degradation temperatures, absorbed moisture content of materials, the level of inorganic and organic components in materials, decomposition points of explosives, and solvent residues. It is also often used to estimate the corrosion kinetics in high temperature oxidation.

In this study, the used TGA instrument was Perkin Elmer TGA 4000. Samples were heated starting from the ambient temperature to 950 °C in the presence of nitrogen gas.

3.2.7. Melt Viscosity Measurement with MFI

The melt flow rate is a measure of the ability of the material's melt to flow under pressure and it is inversely proportional to the viscosity of the melt at the conditions of the test. The schematic drawing of MFI is given in Figure 4.2.

To investigate the effect of clay structure on polyethylene nanocomposites and the interaction between clay and bulk PE, the 'control' polymer matrix effect should be excluded. Therefore, in this study, a normalized MFI (n-MFI) was calculated as shown below and was then compared to n-MFI of polyethylene nanocomposites.

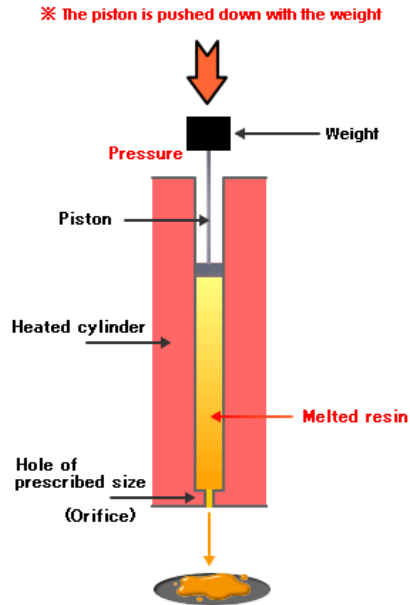


Figure 4.2: Schematic drawing of a melt flow indexer [149].

$$\text{Normalized MFI} = \frac{\text{MFI of composite}}{\text{MFI of corresponding control}} \quad (3.2)$$

The test temperature was set to 190°C and a dead weight load of 2.16 kg was applied as usual for polyethylenes [150]. For each composite sample, the final results were the averages of three sets of measurements.

In this study, HAAKE Melt Flow MT is used to measure MFI and n-MFI values of sample.

3.2.8. Polarized Microscopy Method (POM)

To obtain dispersion of nanoclay and ethylene absorber additives in the low density polyethylene polymer matrix, Leica DM LM.(Germany) trademarked 020-520-714 DM model polarized microscopy was used. The images were obtained at x50 zoom.

3.2.9. Mechanical Analysis

The measurement of mechanical properties is concerned with load-deformation or stress-strain relationships. The results of these tests are important to classify the polymeric material. In this study, for evaluation of mechanical properties, tensile test method was used.

Tensile test is a measure of the withstanding ability of material to the force of pulling and shows the stretching amount of material until breaking. The tensile profile of the sample is expressed in terms of a curve showing the reaction of the material against applied pulling force. Figure 4.3 shows a typical tensile test curve.

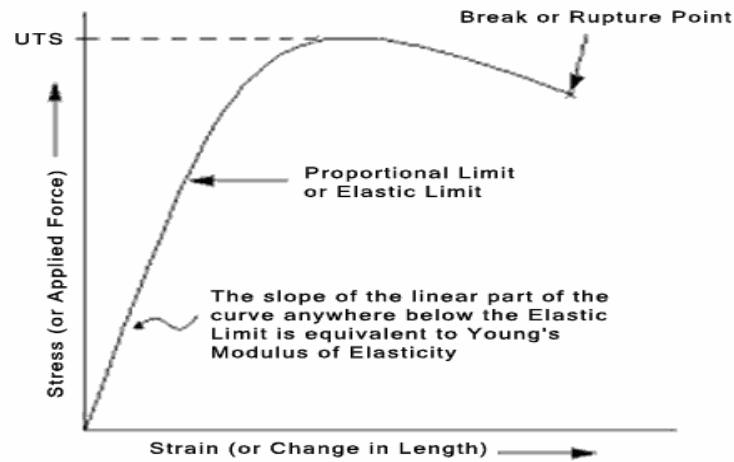


Figure 4.3: Typical tensile test curve [151].

For most tensile testing of materials, in the initial portion of the test, the relation between applied force, or load, and the elongation of the specimen is linear. The constant slope of this linear region is called as “Young's modulus” or “tensile modulus”.

$$\text{Tensile modulus (E)} = \frac{\Delta \text{ Stress } (\sigma)}{\Delta \text{ Strain } (\epsilon)} \quad (3.3)$$

where stress is the force applied per unit area.

$$\text{Stress}(\sigma) = F/A_0 \quad (3.4)$$

and strain is defined as the amount of deformation that the sample shows under stress. It is expressed as the ratio of the elongation to the original gage length.

$$\text{Strain } (\epsilon) = \Delta L / L_0 \quad (3.5)$$

Tensile strength is the force divided by the cross-sectional area of the specimen and expressed in terms of MPa.

$$\text{Tensile strength} = \frac{\text{Force (F)}}{\text{Cross sectional area (A}^0\text{)}} \quad (3.6)$$

In this study, to obtain mechanical properties of polymer nanocomposites, mechanical tests were made by using Zwick/Roell Z0.5 TH universal testing machine. Pre-load was 1 MPa, grip to grip separation at the start position was 100 mm and test speed was 50 mm/min.

3.2.10. Colour Measurements of Nanocomposite Films

In the Hunter system, color is represented as a position in a three-dimensional sphere, where the vertical axis “L” indicates the lightness (ranging from black to white), and the horizontal axes, indicated by a and b, are the chromatic coordinates (ranging from “a”: greenness to redness and “b”: blueness to yellowness). Hunter L, a, and b values were averaged from five

readings across for each coating replicate. The total color difference (ΔE) can be calculated by the following equation;

$$\Delta E = \sqrt{(\Delta L)^2 + (\Delta a)^2 + (\Delta b)^2} \quad (3.7)$$

In this study, for each film, at least five measurements on different positions of film surface were made. The results were expressed as ΔE values, with the substrate standard LDPE film as reference.

3.2.11. Oxygen and Carbon Dioxide Gas Permeability Analysis

Permeability is the steady-state rate of transport of a permeant molecule through a polymer of unit area per unit thickness as a result of combined effects of diffusion and solubility.

Characterizing the relations between permeability of solute and polymer structure is crucial in terms of designing barrier films in food packaging.

The principle of this measuring method which is called as equal pressure is on one side testing gas (oxygen or carbondioxide) flows and on the other side dry case (nitrogen) flows. Pressure of the two sides is equal but oxygen partial pressure is different. Oxygen transmits through the film and carried to the sensor by nitrogen. Sensor measures the oxygen permeance in nitrogen carrier gas and provides the oxygen and carbon dioxide transmission rate. Unit of this method is cc/m².24h.

In this study, Extrasolution Multiperm oxygen-carbondioxide permeability instrument was used to determine oxygen and carbon dioxide permeability of polyethylene and polyethylene nanocomposite film samples used for food packaging.

The measurement temperature was 25 °C, relative humidity was 90%, surface area 50 cm².

3.3. Instrument and Characterization Method for Food Application

In order to evaluate the quality of products, there are some criterias depening on product type. With this purpose, we chose some available testing methods and presented below.

3.3.1. Storage Conditions

A known weight of strawberry (around 120 g corresponding to four pieces), parsley (around 20 g) and iceberg lettuce (around 35g) which were bought from a supermarket as fresh were packaged in 10 cm×15 cm ($S = 0,03 \text{ m}^2$) flexible pouches and stored at 0 °C (which is optimum storage temperature for these used foodstuffs) typical retail conditions for nearly 15 days. Six type of polyethylene nanocomposite packaging film and standart polyethylene packaging film (as control sample) were used to store foodstuffs. In order to use in

intermediate steps, 4-6 parallel samples (depending on durability of used foodstuffs) were initiated and for every step one of each samples were used for analysis.

3.3.2. Oxygen, Carbon Dioxide, Ethylene Changes In Package Versus Time

Oxygen, carbon dioxide and ethylene gas concentrations in packages are crucial regarding the shelf life determination.

The concentration of oxygen and carbon dioxide inside the packages were monitored using an OxyBaby (WITT-GASETECHNICK type) (Figure 4.4). Analyses were performed by inserting the test probe through a rubber seal (Toray Engineering Co. Ltd., Osaka, Japan) attached to the outside of the packaging. The instrument was calibrated towards air. Measurements were performed everyday.

The concentration of ethylene gas in package was monitored by using ICA 56 instrument (Figure 4.5). This analyser is a simple hand held instrument with a built in pump that provides a direct reading of the ethylene concentration within a produce storage or ripening area.



Figure 4.4: OxyBABY oxygen and carbon dioxide analyser instrument.



Figure 4.5: ICA56 Smart Fresh ethylene analyser instrument.

3.3.3. Weight Lose Analysis

Weight lose in fruits and vegetables arises from water lose. Water loses starting after harvest occurs properly according to futures of produces and environmental conditions. Product loses water afterwards creases because of decrease in turgor pressure. All samples were weighted before packaged and saved. During two weeks, once in two days weight lose values were

saved as percentages. Weight loss percentages of foodstuffs packed in films with different compositions were monitored. The results were given as weight loss percentage. The percentage weight loss was determined according to the following expression:

$$\%WL(t) = \frac{W_o - W(t)}{W_o} \cdot 100 \quad (3.8)$$

where %WL(t) is the percentage weight loss at time t, W_o is the initial sample weight and $W(t)$ is the sample weight at time t. At each sampling time, three replicates were made. The weights of foodstuffs were measured by Sartorius isoCAL 211S model weighter.

3.3.4. pH Analysis

The pH values of the strawberry, parsley and bean homogenates were analysed by a Thermo Orion trademarked 3-Star model pH meter (Figure 4.6) in duplicate measurements on every two days. Results were given as graph of pH changes versus time.



Figure 4.6: Orion 3-star pH meter instrument.

3.3.5. Taste and General Quality Evaluation

A quantitative descriptive analysis was used to evaluate the sensory properties of each samples. The analyses were carried out on every two days for each type of product and were performed by a panel consisting of 4 people. The panel members were trained to evaluate smell, flavour, taste, texture attributes and appearance as well as overall quality of the foodstuffs. A number of sensory attributes were developed and described in numbers by comparing foodstuffs that had large differences in sensory quality. In the training, a reference sample of fresh strawberries was used.

A four point scoring scale was employed:

4: very good / 3: good / 2: acceptable / 1: unacceptable.

Scores below two for any of attributes assessed were considered as an indicator of the end of the acceptable quality. The results were given as graph of general quality changes versus time.

3.3.6. Sugar Amount Analysis

The samples opened were homogenised by a mixer for 15 seconds separately each other. The homogenate was used for analysing sugar. The Brix value of the homogenate was measured by a refractometer (Brix Co. Ltd., Tokyo, Japan) (Figure 4.7). Five measurements were made on each sample on every two days and sugar amount changes versus time were given as graph.



Figure 4.7: Brix refractometer.

4. RESULTS AND DISCUSSION

Six different low density polyethylene (LDPE) nanocomposite masterbatches were prepared by using LDPE, nanoclay, compatibilizer with/without ethylene absorber. Two of them contain only nanoclay, 2 of them contain only ethylene absorber and the other contain both of nanoclay and ethylene absorber. LDPE film was used as standart for comparison. These nanocomposite formulations used for strawberry, parsley and iceberg lettuce packaging and their shelflife analysis.

In this study, low density polyethylene nanocomposites which contain nanoclay, compatibilizer were produced with different compositions in counter rotating twin screw extruder. Ethylene absorber was added to some compositions. Using these nanocomposites, polyethylene nanocomposite films were prepared and these films were used as packaging materials. Pre-works were done in order to determine the optimum extrusion conditions and best compositions. In this study, in order to see the effects of ethylene absorber and nanoclay on film properties and food packaging, the obtained best results were given and discussed here.

In this study two kind of nanoclay and ethylene absorber were used. Compatibilizer (PE-g-MA) was added the compositions including nanoclay. Firstly, a masterbatches including clay were formed by mixing 20% F2-12 LDPE with 60% PE-g-MA and 20% nanoclay in the Werner&Pfleider GmbH. Trademarked Z SK 25 model (Diameter=25 mm, L/D=48) counter-rotating twin screw extruder. The other masterbatches including ethylene absorber were formed by mixing 50% wt LDPE with 50% wt active ingredient of ethylene absorber additive in the twin screw extruder. LDPE nanocomposite masterbatches were prepared by using LDPE, nanoclay, compatibilizer with/without ethylene absorber with determined proportions by melt compounding in a counter-rotating twin screw extruder. Nanocomposites pellets were prepared by mixing of 25% the named masterbatch with 75% LDPE. The final compositions of these films were defined as 85% LDPE, 10% compatibilizer, and 5% nanoclay or 82.5% LDPE, 9% compatibilizer, 4.5 % nanoclay, and 4% ethylene absorber. 2 kinds of nanoclay

and 2 kinds of ethylene absorber were used in this study. 100% LDPE film and 4% both of ethylene absorber types containing films.

Sample number and their compositions were listed below in Table 4.2.

Table 4.2: Sample number and their compositions.

SAMPLE NO	FINAL FORMULA
1	LDPE
2	85% LDPE + 10% PE-g-MA + 5% I44
3	85% LDPE + 10% PE-g-MA + 5% DK4
4	92% LDPE + 8% N10774
5	92% LDPE + 8% N10776
6	82.5% LDPE + 9% PE-g-MA + 4.5 % I44 + 4% N10774
7	82.5% LDPE + 9% PE-g-MA + 4.5 % DK4 + 4% N10774

The results of these tests were given as 2 basic parts: characterization of film samples and food application.

4.1. Characterization Results

In order to evaluate the characteristic properties of film samples, some characterization methods were used and results were discussed.

4.1.1. XRD Analysis Results

The results of the XRD measurements of some samples are given in Appendices as Figure A.1, A.2, A.3, A.4, A.5 and A.6.

In 5% DK4 nanoclay containing low density polyethylene nanocomposite sample (No:3) (Table A.4.), it can be clearly seen that, addition of 5% organoclay (with 15% compatibilizer) is really effective to increase the interlayer spacing. Also with addition of organoclay to matrix, some peaks of DK4 nanoclay shifts to left while some peaks are lost. It can be judged that the organoclay has an exfoliated/intercalated morphological structure in low density polyethylene matrix.

Active ingredient of ethylene absorber shows four peaks (Figure A.3) which are $2\theta = 7,4; 10,4; 12,6; 16,7$. These peaks can be seen in XRD graphs of 4.5% I44 nanoclay + 4% N10774 ethylene absorber containing LDPE (No:6) and 4.5% DK4 nanoclay + 4% N10774 ethylene absorber containing LDPE (No:7).

4.1.2. FTIR Test Results

FTIR spectrums of all film samples were obtained and given in Appendices part as A.7, A.8, A.9, A.10, A.11, A.12, A.13. The peaks of six nanocomposites samples were compared with peaks of low density polyethylene film without additive.

1075,83 cm^{-1} and 1044,98 cm^{-1} peaks which belongs to 5% I44 nanoclay LDPE (No:2) and 1091 cm^{-1} and 1032 cm^{-1} peaks which belongs to 5% DK4 nanoclay LDPE (No:3) are identified as absorption of the silicate groups. The peaks between 847-918 cm^{-1} are identified as $\text{AlMg}(\text{Fe}_2\text{Al}_3)\text{OH}$ peak and these peaks are present in both of two spectrums. And also between 600-400 cm^{-1} Si-O-Si and Si-O-Al bending peaks are observed in both spectrums. These nanoclays having familiar structures resemble each other in terms of FTIR graphs.

As I mention before, 4% N10774 (No:4) and 4% N10776 (No:5) ethylene absorbers have same structure but different pore diameter. So, FTIR spectrums are almost same. Around 950-1150 cm^{-1} , vibration bands of Si-O bonds are observed and No:4 and No:5 have a this kind of group in their structures. And also between 600-400 cm^{-1} Si-O-Si and Si-O-Al bending peaks are observed in both spectrums.

In spectrums of nanocomposites including nanoclay and ethylene absorber (No:6 and No:7), peaks belonging to both of organoclay and ethylene absorber can be clearly seen.

4.1.3. DSC Test Results

Differential Scanning Calorimeter analysis results of samples were given in Table 4.3 and DSC graphs are added to Appendices as A.14, A.15, A.16, A.17, A.18, A.19, A.20.

Since glass transition temperature (T_g) of LDPE is around -120 $^{\circ}\text{C}$, we did not obtain T_g changes in nanocomposite samples.

where T_m is melting temperature, T_{mp} is the peak point of melting temperature, ΔH_m is enthalpy of melting, T_c is crystallization temperature, T_{cp} is the peak point of crystallization temperature, ΔH_c is enthalpy of crystallization and X% is crystallinity percentage.

It is shown in Table 4.2 that both of ethylene absorbers do not have an effective role on the melting point and crystallization point.

However, it was observed that melting point (T_m) increased a little with the clay addition when compared to pristine LDPE materials while ΔH_m decreased. This can be explained in two ways. One of the suggestions is that the prevention of motions of polymer chains by the presence of nanoclay layers causes the increasement in melting point and decrease in crystallization content and also in ΔH_m . The other suggestion is the nucleating behaviour of nanoclay layers. Nanoclay layers are dispersed in the polymer matrix as small crystal parts and this increases the melting point and decreases the crystallization content and ΔH_m .

Table 4.3: DSC test results of samples.

SAMPLE NO	HEATING			COOLING			X%
	T_m ($^{\circ}\text{C}$)	T_{mp} ($^{\circ}\text{C}$)	ΔH_m (J/g)	T_c ($^{\circ}\text{C}$)	T_{cp} ($^{\circ}\text{C}$)	ΔH_c (J/g)	
1	98.6	110.3	82.8	101.6	98.2	72.1	28.0
2	103.9	122.6	72.1	111.1	108.6	64.5	25.8
3	101.9	113.8	68.9	105.0	101.1	66.2	24.7
4	98.5	109.7	71.8	101.6	98.7	66.3	25.5
5	100.3	110.3	69.2	101.6	98.3	69.1	24.5
6	104.2	122.0	64.1	111.5	109.1	63.9	23.8
7	100.7	113.2	62.2	105.1	101.8	61.2	23.2

4.1.4. TGA Test Results

Thermal gravimetric analysis results of samples and pure additives were given in Table 4.4 and TGA graphs are added to Appendices part as A.21, A.22, A.23, A.24, A.25, A.26, A.27, A.28, A.29, A.30.

Three degradation temperatures exist for each nanocomposite sample which are beginning point of degradation ($(T_{deg})_{start}$), finishing point of degradation ($(T_{deg})_{finish}$) and midpoint of degradation ($(T_{deg})_{mid}$).

Degradation temperature is decreased by addition of inorganic additives. Since inorganic materials increase in polyethylene matrix, residue amount increases proportionally with percentage of additives.

4.1.5. MFI Results

The influences to the processability of nanoclays to the polymer nanocomposites were observed by melt index measurements. MFI and n-MFI values of PPNC samples were given in Table 4.5.

MFI is a pressure-imposed, capillary flow experiment and was used to study the relationship between low strain rate shear flow properties and clay structure in nanocomposites and the interaction between clay and matrix of LDPE nanocomposite samples.

In the interaction between clay and bulk LDPE, the “control” polymer matrix effect should be excluded to investigate the effect of clay on LDPE nanocomposite samples. For this purpose,

normalized MFI (n-MFI) values were calculated and then the results were compared. The corresponding control units contained matrix LDPE and the compatibilizer.

Control unit for first 5 samples were prepared in the extruder, with 10% w/w compatibilizer without containing any organoclay. The other control unit for sample 6 and 7 include ethylene absorber besides of compatibilizer and matrix LDPE.

As it can be understood from the MFI and n-MFI values of samples. The addition of DK4 nanoclay increased the processability, while I44 nanoclay decreased. This results were confirmed on the Samples No.2; 3 and 6; 7.

Table 4.4: TGA Analysis results of film samples.

Sample No	(T _{deg}) _{start}	(T _{deg}) _{finish}	(T _{deg}) _{mid}
1	390.1	508.9	489.1
2	264.4	583.2	493.1
3	221.8	577.2	494.1
4	160.4	529.7	488.1
5	132.7	602.0	474.3
6	155.4	657.4	501.0
7	136.6	654.5	496.0
I44 nanoclay	170.4	407.0	891.3
DK4 nanoclay	131.3	332.3	879.8
Active ingredient of N10774	30.3	833.3	158.6

Table 4.5: MFI and n-MFI Results of LDPE samples.

Sample No	MFI (g/10 min.)	n-MFI
1	2.1	-
2	3.3	0.8
3	8.3	1.9
4	2.2	-
5	2.1	-
6	2.6	0.5
7	7.0	1.3

4.1.6. POM Analysis Results

To see the effects of addition of additives on dispersion in LDPE matrix, polarized microscopy images were investigated. The images of most important 5 sample were given in Appendices as A.31, A.32, A.33, A.34, A.35.

5% I44 and DK4 nanoclay have good dispersion in LDPE matrix. Since ethylene absorber has bigger particle size, it is clearly seen from the Figure 23, 24 and 25 as intense images. These three images are darker comparing to the other images of samples with nanoclay.

4.1.7. Mechanical Analysis

Tensile test was applied to LDPE nanocomposite samples by using Zwick universal testing machine and results were given in Table 4.6. Stress at break, strain at break and 3% secant modulus of samples were obtained as average value of 3 parallel samples. Samples had 2 cm diameter and 15 cm length. Tensile test were performed on film samples on the main direction (orientation way) and cross direction.

It is clear that, strength of samples on main direction is higher comparing to cross direction due to molecular orientation. %5 I44 LDPE and 5% I44 + 4% N10774 samples have the best strength values. Even at 700% strain value, there was no break, so the strength values of these samples were not be able to obtained.

Addition of 5% DK4 nanoclay to polymer matrix, strength of nanocomposite film sample decreases almost by 50% but increases elongation by 55%. Since ethylene absorber has nearly no effect on strength and 3% secant modulus, the same situation for DK4 was obtained in 5% DK4 + 4% N10774 sample.

4.1.8. Colour Measurement of Nanocomposite Films

This colour model was selected based on its documented adequacy for theoretically quantifying colour changes in film samples and for its matching of sensitivity of human eyes L^* is the luminance or lightness and ranges from 0 to 100, a^* (from green to red) and b^* (from blue to yellow) are the two chromatic components and range from -120 to +120. As values of L^* , a^* and b^* were preferred in this work to describe colour changes, since they represent a kind of standardisation. Here the values (DL, Da, Db) were given as compared with standart value of LDPE film, and this equation was used : $\Delta X^* = X_t^* - X_o^*$.

Also opacity and transparency changes were listed to compare with standart LDPE film sample in Table 4.7.

Table 4.6: Mechanical analysis test results.

SAMPLE NO	MAIN DIRECTION			CROSS DIRECTION		
	Strength at break (MPa)	Strain at break (MPa)	3% Secant Modulus	Strengt h at break (MPa)	Strain at break (MPa)	3% Secant Modulus
1	20.9	165	187.3	10.2	190	186.7
2	22	1010	306.7	20	1006.7	292
3	14	403.3	300.3	10.9	42.5	244.3
4	21.9	170	191.3	9.1	156.7	202.3
5	19.5	186.7	185.2	12	420	195.2
6	21	825	303	18.6	865	359.3
7	14.1	273.3	271.4	8.3	29	288.3

Table 4.7: Colour, opacity and transparency measurements of LDPE film samples.

Sample No	DL*	Da*	Db*	Opacity/Transparency
1	-0.28	-0.03	-0.03	18.84/80.38
2	-4.47	+0.38	7.72	19.64/76.08
3	-2.18	-0.38	+3.88	19.11/78.48
4	-0.25	-0.22	-0.11	18.29/80.85
5	-1.00	-0.85	+4,27	18.85/79.80
6	-5.35	+0.66	+10.30	23.34/71.80
7	-2.47	-0.38	+5.35	23.04/75.10

Addition of 4% N10774 to LDPE matrix has almost no effect in terms of lightness but 4% N10776 decrease the lightness. 5% I44 nanoclay addition decrease the lightness of standart film sample, increase the redness a bit and yellowness so much. So, opacity of film sample is increased while transparency is decreased. This effect can be clearly seen in Sample no 6.

5% DK4 nanoclay addition decrease the lightness, increase greenness and blueness. So, opacity of film sample is increased, transparency is decreased.

As a result of these evaluations, addition of additive such as nanoclay, ethylene absorber, generally transparency of film samples is decreased and opacity is increased. By colour of additive, the film samples gets a colour.

4.1.9. Oxygen and Carbon Dioxide Gas Permeability Test Results

Oxygen and carbon dioxide gas permeability tests were applied to LDPE and LDPE nanocomposite samples and results were given in Table 4.8.

Table 4.8: Oxygen and Carbondioxide permeability test results.

Film Sample (100-110 μ)	Oxygen permeability (cc/m ² .24h)	Carbon dioxide permeability (cc/m ² .24h)
1	1995.5	6159.7
2	1333.0	4136.6
3	1374.7	4234.8
4	1451.1	6490.5
5	2001.5	6212.7
6	1268.5	4048.6
7	1261.5	4753.6

As it can be seen from the table, oxygen and carbon dioxide gas permeability were decreased by 35% through addition of 5% I44 nanoclay. Ethylene absorber effect is too low. But addition of both of ethylene absorber and nanoclay lowered the permeability amount greatly.

4.2. Analysis Results For Food Packaging

The prepared nanocomposite films were used to pack starwberry and parsley. The analysis performed on these foodstuffs will be given seperately each other.

4.2.1. Analysis Results of Strawberry

A known weight of strawberries (around 120 g corresponding to four pieces) were packed in 7 different pouches and stored at 0°C. 4 parallel study was initiated because of short shelf life of strawberry. For evaluation of changes occurring in strawberry samples, some criterias were determined and tests were performed.

4.2.1.1. Gas composition changes

Two series of samples were used to monitore gas changes. The results were given as avarage of these two series. The graphs of C₂H₄, O₂ and CO₂ gas changes of samples versus time were given in Appendice as Figure A.36, A.37, A.38, A.39, A.40, A.41, A.42.

According to these graphs, it is clear that LDPE packages without additive have high ethylene concentration and high amount of oxygen gas (at the same time CO₂ gas amount is increasing so fast in package) amount allow to fast spoilage. Respiration rate of strawberry in LDPE package is so fast therefore spoilage is accelerated.

By addition of nanoclay to polymer matrix, oxygen permeability is decreased, so respiration rates of strawberries are lowered.

By addition of ethylene absorber, ethylene concentration is lowered by 50% comparing to LDPE control package, acceleration effect of ethylene gas was eliminated. Among two kind of ethylene absorber additives which are N10774 and N10776, N10774 one was more effective and had more ethylene absorption capacity regarding previous pre-studies. Therefore, it was preffered to use N10774 encoded ethylene absorber in packages including nanoclay and ethylene absorber.

In the packages including both barrier additive and ethylene absorber additive, it was managed to decrease oxygen and ethylene amount in headspace of packages.

It was determined that, the nanocomposite materials are much better than LDPE packages in terms of gas changes results.

But, more effective packages were sample 6 and 7 which have nanoclay and ethylene absorber to increase shelf-life since oxygen and ethylene amount is decreased to desired value.

4.2.1.2. Weight lose analysis

This parameter was crucial, due to every loss in weight being translated into an economical loss. Weight lose is important parameter to monitor spoilage rate. Because during respiration, strawberries lose water so much. In this study, at the end of the 10 days storage of strawberries, weight lose difference becomes more obvious. The weight lose graphs were

given in Appendice as Figure A.43. Ten days later, weight lose in LDPE packages reached to 6,41% while in the other packages around 1-2%. Especially in the sample no 6 and 7 (which have both barrier and ethylene absorber additive), the weight lose was around 0,40-0,10%. This was an expected result because of lowered respiration rate and controlled gas configuration.

4.2.1.3. pH changes

During storage of strawberries, organic nutrition materials within the foodstuff are broken down to come up carboxyl acid materials. But acidity of these groups are not so high. So during 10 days storage, acidity does not change exceedingly. Acidity changes of strawberries during 10 days storage versus time was given in Appendice as Figure A.44.

4.2.1.4. Sugar amount analysis

As it is known, because of the broken of starch within strawberry, increase in sugar amount is an expected result. But sugar amount can not be understood previously, it is related to maturity of product. Therefore sugar amount changes were floating. Brix changes of strawberries during 10 days storage versus time was given in Appendices part as Figure A.45.

4.2.1.5. Taste and general quality evaluation results of strawberry

The graph of general quality changes of strawberries during 10 days storage versus time was given in Appendice as Figure A.46. According to results; after 5 days, strawberries stored in LDPE decreased down to acceptable limit while the other all packages are fresh and eatable. But at 8th day, strawberries stored in the sample no 2, 3, 4 and 5 packages becomes spoiled while strawberries stored the sample no 6 and 7 was still above acceptable limit. At the end of 10 days, according to trainers estimation, the strawberries stored the sample no 6 and 7 was still eatable.

4.2.1.6. Shelf life analysis results of strawberry

Every two days also photographs of 2 standard series were taken and all period were observed on these series. In this way, the conducted study was proved with photographs. The pictures of starwberries stored in sample no 1, 2, 3, 4, 5, 6 and 7 at 3th, 5th, 8th, 10th were given in Appendices part as Figure A.47, A.48, A.49, A.50, A.51, A.52 and A.53. By using nanocomposites packages, controlling the headspace gas concentration it can be achieved to increase shelflife of foodstuffs. All these tests conducted periodically confirm the pictures and shelflife analysis.

4.2.2. Analysis Results of Parsley

A known weight of parsley (around 20 g) were packed in 7 different pouches and stored at 0°C. 6 parallel study was initiated because of longer shleflife comparing to strawberry. For evaluation of changes occuring in parsley samples, some criterias were determined and tests were performed.

4.2.2.1 Gas composition changes

Two series of samples were used to monitore gas changes. The results were given as avarage of these two series. The graphs of C₂H₄, O₂ and CO₂ gas changes of samples versus time were given in Appendices part as Figure A.54, A.55, A.56, A.57, A.58, A.59, A.60.

According to these graphs, it is clear that LDPE packages without additive have high ethylene concentration and high amount of oxygen gas (at the same time CO₂ gas amount is increasing so fast in package) amount allow to fast spoilage. Respiration rate of parsley in LDPE package is so fast therefore spoilage is accelerated. But comparing to parsley, respiration rate of parsley is lower and shelflife is longer.

By addition of nanoclay to polymer matrix, oxygen permeability is decreased, so respiration rates of parsleys are lowered.

By addition of ethylene absorber, ethylene concentration is lowered by 50% comparing to LDPE control package, acceleration effect of ethylene gas was eliminated. Therefore, it was preffered to use N10774 encoded ethylene absorber in packages including nanoclay and ethylene absorber.

In the packages including both barrier additive and ethylene absorber additive, it was managed to decrease oxygen and ethylene amount in headspace of packages.

It was determined that, the nanocomposite materials are much better than LDPE packages in terms of gas changes results.

But, more effective packages were sample 6 and 7 which have nanoclay and ethylene absorber to increase shelf-life since oxygen and ethylene amount is decreased to desired value.

4.2.2.2. Weight lose analysis

At the end of the 17 days storage of parsleys, weight lose difference becomes more obvious. The weight lose graphs were given in Appendices part as Figure A.61. 17 days later, weight lose in LDPE packages reached to 10,328% while in the other packages around 4-6%. Especially in the sample no 6 and 7 (which have both barrier and ethylene absorber additive),

the weight loss was around 2,3-2,5%. This was an expected result because of lowered respiration rate and controlled gas configuration.

4.2.2.3. pH changes results

During storage of parsleys, organic nutrition materials within the foodstuff are broken down to come up carboxyl acid materials. But acidity of these groups are not so high. So during 17 days storage, acidity does not change exceedingly. Acidity changes of parsleys during 17 days storage versus time was given in Appendices part as Figure A.62.

4.2.2.4. Taste and general quality evaluation results

The graph of general quality changes of parsleys during 17 days storage versus time was given in Appendices part as Figure A.63. According to results; after 12 days, parsleys stored in LDPE started to turn yellow while the other all packages are fresh, green and eatable. But at 15th day, parsleys stored in the sample no 2, 3, 4 and 5 packages turns yellow while parsleys stored the sample no 6 and 7 was still above acceptable limit. At the end of 17 days, according to trainers estimations, the parsleys stored the sample no 6 and 7 was still green and eatable.

4.2.2.5. Shelf life analysis

Every two days also photographs of 2 standard series were taken and all period were observed on these series. In this way, the conducted study was proved with photographs. The pictures of parsleys stored in sample no 1, 2, 3, 4, 5, 6 and 7 at 5th, 12th, 15th, 17th were given in Appendices part as Figure A.64, A.65, A.66, A.67, A.68, A.69 and A.70. By using nanocomposites packages, controlling the headspace gas concentration it can be achieved to increase shelflife of foodstuffs. All these tests conducted periodically confirm the pictures and shelflife analysis.

4.2.3. Analysis Results of Iceberg Lettuce

A known weight of iceberg lettuce (around 35 g) were packed in 7 different pouches and stored at 0°C. 6 parallel study was initiated because of longer shelflife comparing to strawberry. For evaluation of changes occurring in iceberg lettuce samples, some criterias were determined and tests were performed.

4.2.3.1. Gas composition changes

Two series of samples were used to monitor gas changes. The results were given as average of these two series. The graphs of C₂H₄, O₂ and CO₂ gas changes of samples versus time were given in Appendices as Figure A.71, A.72, A.73, A.74, A.75, A.76, A.77.

According to these graphs, it is clear that in the LDPE packages containing ethylene absorber, ethylene amount did not increase since absorption mechanism of ethylene gas works perfectly.

Because of so low respiration rate of iceberg lettuces, oxygen and carbon dioxide gas concentration changes did not give an idea. Only because of their visual difference, it was approved to be used in this work.

4.2.3.2. Weight loss analysis

At the end of the 22 days storage of iceberg lettuces, weight loss difference becomes more obvious. The weight loss graphs were given in Appendices as Figure A.78. 22 days later, weight loss in LDPE packages reached to 15.45% while in the other packages around 8-9%. Especially in the sample no 6 and 7 (which have both barrier and ethylene absorber additive), the weight loss was around 6%. This was an expected result because of lowered respiration rate and controlled gas configuration.

4.2.3.3. pH changes results

During storage of iceberg lettuces, organic nutrition materials within the foodstuff are broken down to come up carboxyl acid materials. But acidity of these groups are not so high. So during 22 days storage, acidity does not change exceedingly. Acidity changes of iceberg lettuces during 22 days storage versus time was given in Appendices as Figure A.79.

4.2.3.4. Taste and general quality evaluation results

The graph of general quality changes of iceberg lettuces during 22 days storage versus time was given in Appendices as Figure A.80. According to results; after 15 days, iceberg lettuces stored in LDPE started to get wet much more than the other packages. This caused to accelerate the spoilage of iceberg lettuces. Iceberg lettuces packed in the LDPE film got softer after 18 days and quality dropped dramatically while iceberg lettuces packed in the other packages were eatable and buyable.

4.2.3.5. Shelf life analysis

Every two days also photographs of 2 standard series were taken and all period were observed on these series. In this way, the conducted study was proved with photographs. The pictures of iceberg lettuces stored in sample no 1, 2, 3, 4, 5, 6 and 7 at 7th, 9th, 18th, 22th were given in Appendices as Figure A.81, A.82, A.83, A.84, A.85 A.86 and A.87. By using nanocomposites packages, controlling the headspace gas concentration it can be achieved to increase shelflife of foodstuffs. All these tests conducted periodically confirm the pictures and shelflife analysis.

5. CONCLUSION

The destructive effect of the high oxygen and ethylene concentration in package should be eliminated and it was fulfilled by packaging material instead of using modified atmosphere technology.

Firstly, the LDPE nanocomposite films having 100 micron thickness were prepared by using oxygen barrier and ethylene absorber additives. Two kind of organically modified nanoclays were used as oxygen barrier additive. N10774 and N10776 encoded additives obtained from Aksoy Plastic A.S. were used ethylene absorbers. 6 kind of LDPE nanocomposite films were prepared with different proportions. LDPE nanocomposite masterbatches were prepared by using counter-rotating twin screw extruder. Then, by using cast film line, film samples to be used in food packaging were prepared.

The prepared 6 LDPE nanocomposite and 1 LDPE films were investigated structurally by XRD, POM and FTIR; mechanically by universal testing machine; thermally by DSC and TGA; process ability by MFI measurements points of view.

According to XRD results, in nanocomposite materials which include nanoclay, exfoliated/intercalated mixture of morphology was obtained. This result is enough to obtain barrier property.

FTIR results give the characteristic peaks belonging to nanoclay and ethylene absorber separately.

By using DSC analysis, T_m and T_c points were determined of samples. It was obtained that addition of nanoclay and ethylene absorber to LDPE matrix increase T_m and T_c while ΔH_m and ΔH_c decrease.

Degradation temperatures were obtained from TGA graphs and addition of additives decrease the degradation temperature and all of nanocomposite samples start to decompose at earlier temperatures.

POM images help to see the dispersion of additives in polymer matrix.

Process abilities of LDPE nanocomposite samples were measured by MFI measurement technique and n-MFI values were calculated. By addition of DK4 nanoclay, melt flow was increased by 300%. I44 nanoclay does not have an effect on melt flow of LDPE.

Mechanical properties of the LDPE nanocomposite samples were investigated from the main and cross direction of film samples separately and strength at break, strain at break and 3% secant modulus values were calculated. Addition of clay increase elongation of samples while decrease strength of material comparing to pristine LDPE film. Ethylene absorbers do not have an effect on mechanical properties of samples.

Colour measurements of samples were measured in terms of their lightness, redness-greenness, yellowness-blueness and opacity-transparency. Depending on the colour of additive, the film samples gain a colour a bit. Generally by addition of nanoclay and ethylene absorber, transparency was decreased and opacity is increased.

Afterwards these investigations, strawberry, parsley and iceberg lettuce were stored in these different 7 packaging materials. One of these packaging materials is LDPE without additive and used as a standard. O₂, CO₂, C₂H₄ gas changes, weight loose, sugar amount changes, pH changes, general quality changes versus time were evaluated.

As a result of overall these tests, the best packages were determined as sample no 6 and 7 which have both of nanoclay and ethylene absorber additive. The desired gas values were obtained, weight loose was lower comparing to the other packaging materials. pH and sugar amounts did not give significant results for comparison. Taste and quality changes were monitored versus time and the result confirmed all of the other results.

As a result of this study, it was obtained that, there is a big difference between LDPE packages and LDPE composite packages from the point of the taste and quality. Removing the gases which are playing crucial role on shelf life period of products increases shelf life of foodstuffs. Therefore, the packages including both barrier and ethylene absorber additives were best packages since these additives provide desired gas configuration in packages.

APPENDICES

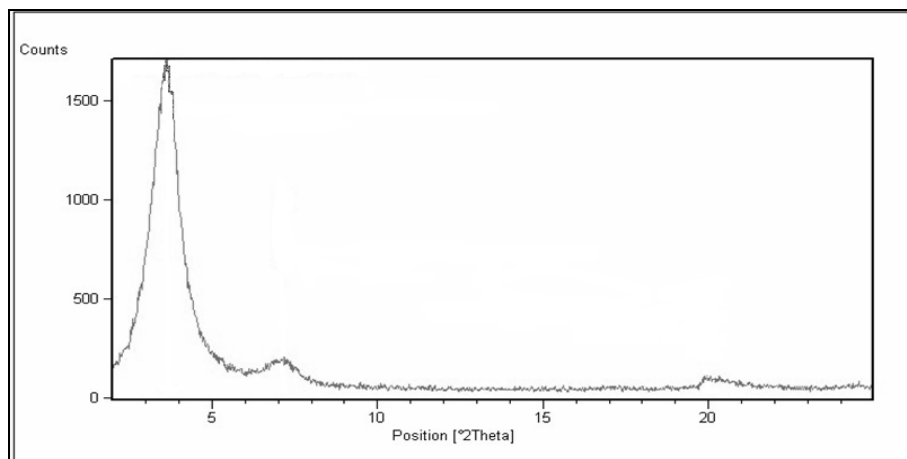


Figure A.1: XRD result of I44 nanoclay.

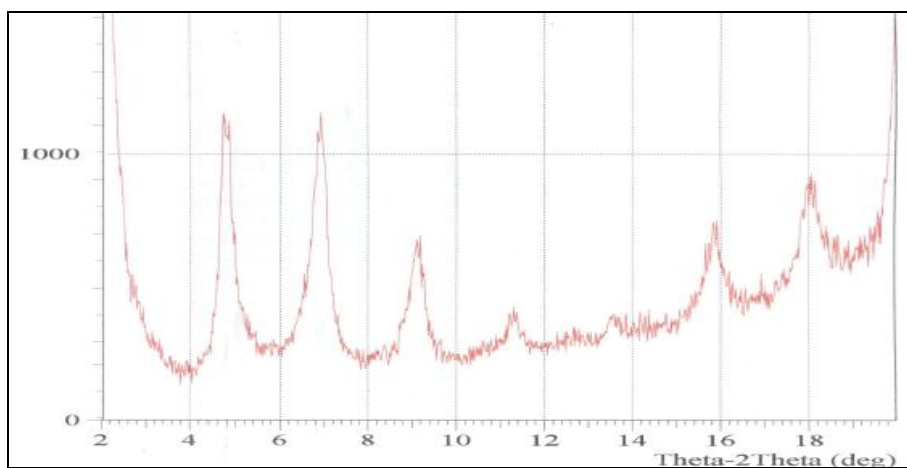


Figure A.2: XRD result of DK4 nanoclay.

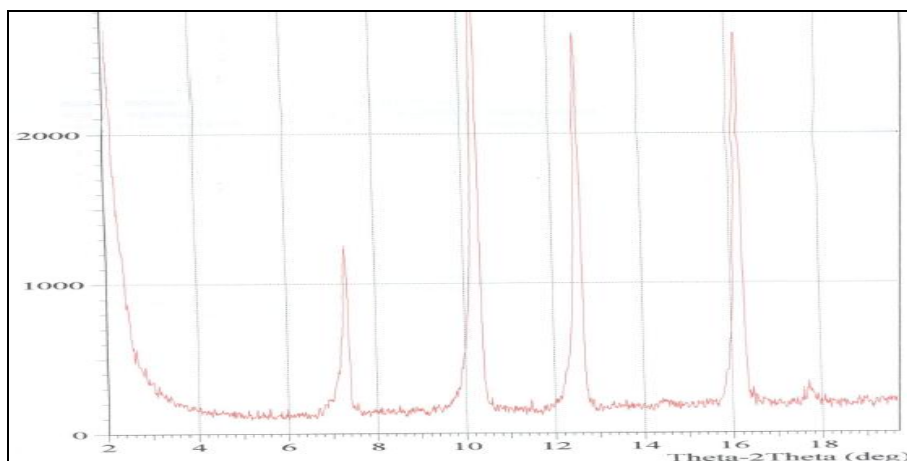


Figure A.3: XRD result of active ingredient of N10774.

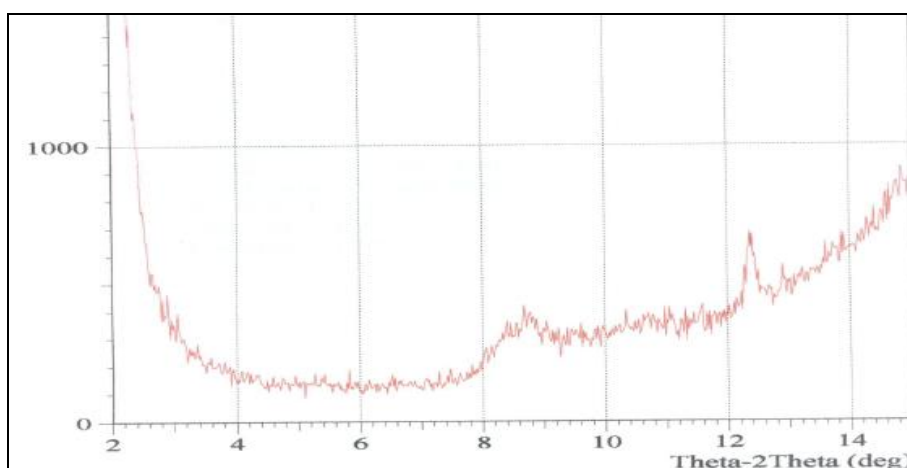


Figure A.4: XRD result of 5% DK4 nanoclay containing LDPE (Sample no:3).

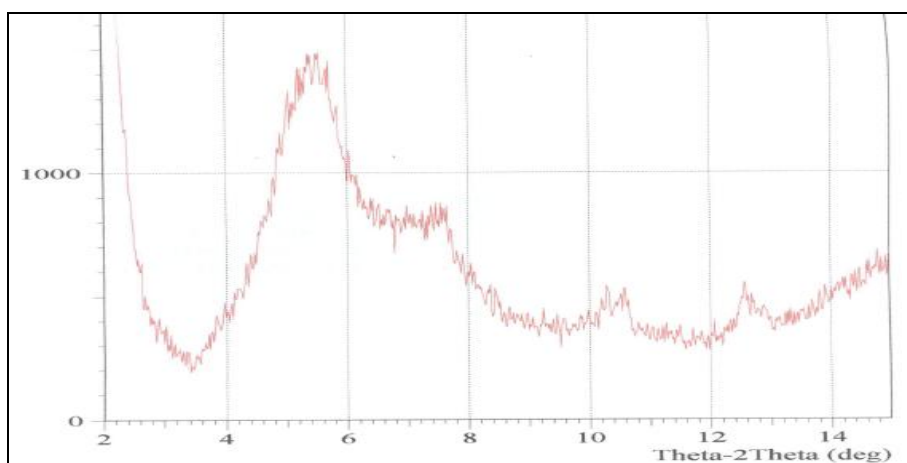


Figure A.5: XRD result of 4.5% I44 nanoclay+ 4% N10774 ethylene absorber containing LDPE (Sample no:6).

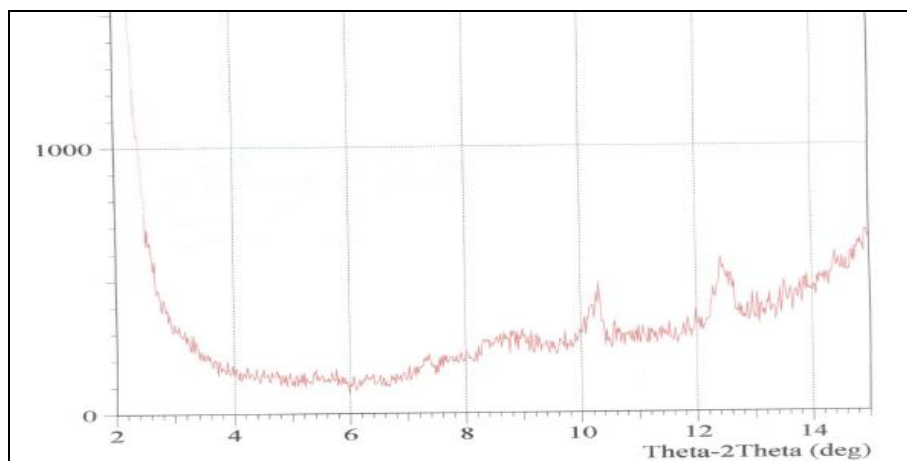


Figure A.6: XRD result of 4.5% DK4 nanoclay+ 4% N10774 ethylene absorber containing LDPE (Sample no:7).

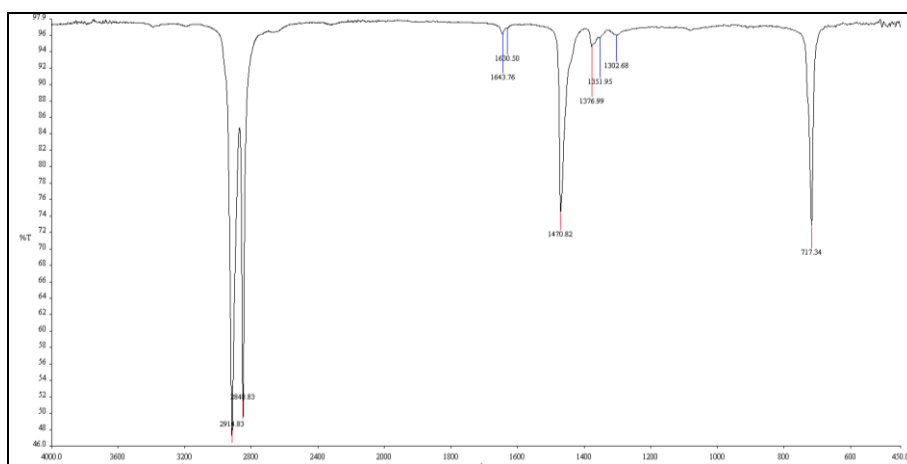


Figure A.7: FTIR spectrum of LDPE (Sample no:1).

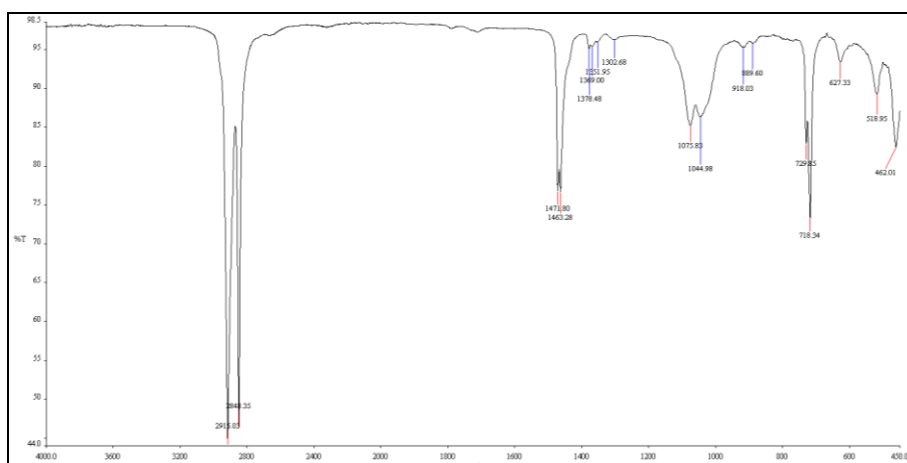


Figure A.8: FTIR spectrum of 5% I44 nanoclay LDPE (Sample no:2).

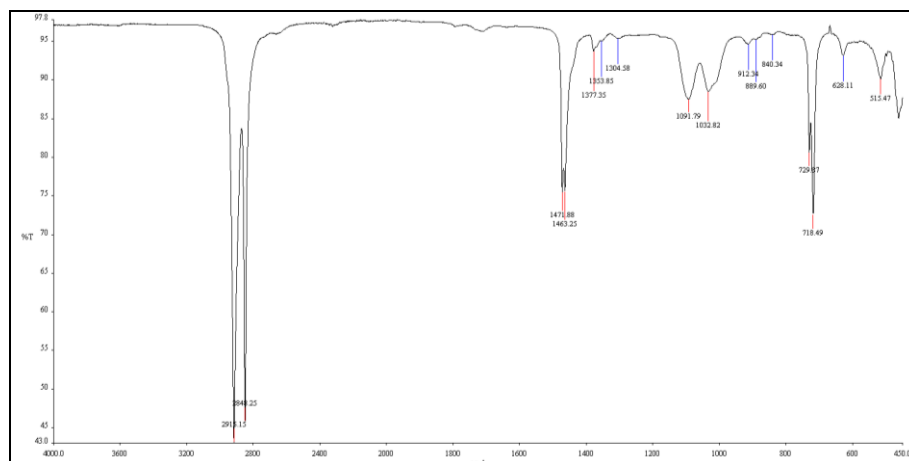


Figure A.9: FTIR spectrum of 5% DK4 nanoclay LDPE (Sample no:3).

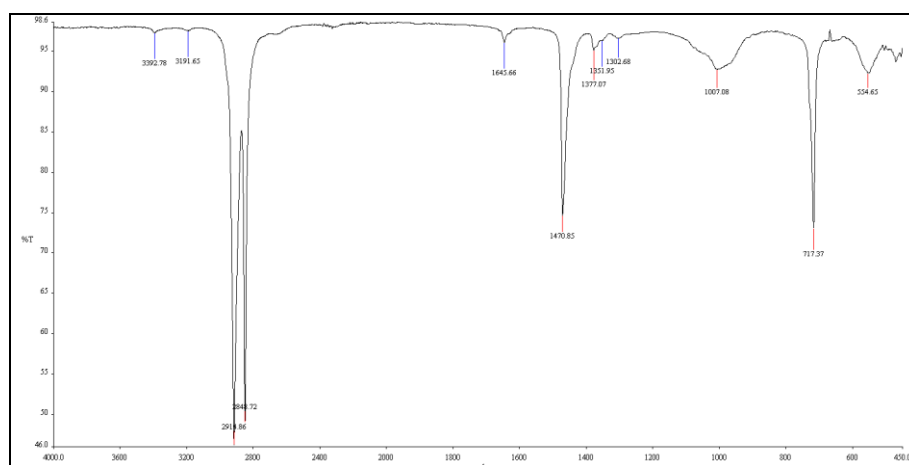


Figure A.10: FTIR spectrum of 4% N10774 LDPE (Sample no:4).

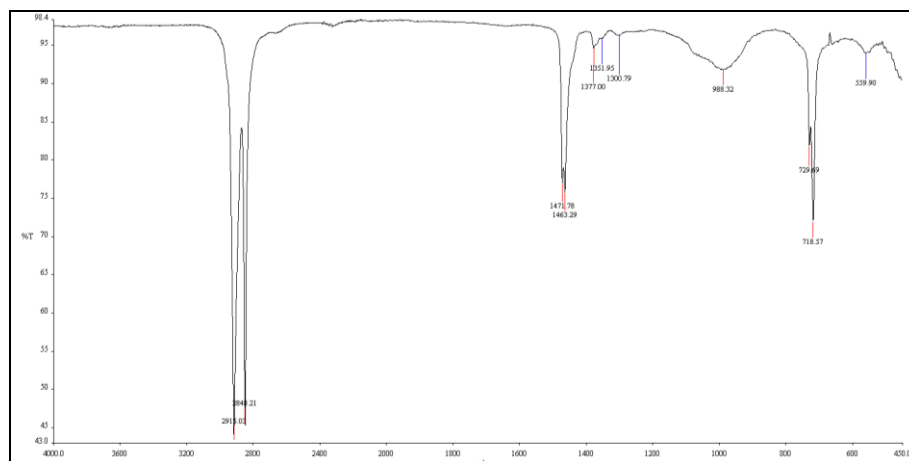


Figure A.11: FTIR spectrum of 4% N10776 LDPE (Sample no:5).

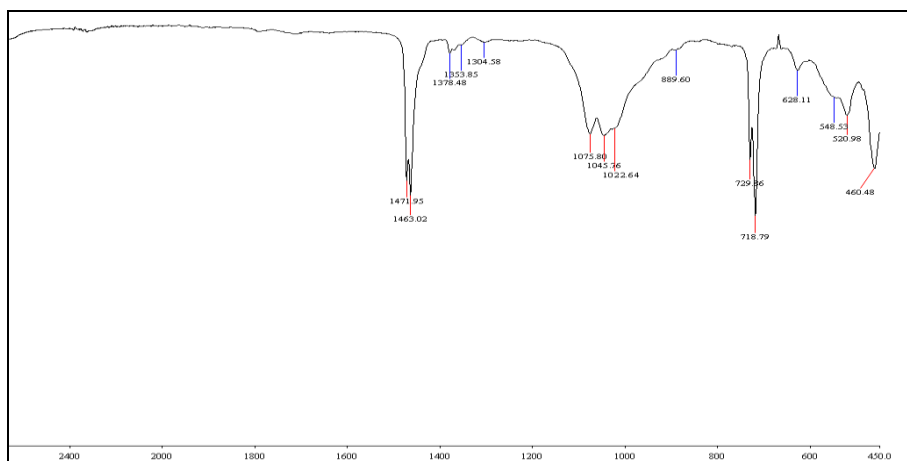


Figure A.12: FTIR spectrum of 4.5% I44 nanoclay + 4% N10774 LDPE (Sample no:6).

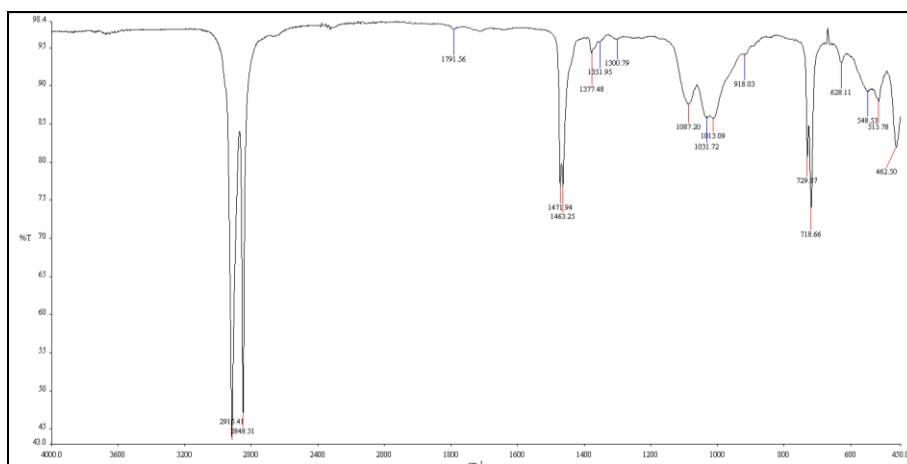


Figure A.13: FTIR spectrum of 4.5% DK4 nanoclay + 4% N10774 LDPE (Sample no:7).

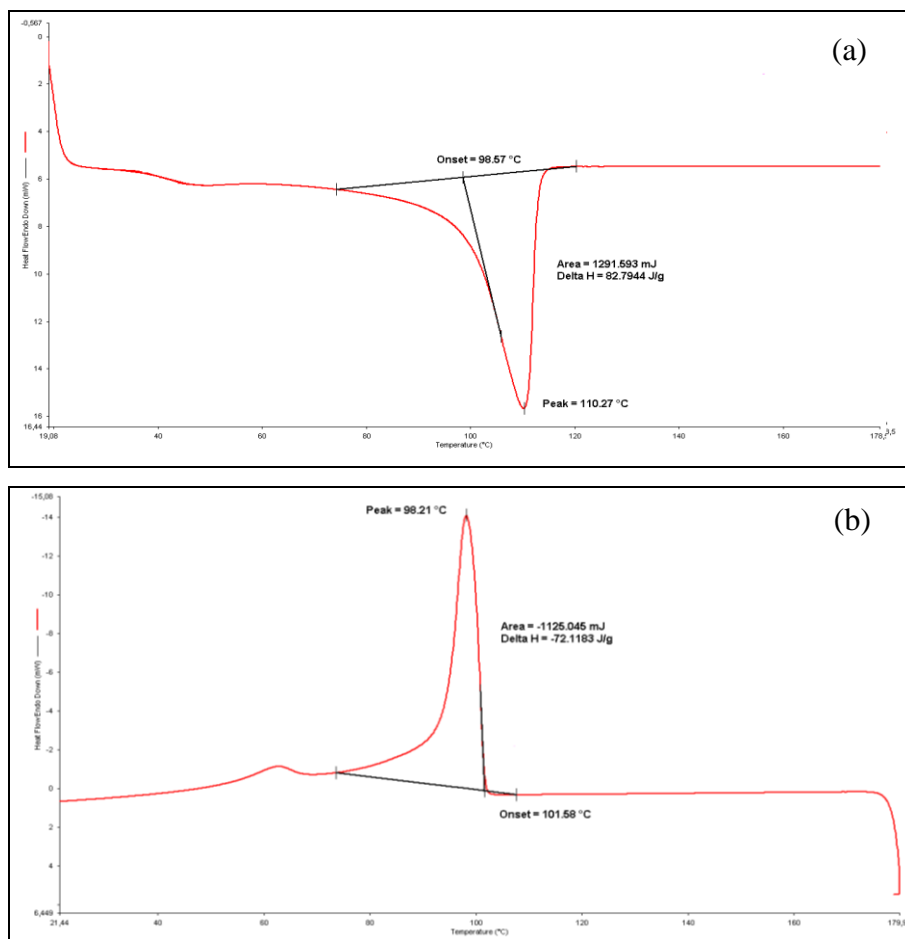


Figure A.14: DSC graphs of LDPE ((a) heating and (b) cooling relatively) (Sample no:1).

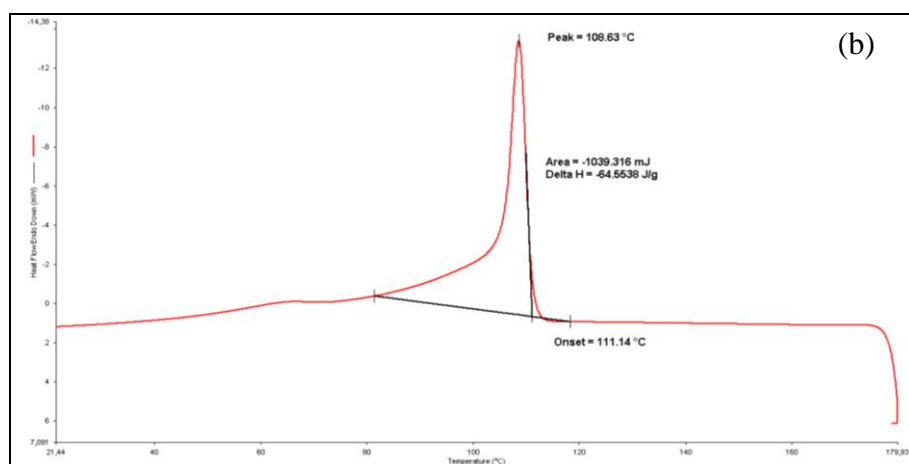
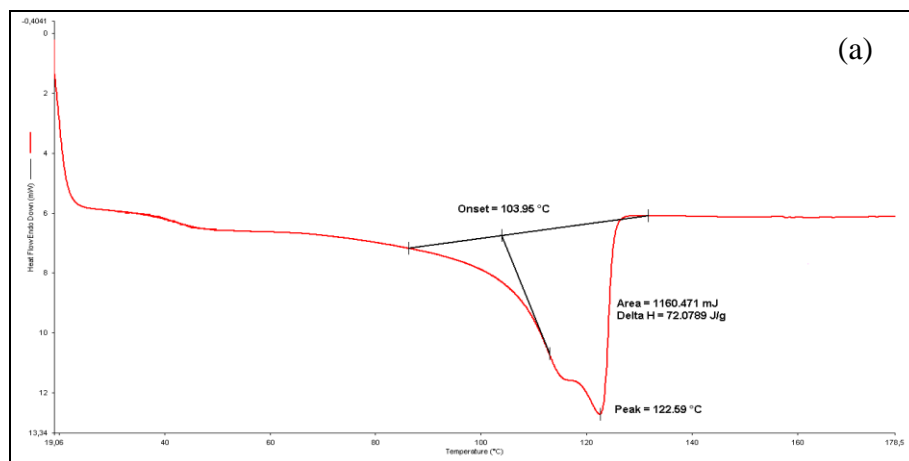


Figure A.15: DSC graph of 5% I44 nanoclay LDPE ((a) heating and (b) cooling relatively) (Sample no:2).

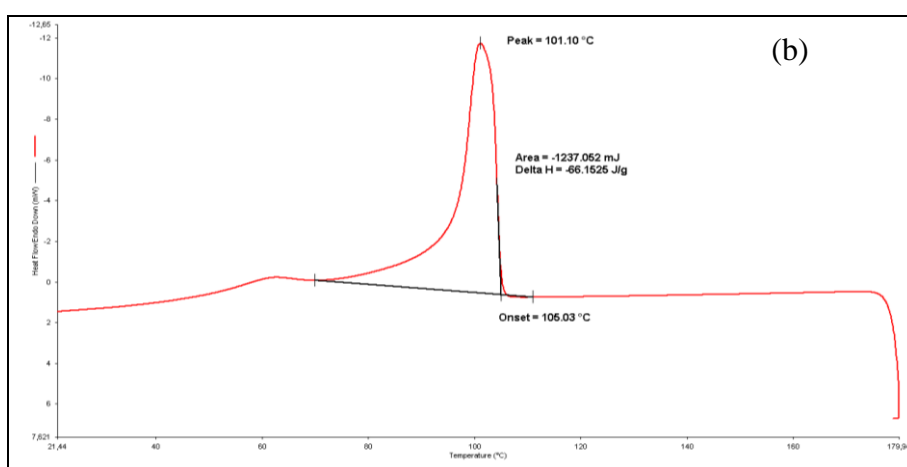
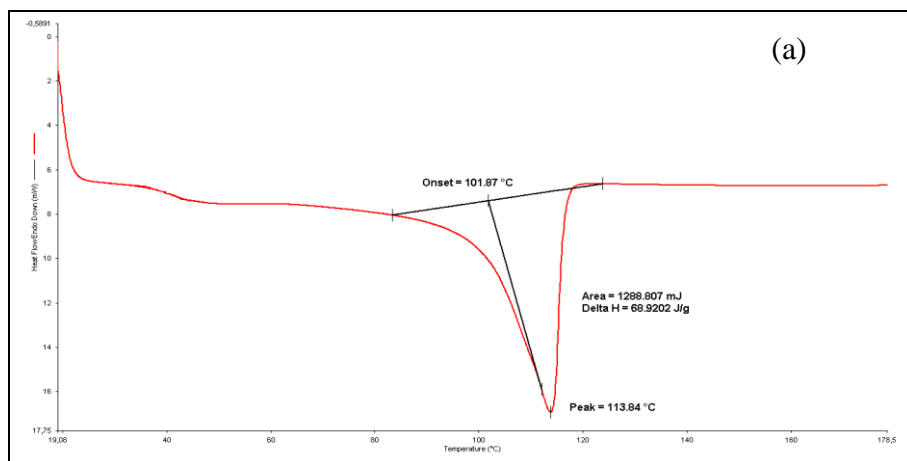


Figure A.16: DSC graph of 5% DK4 nanoclay LDPE ((a) heating and (b) cooling relatively) (Sample no:3).

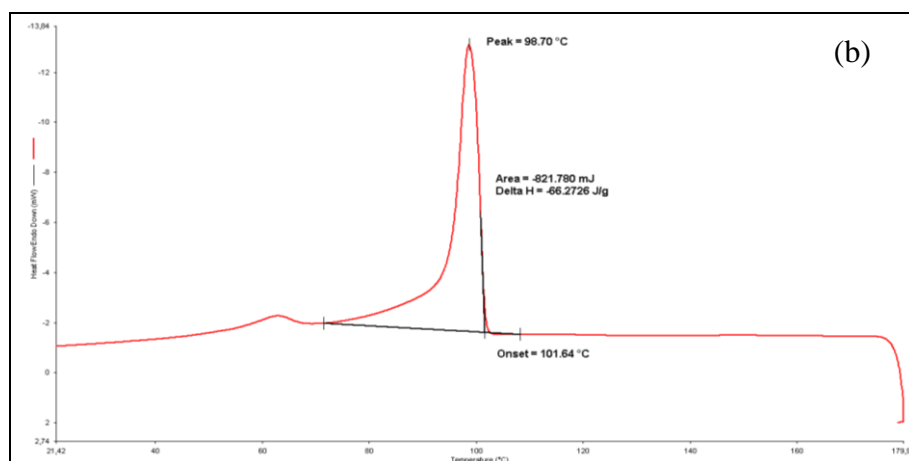
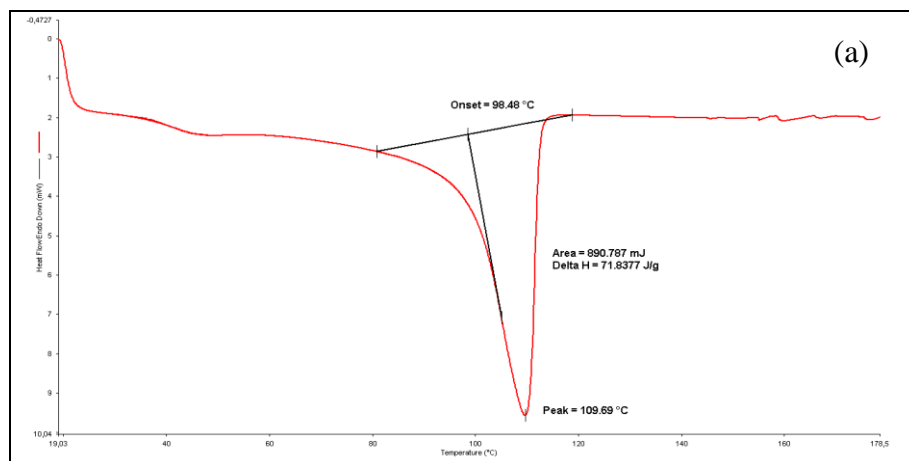


Figure A.17: DSC graph of 4% N10774 LDPE ((a) heating and (b) cooling relatively) (Sample no:4).

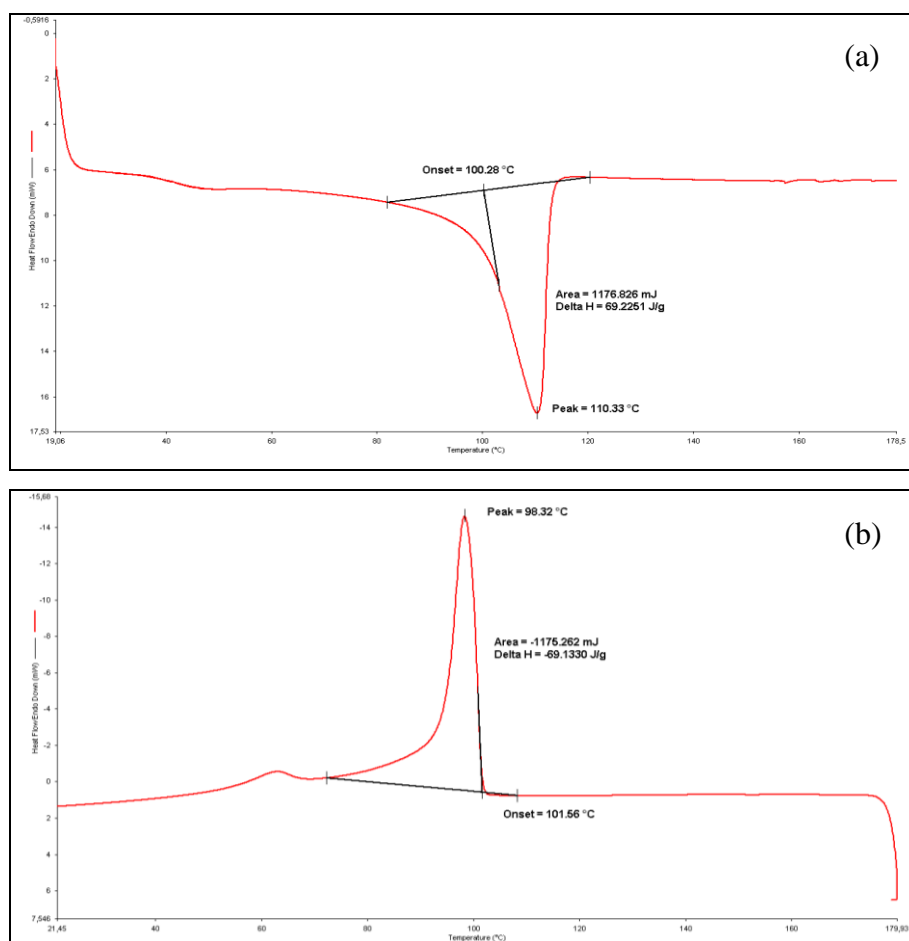


Figure A.18: DSC graph of 4% N10776 LDPE ((a) heating and (b) cooling relatively) (Sample no:5).

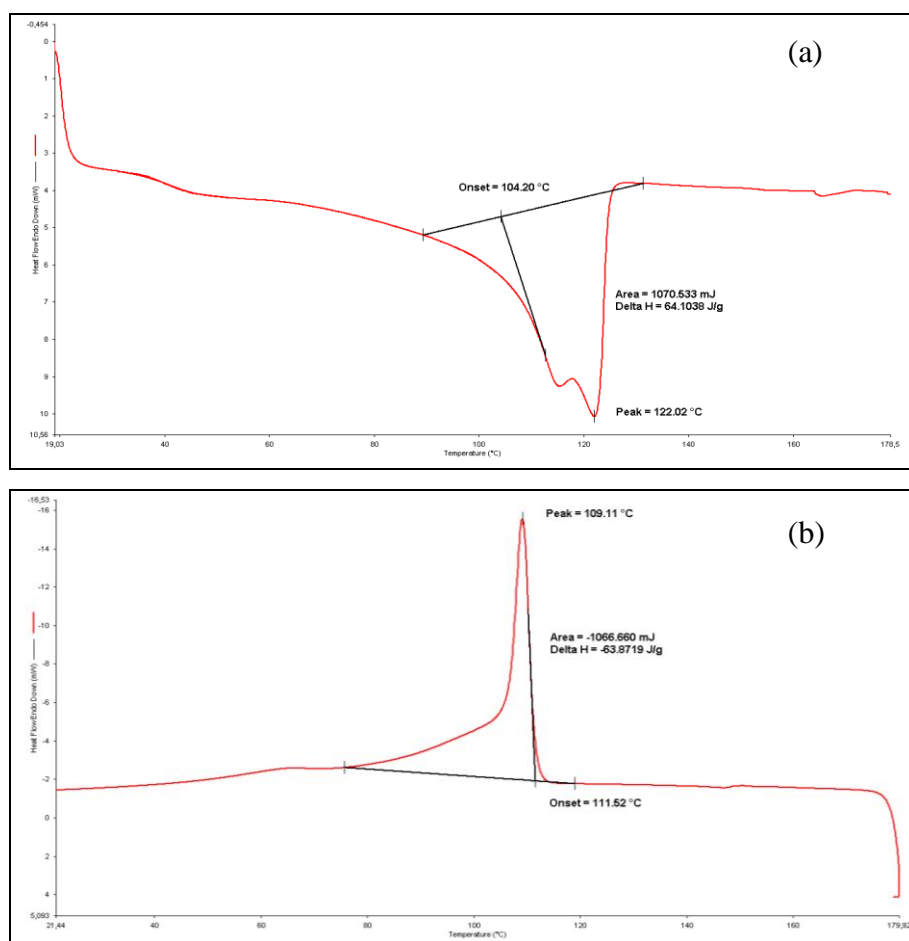


Figure A.19: DSC graph of 4.5% I44 nanoclay + 4% N10774 LDPE
 ((a) heating and (b) cooling relatively) (Sample no:6).

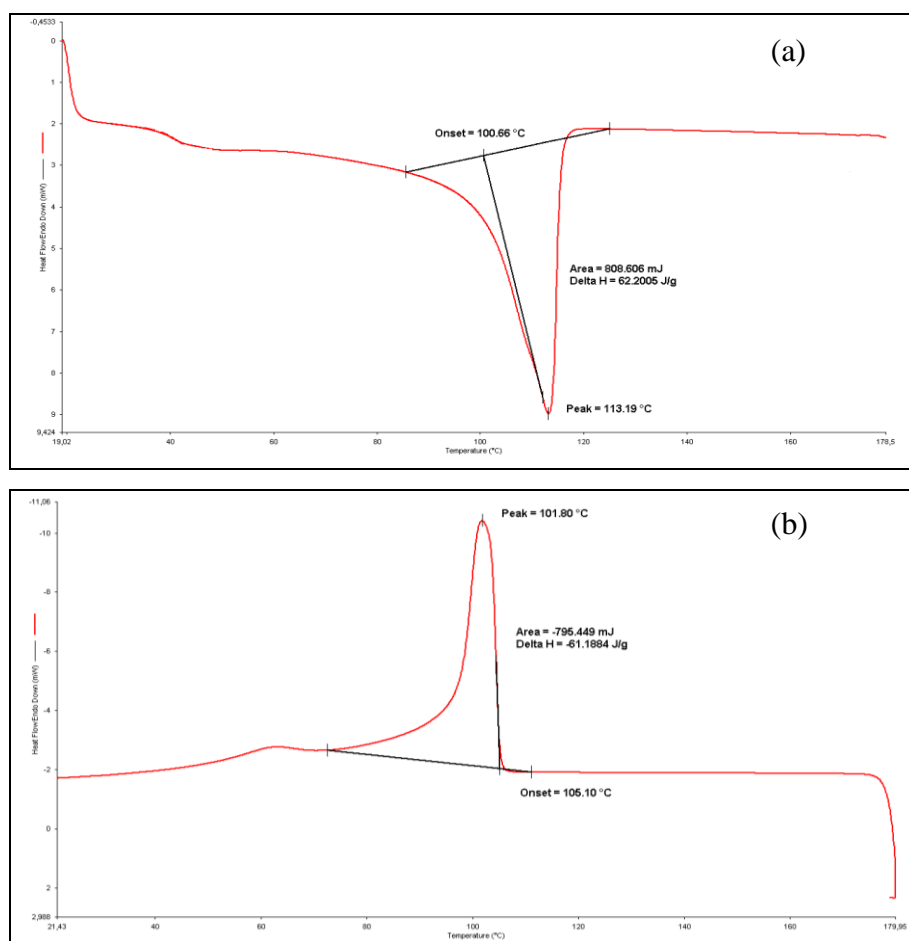


Figure A.20: DSC graph of 4.5% DK4 nanoclay + 4% N10774 LDPE ((a) heating and (b) cooling relatively) (Sample no:7).

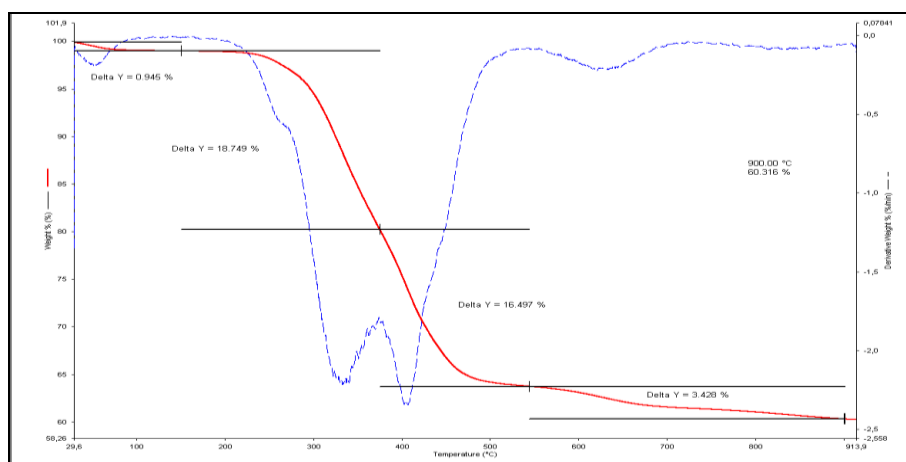


Figure A.21: TGA graph of I44 nanoclay.

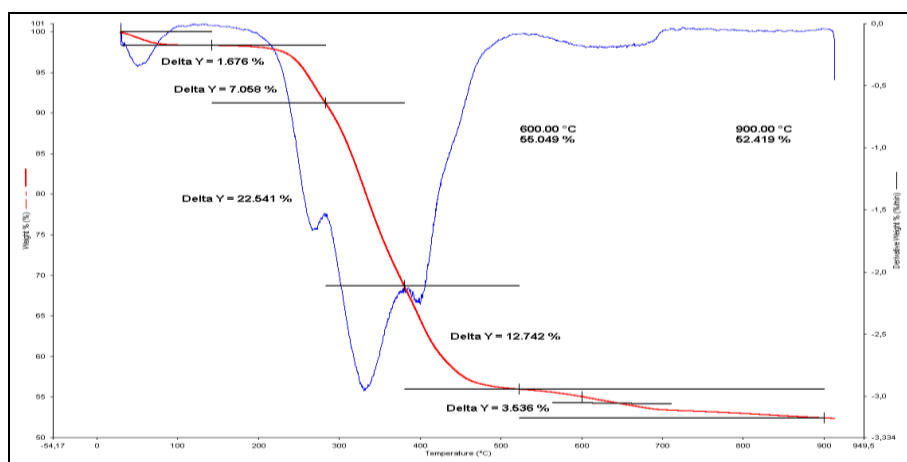


Figure A.22: TGA graph of DK4 nanoclay.

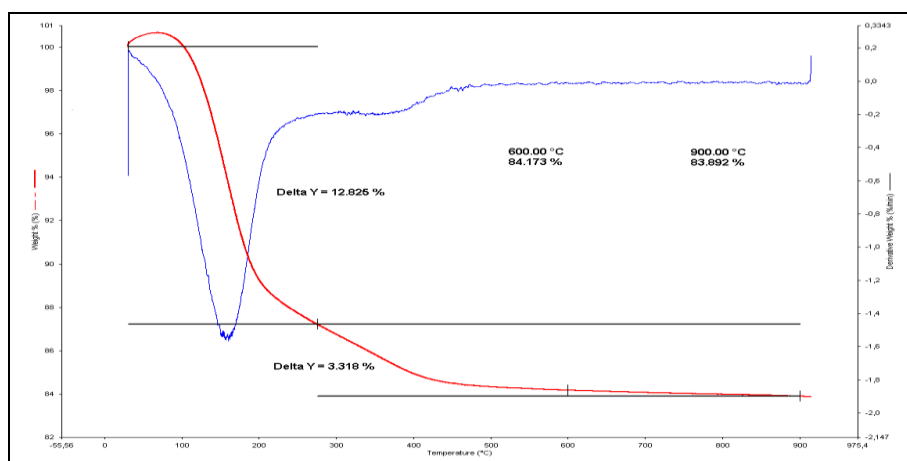


Figure A.23: TGA graph of active ingredient of N10774 ethylene absorber.

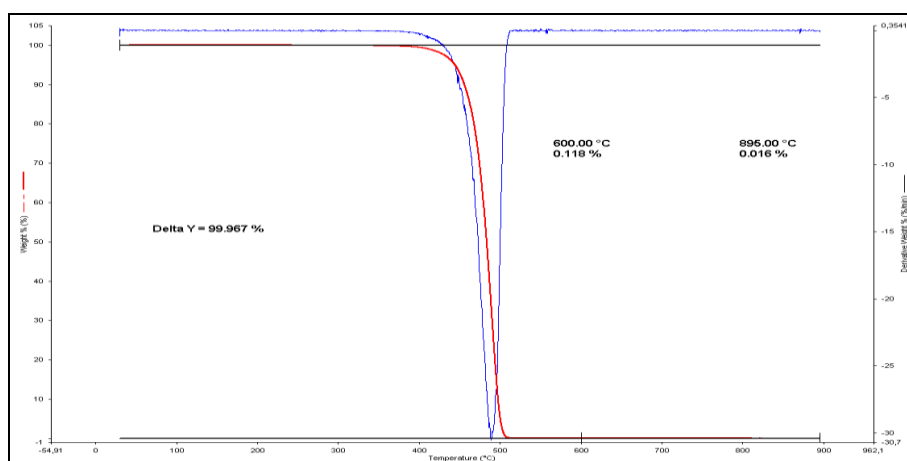


Figure A.24: TGA graph of LDPE (Sample no:1).

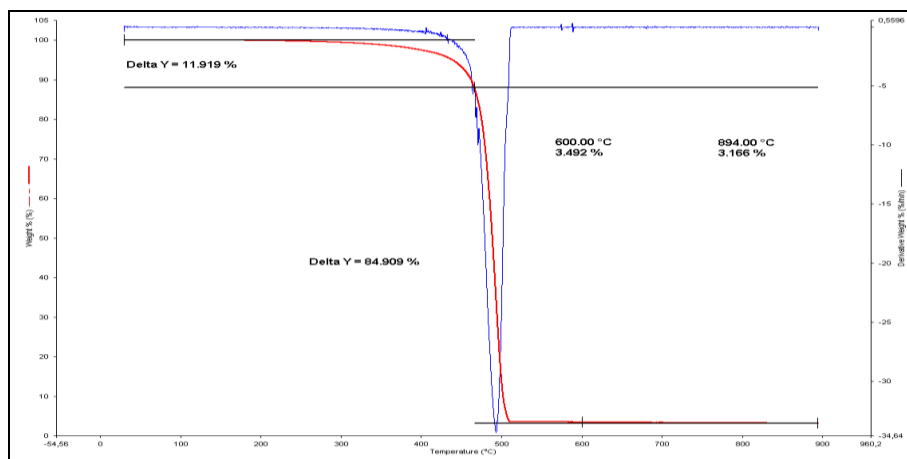


Figure A.25: TGA graph of 5% I44 nanoclay LDPE (Sample no:2).

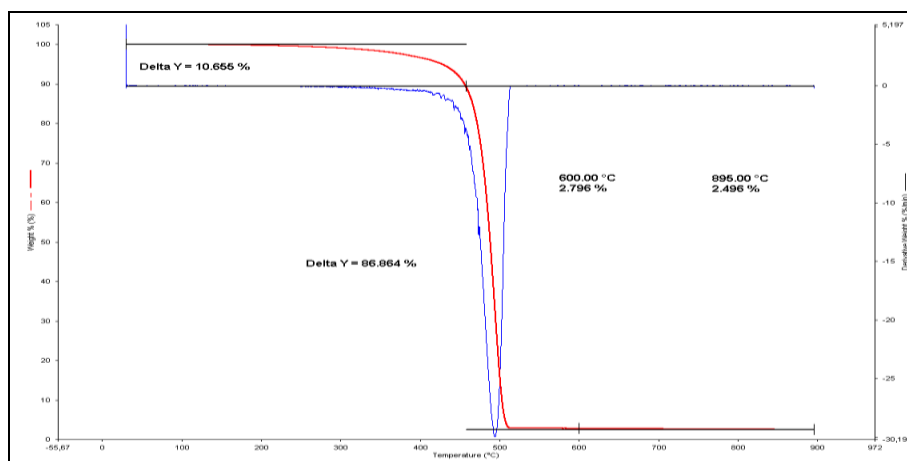


Figure A.26: TGA graph of 5% DK4 nanoclay LDPE (Sample no:3).

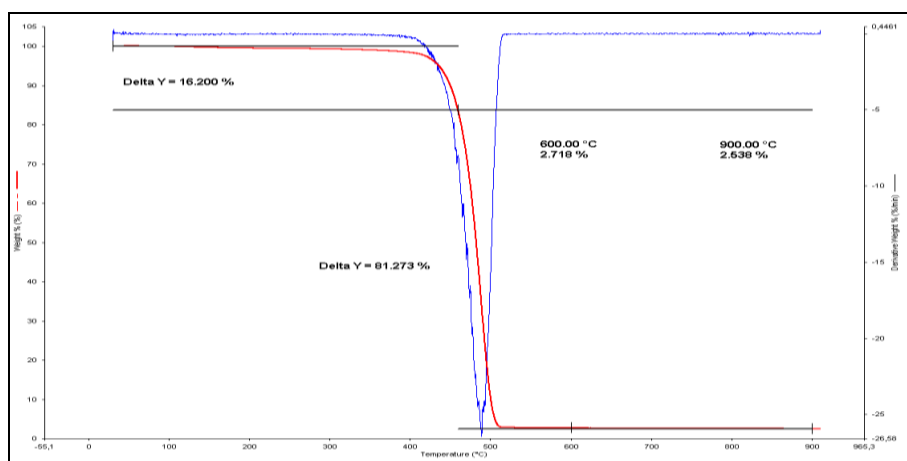


Figure A.27: TGA graph of 4% N10774 LDPE (Sample no:4).

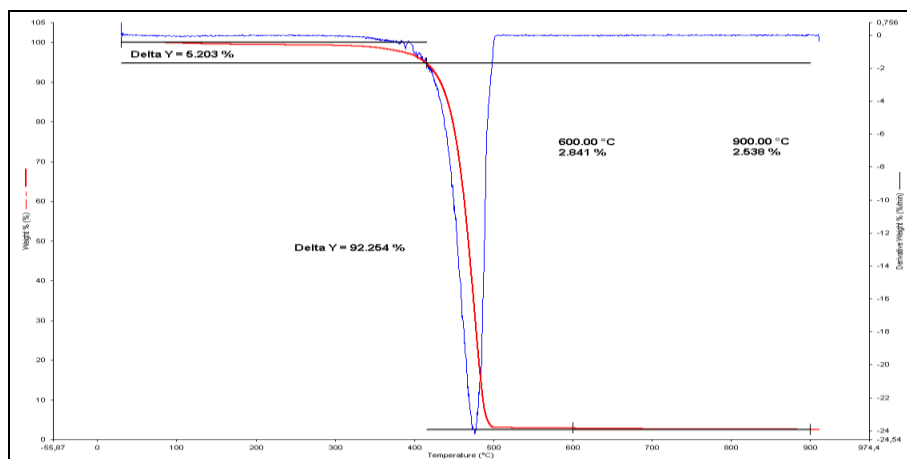


Figure A.28: TGA graph of 4% N10776 LDPE (Sample no:5)

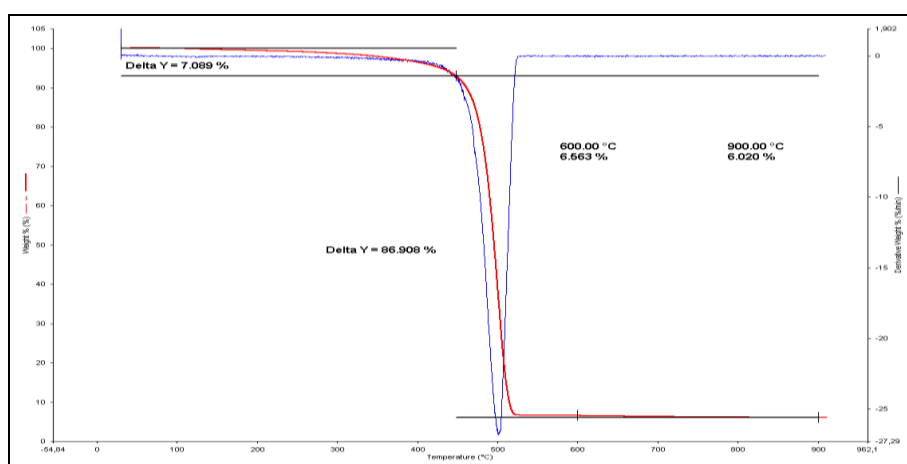


Figure A.29: TGA graph of 4.5% I44 nanoclay + 4% N10774 LDPE (Sample no:6).

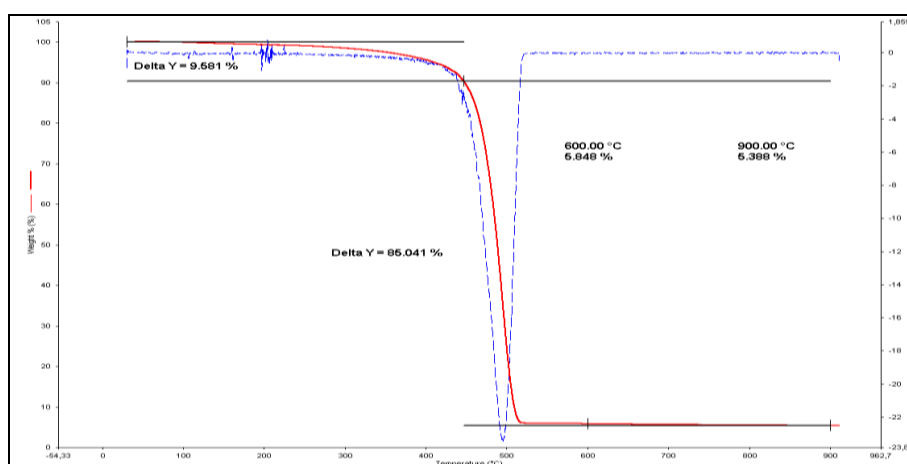


Figure A.30: TGA graph of 4.5% DK4 nanoclay + 4% N10774 LDPE (Sample no:7).

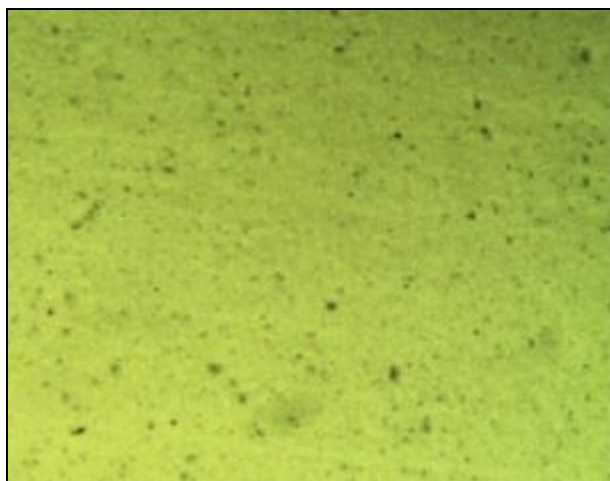


Figure A.31: POM image of 5% I44 nanoclay LDPE film (Sample no:2).

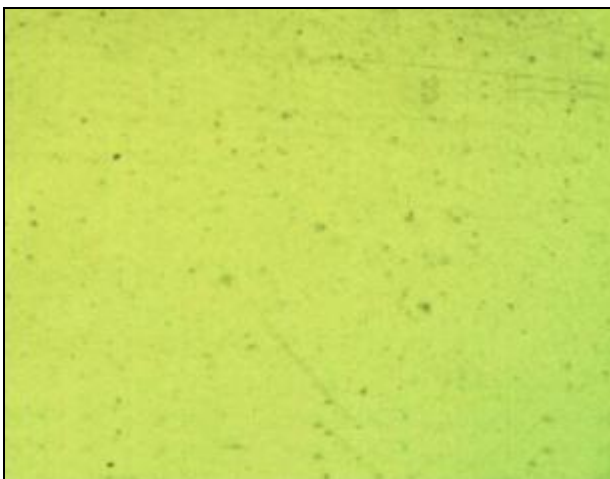


Figure A.32: POM image of 5% DK4 nanoclay LDPE film (Sample no:3).

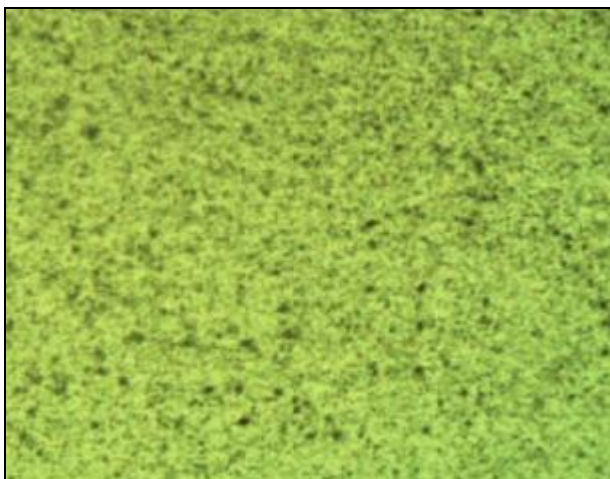


Figure A.33: POM image of 4% N10774 LDPE film (Sample no:4).



Figure A.34: POM image of 4.5% I44 nanoclay + 4% N10774 LDPE (Sample no:6).

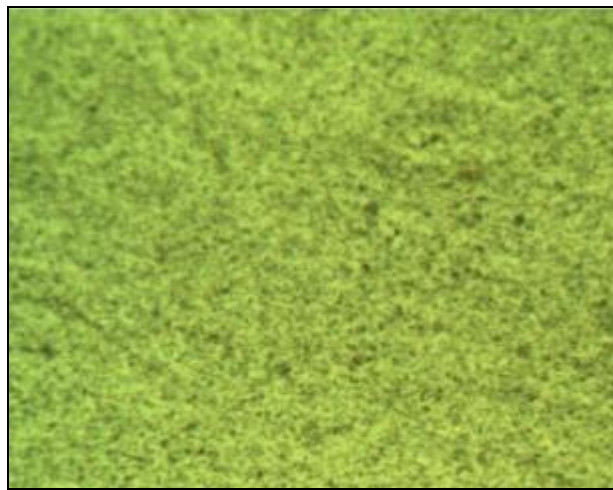


Figure A.35: POM image of 4.5% DK4 nanoclay + 4% N10774 LDPE (Sample no:7).

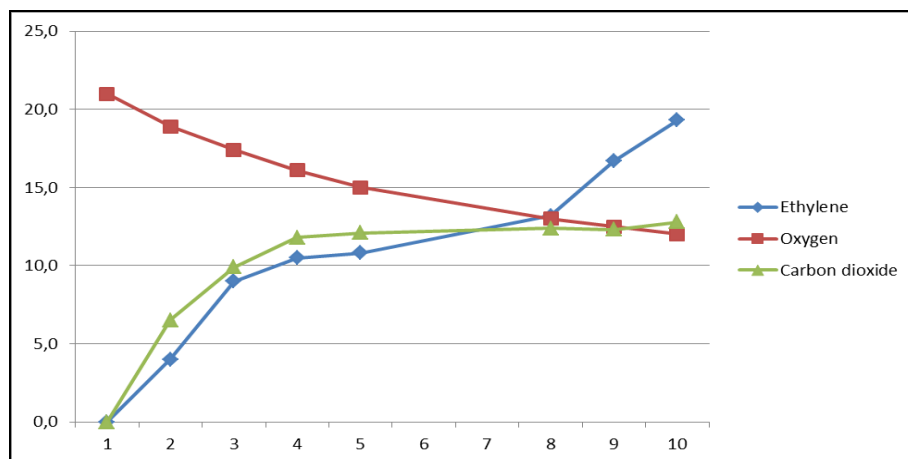


Figure A.36: C_2H_4 , O_2 and CO_2 gas changes versus time of LDPE package for strawberry (Sample no:1).

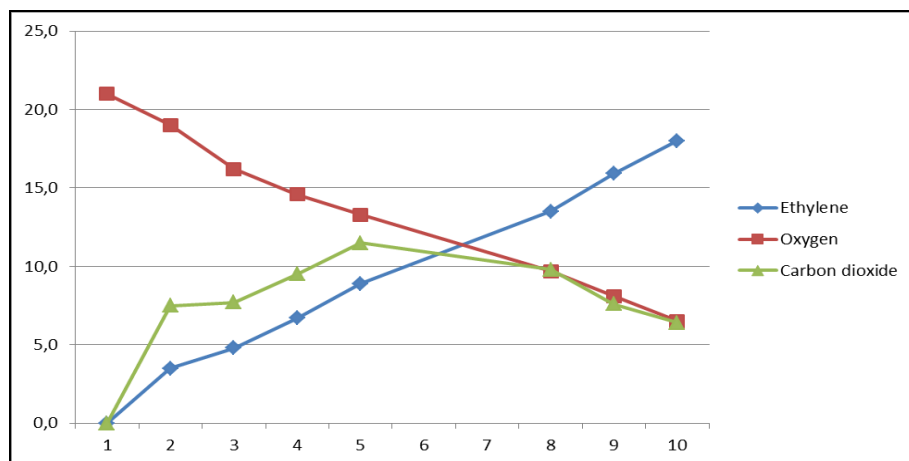


Figure A.37: C_2H_4 , O_2 and CO_2 gas changes versus time of 5% I44 nanoclay LDPE package for strawberry (Sample no:2).

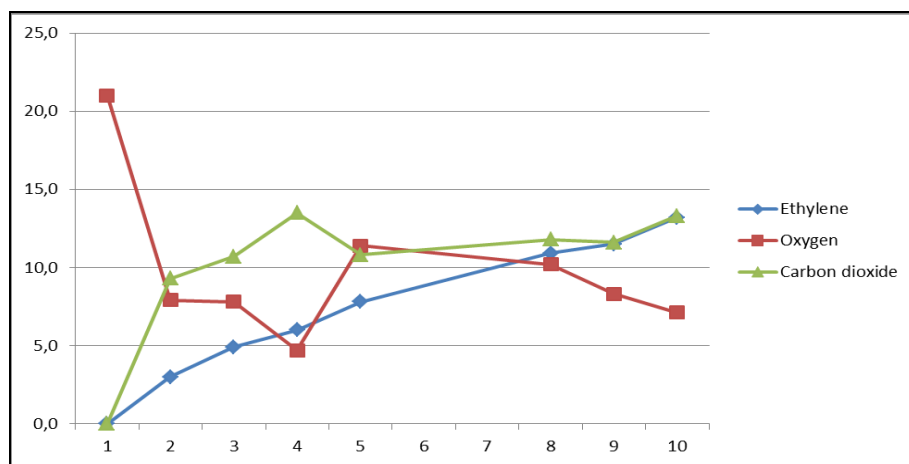


Figure A.38: C_2H_4 , O_2 and CO_2 gas changes versus time of 5% DK4 nanoclay LDPE package for strawberry (Sample no:3).

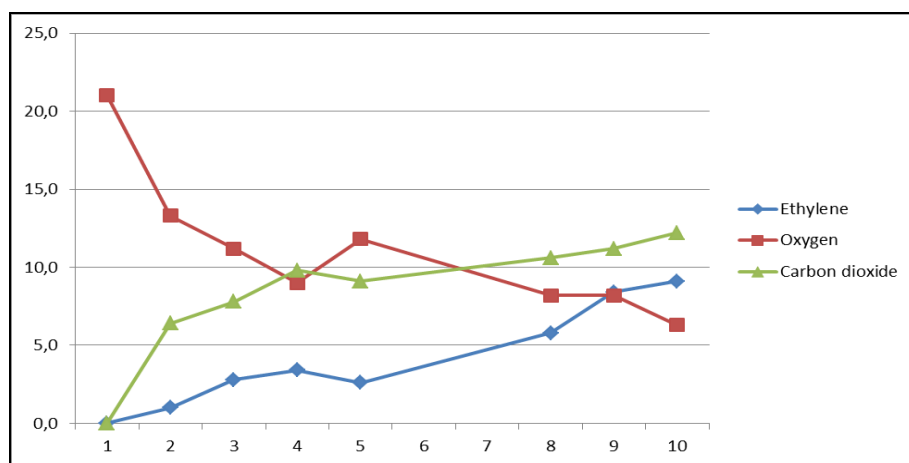


Figure A.39: C_2H_4 , O_2 and CO_2 gas changes versus time of 4% N10774 LDPE package for strawberry (Sample no:4).

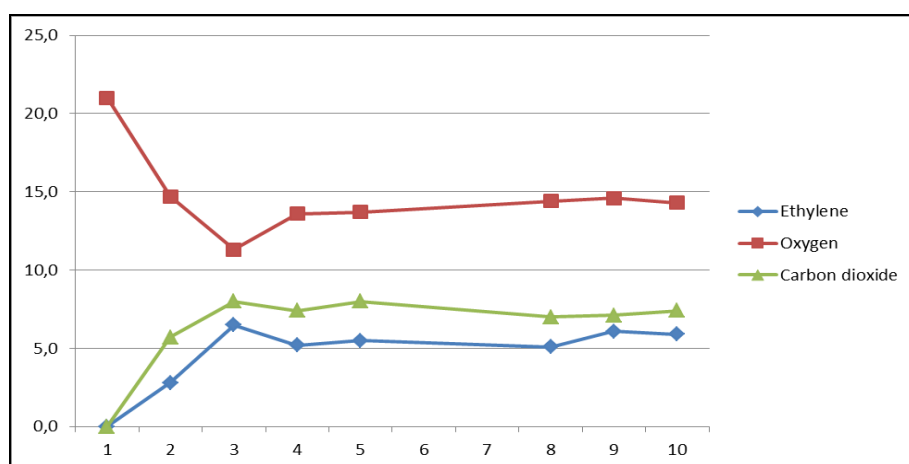


Figure A.40: C₂H₄, O₂ and CO₂ gas changes versus time of 4% N10776 package for strawberry (Sample no:5).

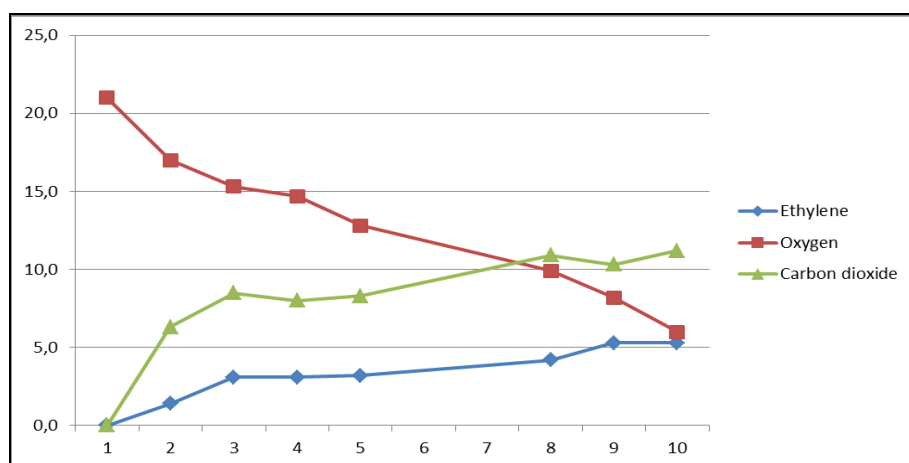


Figure A.41: C₂H₄, O₂ and CO₂ gas changes versus time of 4.5% I44 nanoclay + 4% N10774 package for strawberry (Sample no:6).

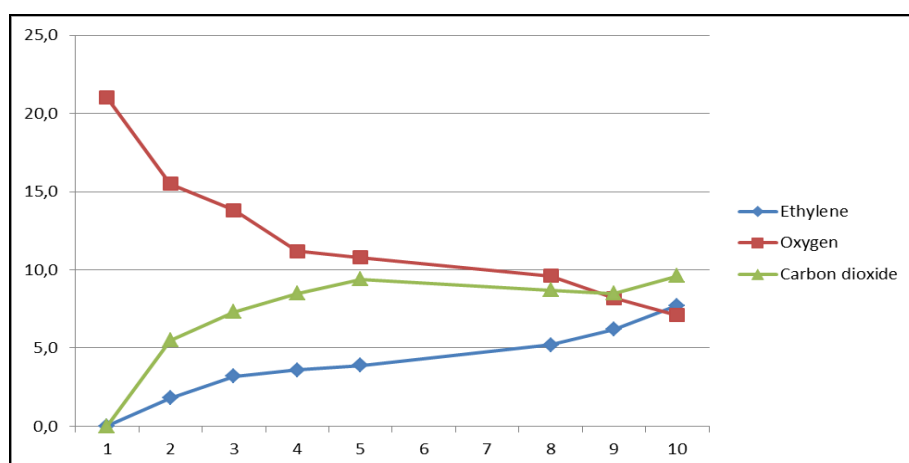


Figure A.42: C₂H₄, O₂ and CO₂ gas changes versus time of 4.5% DK4 nanoclay + 4% N10774 LDPE package for strawberry (Sample no:7).

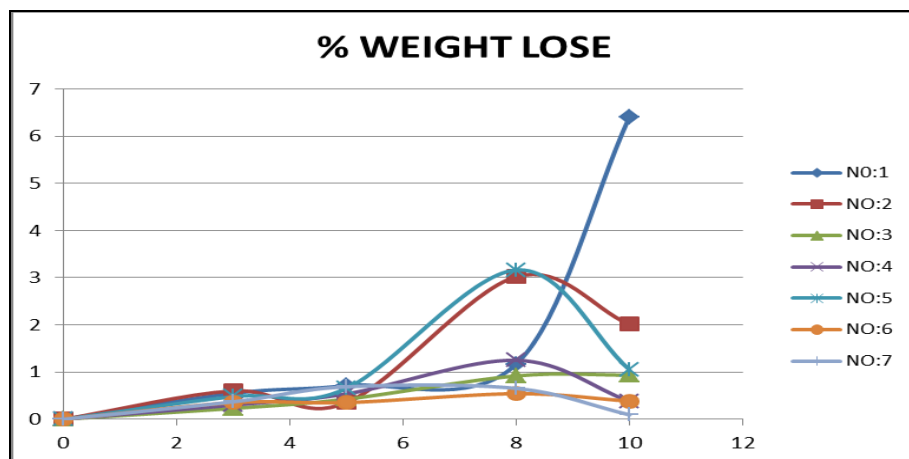


Figure A.43: The graph of weight lose changes of strawberries during 10 days storage versus time.

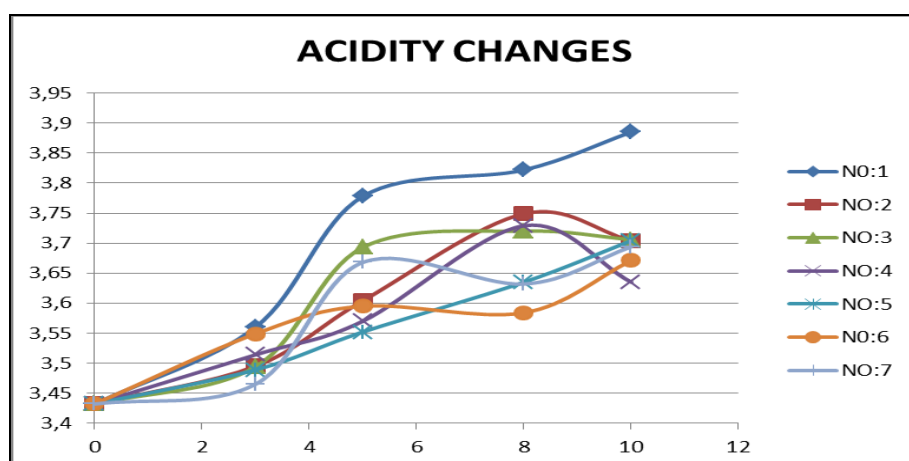


Figure A.44: The graph of pH changes of strawberries during 10 days storage versus time.

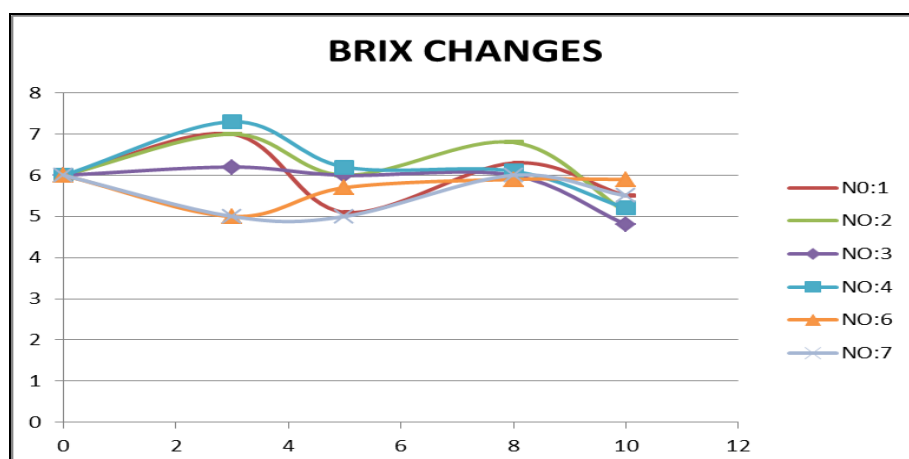


Figure A.45: The graph of brix changes of strawberries during 10 days storage versus time.

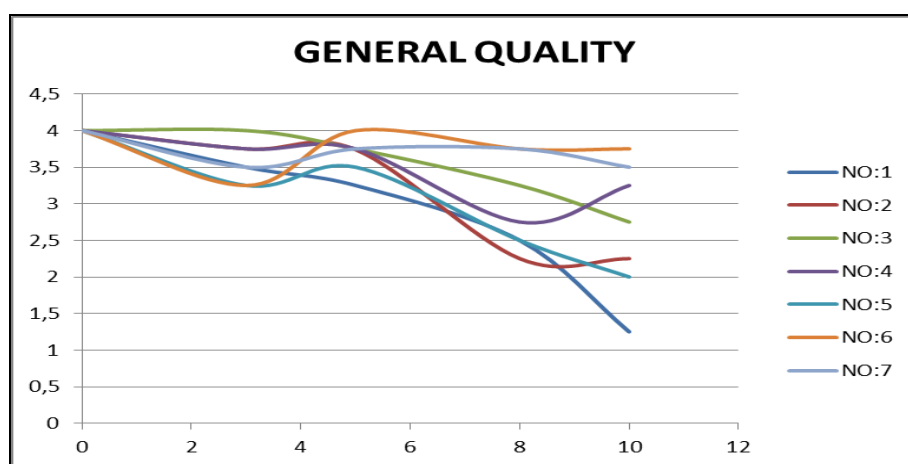


Figure A.46: The graph of general quality changes of strawberries during 10 days storage versus time.



Figure A.47: The strawberry pictures stored in LDPE packages at 3th, 5th, 8th, 10th days (Sample no:1).



Figure A.48: The strawberry pictures stored in 5% I44 LDPE packages at 3th, 5th, 8th, 10th days (Sample no:2).



Figure A.49: The strawberry pictures stored in 5% DK4 LDPE packages at 3th, 5th, 8th, 10th days (Sample no:3).



Figure A.50: The strawberry pictures stored in 4% N10774 LDPE packages at 3th, 5th, 8th, 10th days (Sample no:4).



Figure A.51: The strawberry pictures stored in 4% N10776 LDPE packages at 3th, 5th, 8th, 10th days (Sample no:5).



Figure A.52: The strawberry pictures stored in 5% I44 + 4% N10774 LDPE packages at 3th, 5th, 8th, 10th days (Sample no:6).



Figure A.53: The strawberry pictures stored in 5% DK4 + 4% N10774 LDPE packages at 3th, 5th, 8th, 10th days (Sample no:7).

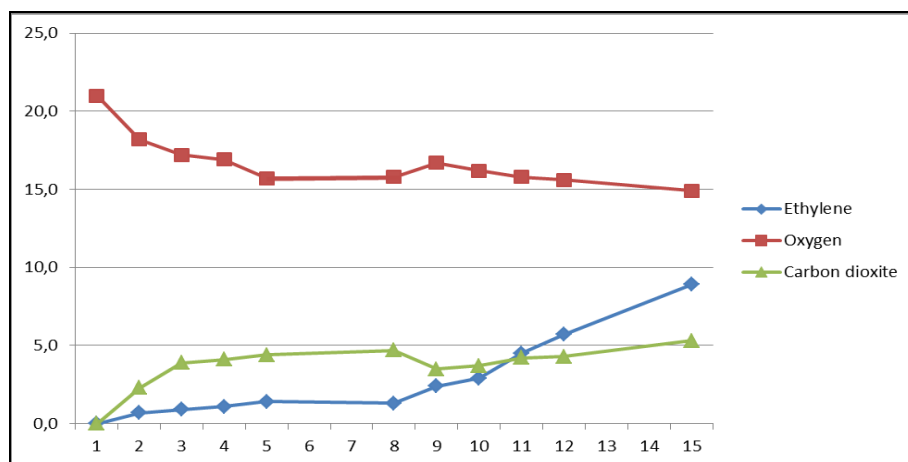


Figure A.54: C₂H₄, O₂ and CO₂ gas changes versus time of LDPE package for parsley (Sample no:1).

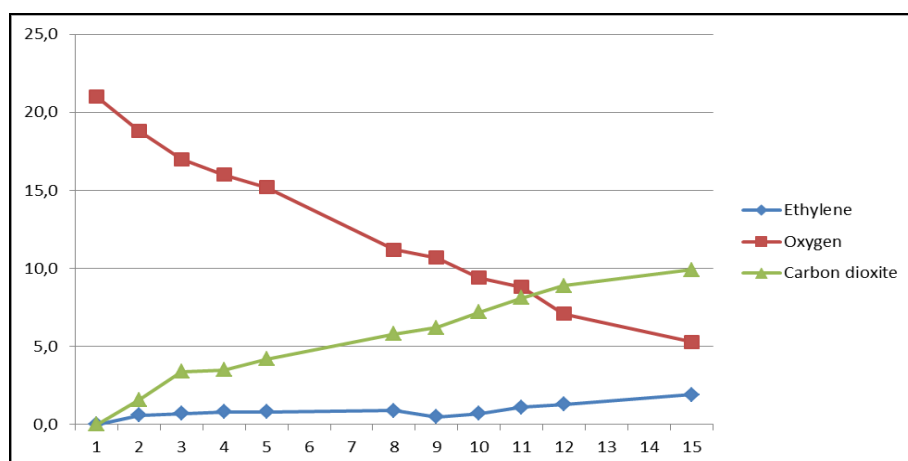


Figure A.55: C₂H₄, O₂ and CO₂ gas changes versus time of 5% I44 LDPE package for parsley (Sample no:2).

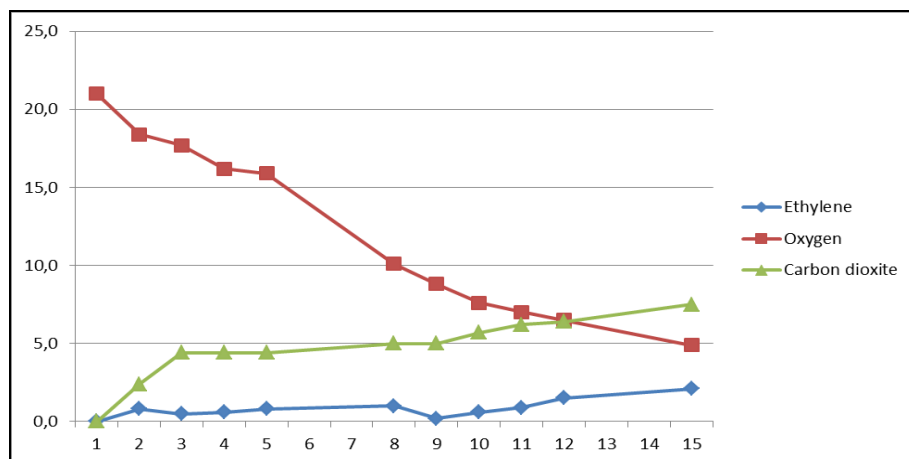


Figure A.56: C_2H_4 , O_2 and CO_2 gas changes versus time of 5% DK4 LDPE package for parsley (Sample no:3).

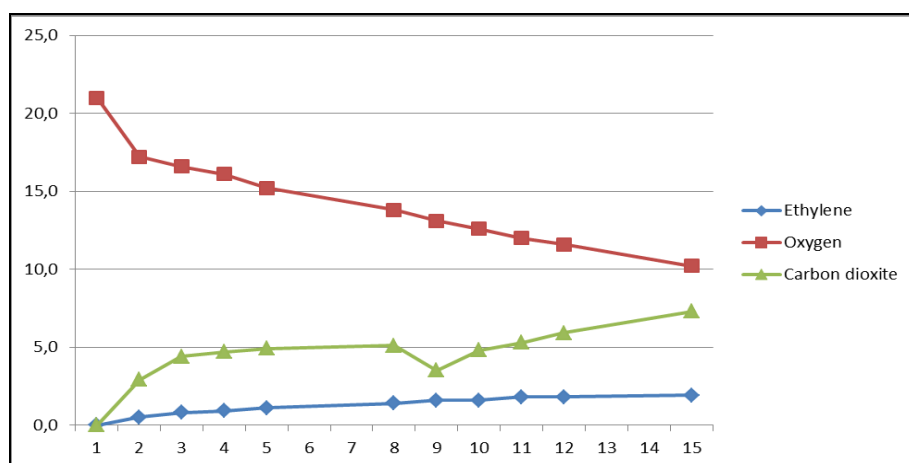


Figure A.57: C_2H_4 , O_2 and CO_2 gas changes versus time of 4% N10774 LDPE package for parsley (Sample no:4).

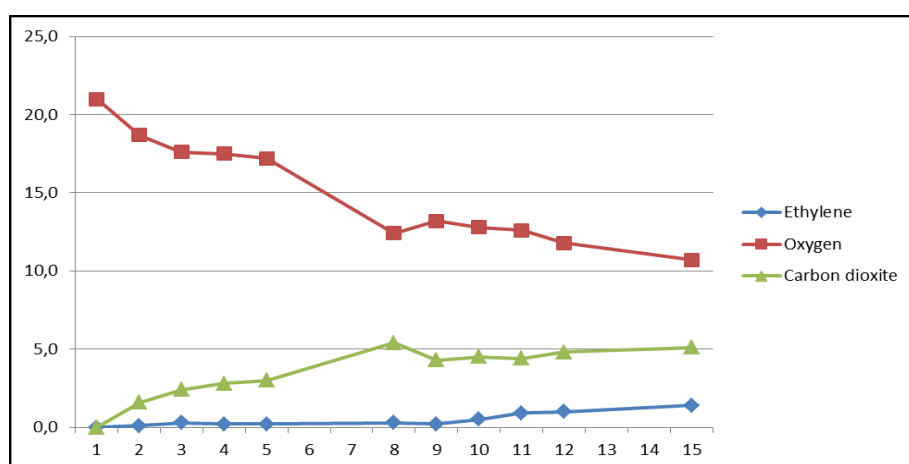


Figure A.58: C_2H_4 , O_2 and CO_2 gas changes versus time of 4% N10776 LDPE package for parsley (Sample no:5).

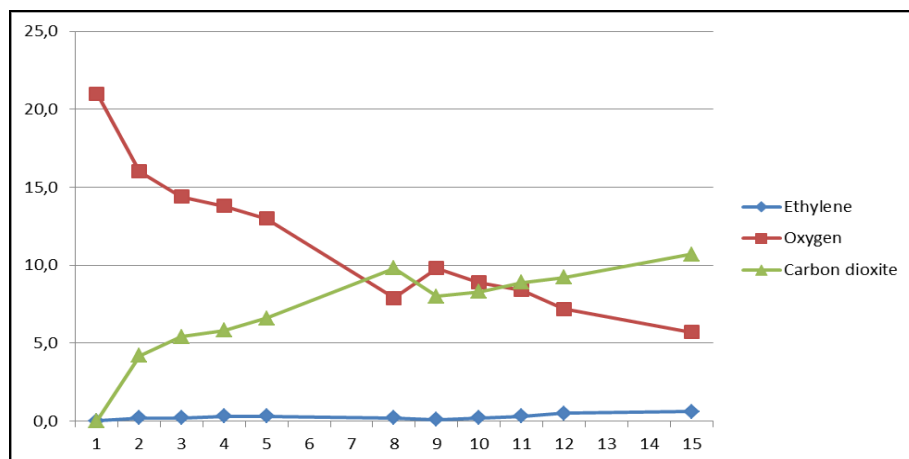


Figure A.59: C₂H₄, O₂ and CO₂ gas changes versus time of 4.5% I44 + 4% N10774 LDPE package for parsley (Sample no:6).

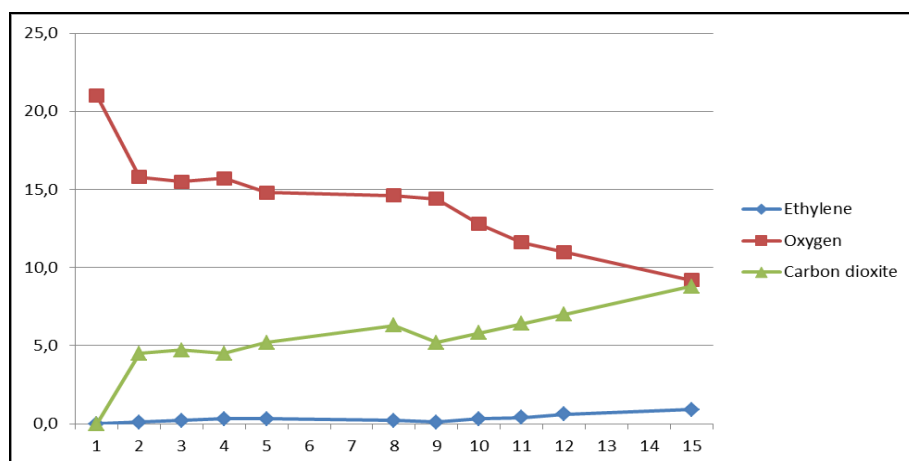


Figure A.60: C₂H₄, O₂ and CO₂ gas changes versus time of 4.5% DK4 + 4% N10774 LDPE package for parsley (Sample no:7).

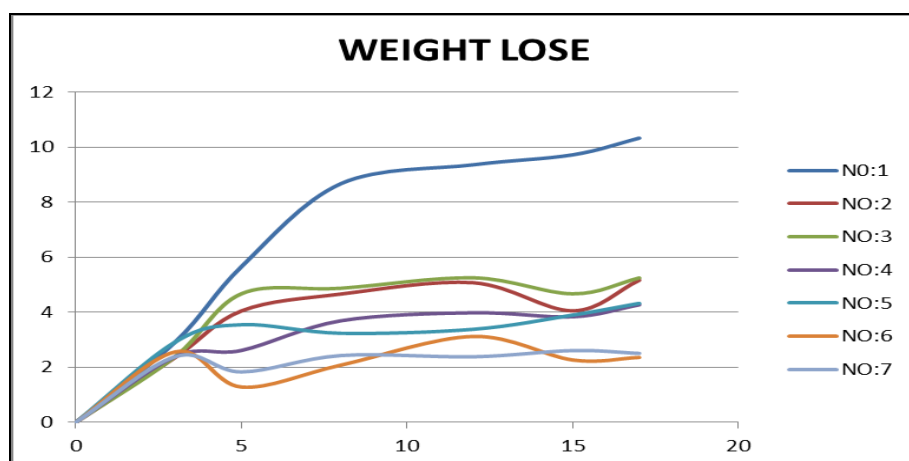


Figure A.61: The graph of weight lose changes of parsley during 17 days storage versus time.

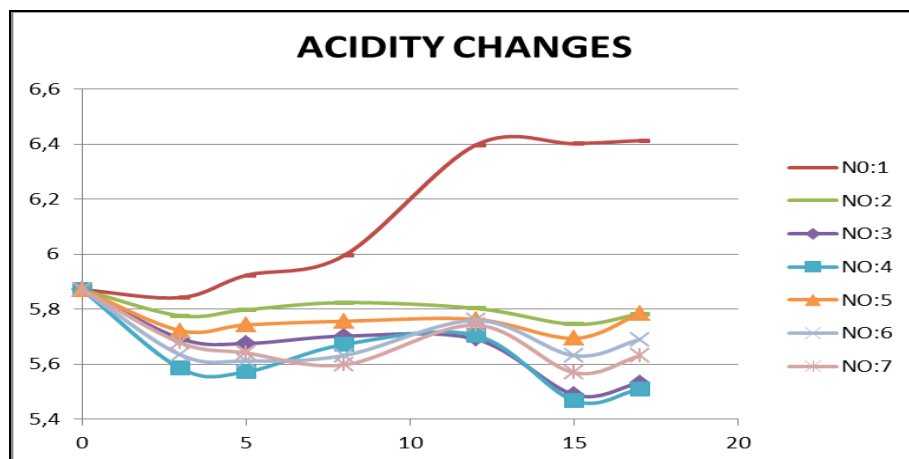


Figure A.62: The graph of pH changes of parsley during 17 days storage versus time.

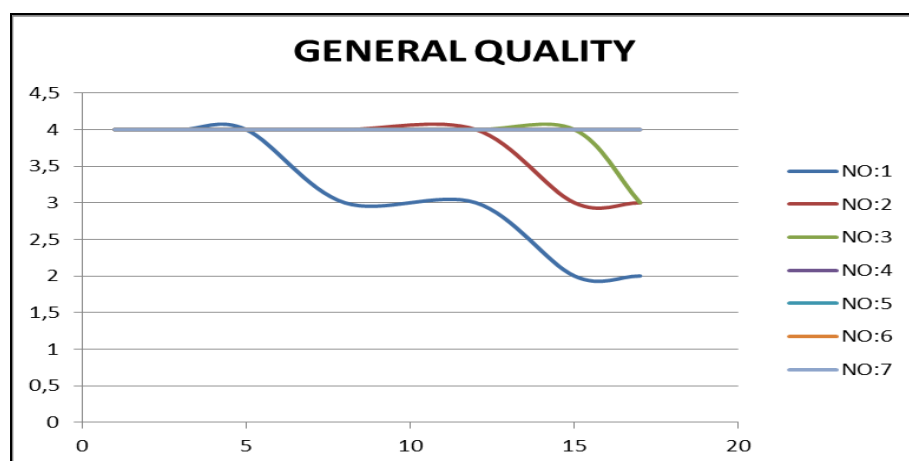


Figure A.63: The graph of general quality changes of parsley during 17 days storage versus time.



Figure A.64: The parsley pictures stored in LDPE packages at 5th, 12th, 15th, 17th days (Sample no:1).



Figure A.65: The parsley pictures stored in 5% I44 LDPE packages at 5th, 12th, 15th, 17th days (Sample no:2).



Figure A.66: The parsley pictures stored in 5% DK4 LDPE packages at 5th, 12th, 15th, 17th days (Sample no:3).



Figure A.67: The parsley pictures stored in 4% N10774 LDPE packages at 5th, 12th, 15th, 17th days (Sample no:4).



Figure A.68: The parsley pictures stored in 4% N10776 LDPE packages at 5th, 12th, 15th, 17th days (Sample no:5).



Figure A.69: The parsley pictures stored in 4.5% I44 + 4% N10774 LDPE packages at 5th, 12th, 15th, 17th days (Sample no:6).



Figure A.70: The parsley pictures stored in 4.5% DK4 + 4% N10774 LDPE packages at 5th, 12th, 15th, 17th days (Sample no:7).

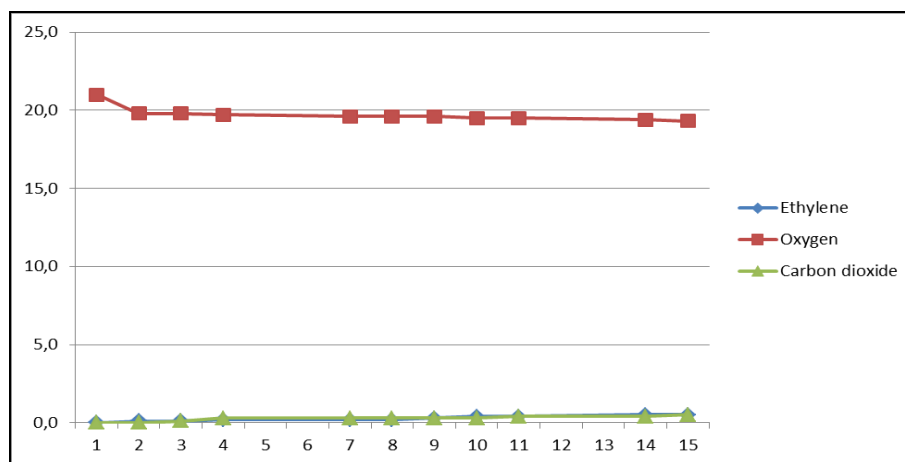


Figure A.71: C₂H₄, O₂ and CO₂ gas changes versus time of LDPE package for iceberg lettuce (Sample no:1).

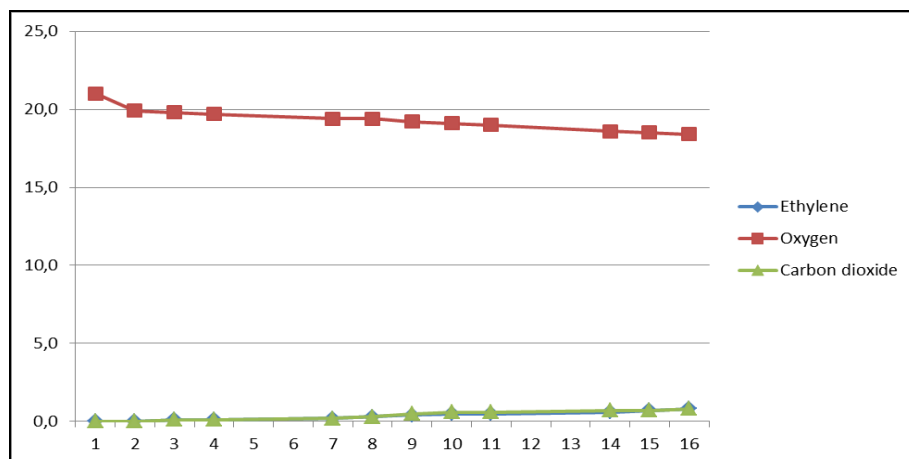


Figure A.72: C_2H_4 , O_2 and CO_2 gas changes versus time of 5% I44 LDPE package for iceberg lettuce (Sample no:2).

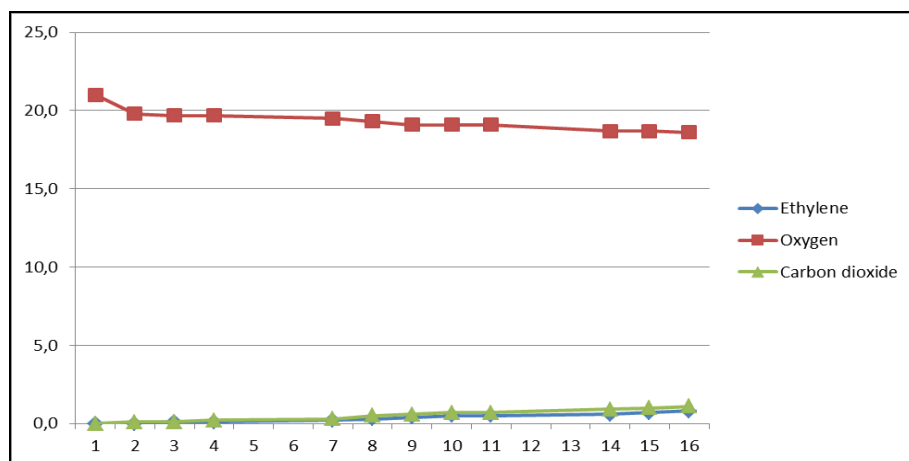


Figure A.73: C_2H_4 , O_2 and CO_2 gas changes versus time of 5% DK4 LDPE package for iceberg lettuce (Sample no:3).

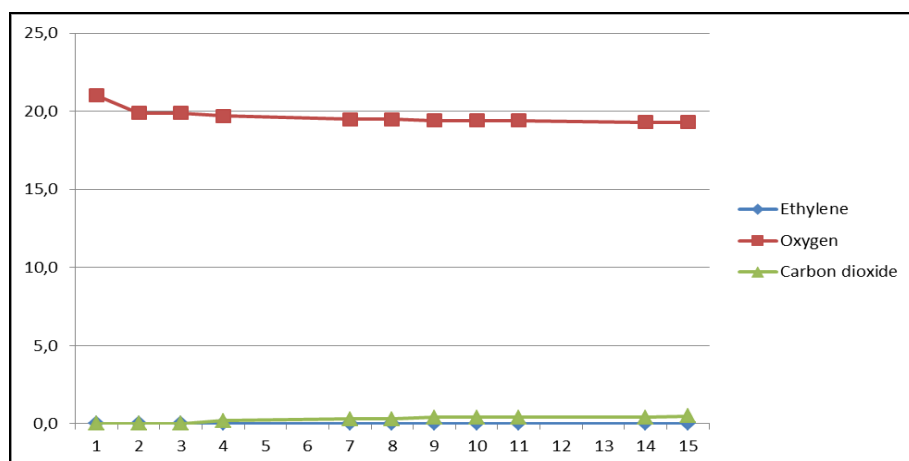


Figure A.74: C_2H_4 , O_2 and CO_2 gas changes versus time of 4% N10774 LDPE package for iceberg lettuce (Sample no:4).

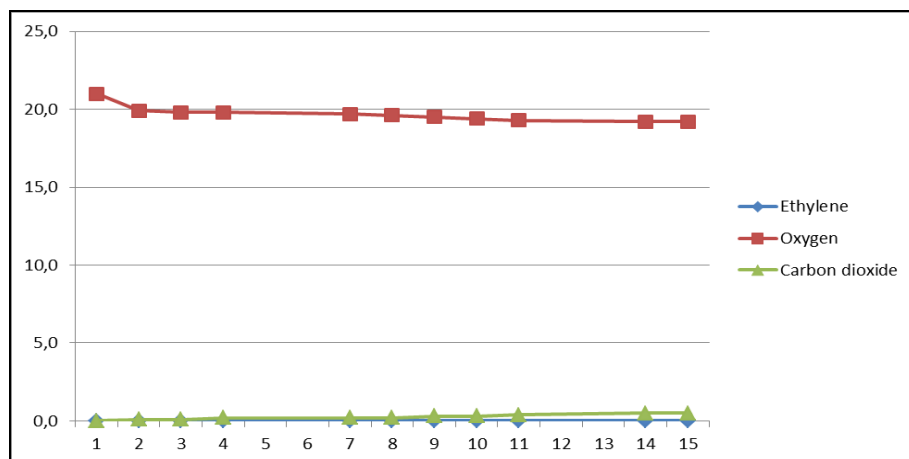


Figure A.75: C₂H₄, O₂ and CO₂ gas changes versus time of 4% N10776 LDPE package for iceberg lettuce (Sample no:5).

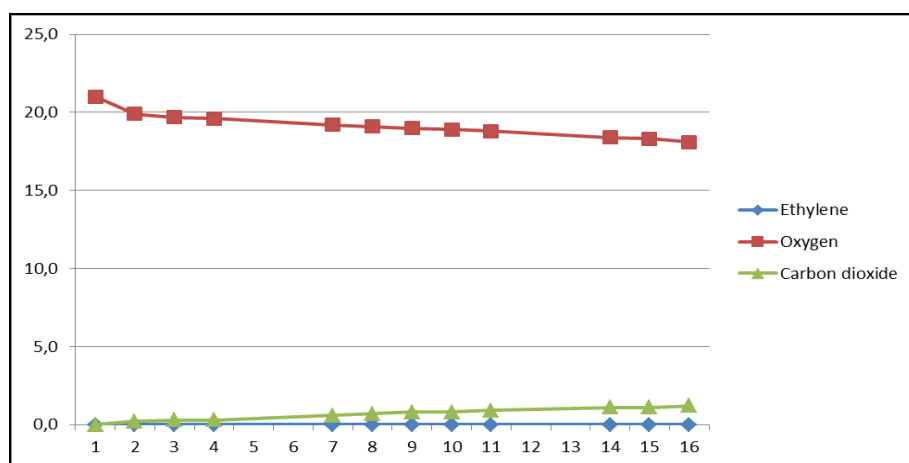


Figure A.76: C₂H₄, O₂ and CO₂ gas changes versus time of 4.5% I44 + 4% N10774 LDPE package for iceberg lettuce (Sample no:6).

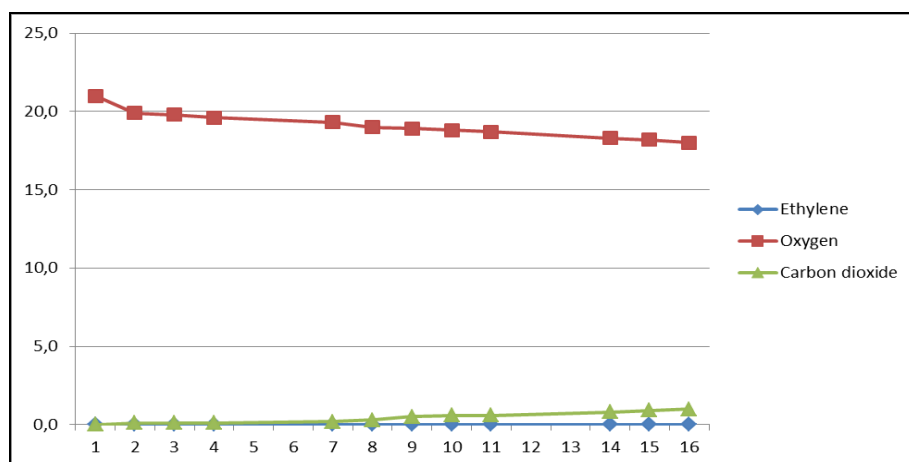


Figure A.77: C₂H₄, O₂ and CO₂ gas changes versus time of 4.5% DK4 + 4% N10774 LDPE package for iceberg lettuce (Sample no:7).

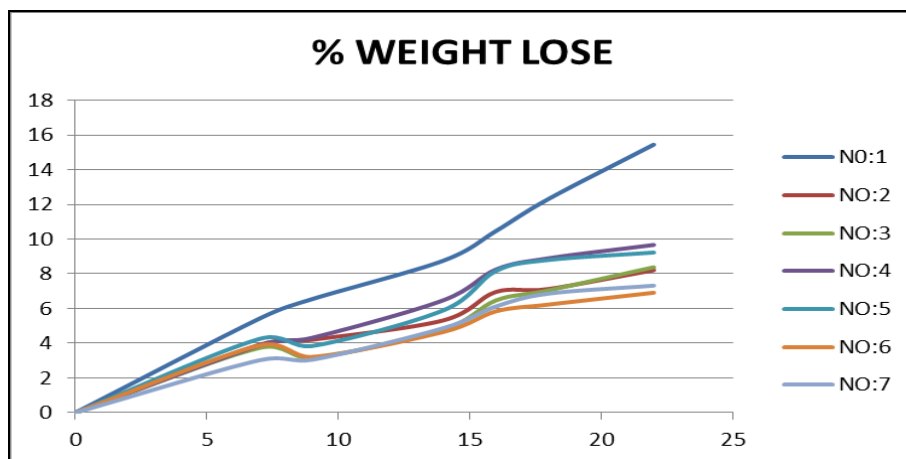


Figure A.78: The graph of weight lose changes of iceberg lettuce during 22 days storage versus time.

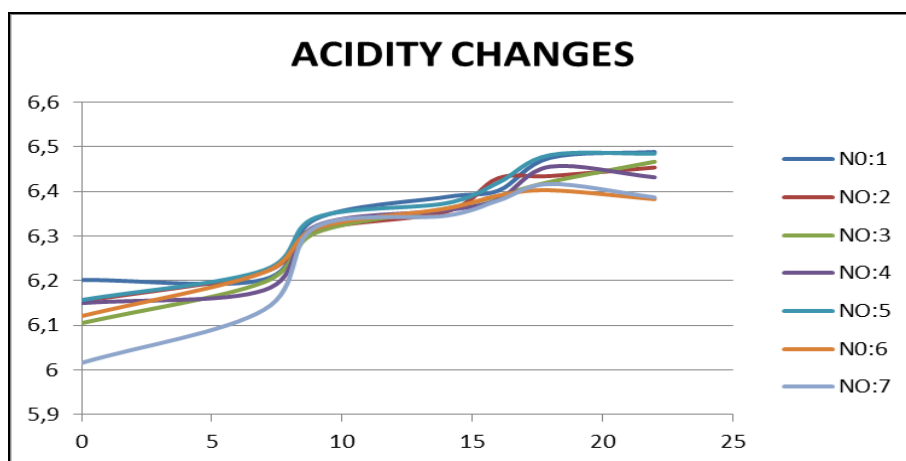


Figure A.79: The graph of pH changes of iceberg lettuce during 22 days storage versus time.

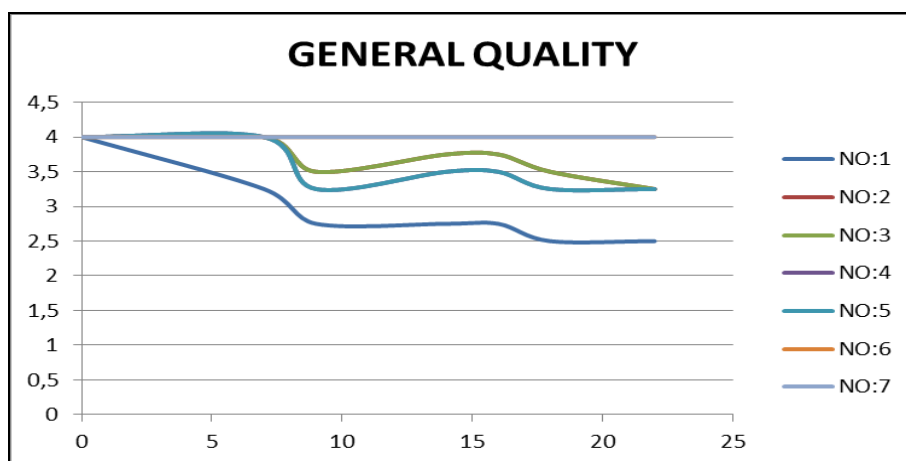


Figure A.80: The graph of general quality changes of iceberg lettuce during 22 days storage versus time.



Figure A.81: The iceberg lettuce pictures stored in LDPE packages at 7th, 9th, 18th, 22th days (Sample no:1).



Figure A.82: The iceberg lettuce pictures stored in 5% I44 LDPE packages at 7th, 9th, 18th, 22th days (Sample no:2).



Figure A.83: The iceberg lettuce pictures stored in 5% DK4 LDPE packages at 7th, 9th, 18th, 22th days (Sample no:3).



Figure A.84: The iceberg lettuce pictures stored in 4% N10774 LDPE packages at 7th, 9th, 18th, 22th days (Sample no:4).



Figure A.85: The iceberg lettuce pictures stored in 4% N10776 LDPE packages at 7th, 9th, 18th, 22th days (Sample no:5).



Figure A.86: The iceberg lettuce pictures stored in 4.5% I44 + 4% N10774 LDPE packages at 7th, 9th, 18th, 22th days (Sample no:6).



Figure A.87: The iceberg lettuce pictures stored in 4.5% DK4 + 4% N10774 LDPE packages at 7th, 9th, 18th, 22th days (Sample no:7).

REFERENCES

- [1] www.nanocompositech.com/review-nanocomposite.htm, 2011.
- [2] Encyclopedia of Polymer Science and Technology, 3rd ed., vol. 12, Wiley Interscience, 2003.
- [3] **Nielsen L.E.** and **Landel R.F.**, “Mechanical Properties of Polymers and Composites”, 2nd ed., Marcel Dekker, Inc., New York, 1994.
- [4] **Wu C.L., Zhang M.Q., Rong M.Z. and Friedrich K.**, “Silica Nanoparticles Filled Polypropylene: Effects of Particle Surface Treatment, Matrix Ductility and Particle Species on Mechanical Performance of the Composites”, Composites Science and Technology, Vol. **65**, 635-645, 2005.
- [5] **Nielsen L.E.**, “Simple Theory of Stress–Strain Properties of Filled Polymer” Journal of Applied Polymer Science, Vol.**10**, 97–103, 1966.
- [6] **Nicolais L.** and **Narkis M.**, “Stress–Strain Behavior of Styrene Acrylonitrile/Glass Bead Composites in the Glassy Region” Polymer Engineering Science, Vol. **11**, 194–199, 1971.
- [7] **Fornes T.D., Yoon, P.J., Keskkula, H., Paul, D.R.**, 2001, Nylon 6 nanocomposites : the effects of matrix molecular weight, Polymer, 42, 9929-9940.
- [8] **Fornes T.D., Hunter, D.L., Paul, D.R.**, 2004, Effect of sodium montmorillonite source on nylon 6/clay nanocomposites, *Polymer*, 45, 2321-2331.
- [9] **Katti, K.S., Sikdar, D., Katti, D.R., Ghosh, P., Verma, D.**, 2006, Molecular interactions in intercalated organically modified clay and clay-polycaprolactam nanocomposites: Experiments and modeling, Polymer, 47, 403-414.
- [10] **Shah, R.K., Paul, D.R.**, 2004, Nylon 6 nanocomposites prepared by a melt mixing masterbatch process, Polymer, 45, 2991-3000.
- [11] **Zhang, X., Yang, G., Lin, J.**, 2006, Synthesis, rheology, and morphology of nylon 11/layered silicate nanocomposite, Journal of Polymer Science,

Part B: Polym Phys., 44, 2161–2172.

- [12] **Li, Y., Ishida, H.**, 2005, A study of morphology and intercalation kinetics of polystyrene-organoclay nanocomposites, *Macromolecules*, 38, 6513-6519.
- [13] **Qi, R., Jin, X., Nie, J., Yu, W., Zhou, C.**, 2005, Synthesis and properties of polystyrene–clay nanocomposites via in-situ intercalative polymerization, *Journal of Applied Polymer Science*, 97, 201–207.
- [14] **Tanoue, S., Utracki, L.A., Garcia-Rejon, A., Tatibouet, J., Cole, K.C., Kamal, M.R.**, 2004, Melt compounding of different grades of polystyrene with organoclay. Part 1: Compounding and characterization, *Polymer Engineering and Science*, 44 (6), 1046-1060.
- [15] **Tanoue, S., Utracki, L.A., Garcia-Rejon, A., Sammut, P., Ton-Hat, M.T., Pesneau, I., Kamal, M.R., Lyngaae-Jorgensen, J.**, 2004, Melt compounding of different grades of polystyrene with organoclay. Part 2: Rheological properties, *Polymer Engineering and Science*, 44 (6), 1061-1076.
- [16] **Sepehr, M., Utracki, L.A., Zheng, X., Wilkie, C.A.**, 2005, Polystyrenes with macro-intercalated organoclay. Part I. Compounding and characterization, *Polymer*, 46, 11557-11568.
- [17] **Kumar, S., Jog, J.P., Natarajan, U.**, 2003, Preparation and characterization of poly(methyl methacrylate)–clay nanocomposites via melt intercalation: The effect of organoclay on the structure and thermal properties, *Journal of Applied Polymer Science*, 89, 1186–1194.
- [18] **Li, Y., Zhao, B., Xie, S., and Zhang, S.**, 2003, Synthesis and properties of poly (methylemethacrylate) / montmorillonite (PMMA/MMT) nanocomposites, *Polymer International*, 52, 892–898.
- [19] **Hwu, J.M., Jiang, G.J., Gao, Z.M., Xie, W., Pan W.P.**, 2002, The Characterization of organic modified clay and clay-filled PMMA nanocomposite, *Journal of Applied Polymer Science*, 83, 1702–1710.
- [20] **Miyagawa, H., Rich, M.J., Drzal, L.T.**, 2004, Amine-cured epoxy/clay nanocomposites. II. The effect of the nanoclay aspect ratio, *Journal of Polymer Science, Part B: Polym Phys.*, 42, 4391–4400.

- [21] **Xu, W.B., Bao, S.P., He, P.S.**, 2002, Intercalation and exfoliation behavior of epoxy resin/curing agent/montmorillonite nanocomposite, *Journal of Applied Polymer Science*, 84, 842–849.
- [22] **Triantafallidis, C.S., Lebaron, P.C., Pinnavaia, T.J.**, 2002, Thermoset epoxy-clay nanocomposites: The dual role of α,ω -diamines as clay surface modifiers and polymer curing agents, *Journal of Solid State Chemistry*, 167, 354-362.
- [23] **Solis, A.S., Rejon, A.G., Manero, O.**, 2003, Production of nanocomposites of PET-montmorillonite clay by an extrusion process, *Macromolecular Symposia*, 192, 281-292.
- [24] **Boesel, L.F., Pessan, L.A.**, 2002, Poly(ethylene terephthalate)-organoclay nanocomposites: Morphological characterization, *Metastable and Nanostructured Materials, Nanomat-2001*, 403, 89-93.
- [25] **Kim, S.H., Park, S.H., Kim, S.C.**, 2005, Novel clay treatment and preparation of poly(ethylene terephthalate)/clay nanocomposite by in-situ polymerization, *Polymer Bulletin*, 53 (4), 285-292.
- [26] **Qu, C.F., Ho, M.T., Lin, J.R.**, 2006, Synthesis and characterization of poly(ethyleneterephthalate) nanocomposites with organoclay, *Journal of Applied Polymer Science*, 91 (1), 140-145.
- [27] **Choi, W.J., Kim, H-J., Yoon, K.H., Kwon, O.H., Hwang, C.I.**, 2006, Preparation and barrier property of poly(ethylene terephthalate)/clay nanocomposite using clay supported catalyst, *Journal of Applied Polymer Science*, 100, 4875-4879.
- [28] **Wu, T-M., Liu, C-Y.**, 2005, Poly(ethylene 2,6-naphthalate)/layered silicate nanocomposites: fabrication, crystallization behavior and properties, *Polymer*, 46, 5621 5629.
- [29] **Ahn, S.H., Kim, S.H., Kim, B.C., Shim, K.B., Cho, B.G.**, 2004, Mechanical properties of silica nanoparticle reinforced poly(ethylene 2,6-naphthalate), *Macromolecular Research*, 12, 293-302.
- [30] **Wu, D., Zhou, C., Zheng, H.**, 2006, A rheological study on kinetics of poly(butylene terephthalate) melt Intercalation, *Journal of Applied Polymer Science*, 99, 1865–1871.

- [31] **Wu, D., Zhou, C., Zheng, H., Mao, D., Bian, Z.**, 2005, Study on rheological behaviour of poly(butylene terephthalate)/montmorillonite nanocomposites, *European Polymer Journal*, 41, 2199-2207.
- [32] **Scatteia, L., Scarfato, P., Acierno, D.**, 2004, Rheology of PBT-layered silicate nanocomposites prepared by melt compounding, *Plastics, Rubbers and Composites*, 33, 85-91.
- [33] **Loyens, W., Jannasch, P., Maurer, F.H.J.**, 2005, Poly(ethylene oxide)/Laponite nanocomposites via melt-compounding : effect of clay modification and matrix molar mass, *Polymer*, 46, 915-928.
- [34] **Homminga, D., Goderis, B., Dolbnya, I., Reynaers, H., Groeninckx, G.**, 2005, Crystallization behavior of polymer/montmorillonite nanocomposites. Part I. Intercalated poly(ethylene oxide)/montmorillonite nanocomposites, *Polymer*, 46, 11359-11365.
- [35] **Ratna, D., Divekar, S., Samui, A.B., Chakraborty, B.C., Banthia, A.K.**, 2006, Poly(ethylene oxide)/clay nanocomposite: Thermomechanical properties and morphology, *Polymer*, 47, 4068-4074.
- [36] **Ray, S.S., Yamada, K., Okamoto, M., Ueda, K.**, 2002, Polylactide-layered silicate nanocomposite: A novel biodegradable material, *Nano Letters*, 2, 1093-1096.
- [37] **Chang, J.H., An, Y.U., Cho, D.H., Giannelis, E.P.**, 2003, Poly(lactic acid) nanocomposites: comparison of their properties with montmorillonite and synthetic mica(II), *Polymer*, 44, 3715-3720.
- [38] **Di, Y.W., Iannace, S., Di Maio, E., Nicolais, L.**, 2005, Poly(lactic acid)/organoclay nanocomposites: Thermal, rheological properties and foam processing, *Journal of Polymer Science, Part B: Polym Phys.*, 43, 689-698.
- [39] **Gong, F.L., Zhao, C.G., Feng, M., Qin, H.L., Yang, M. S.**, 2004, Synthesis and characterization of PVC/montmorillonite nanocomposite, *Journal of Material Science*, 39, 293– 294.
- [40] **Wan, C., Qiao, X., Zhang, Y., Zhang, Y.**, 2003, Effect of different clay treatment on morphology and mechanical properties of PVC-clay nanocomposites, *Polymer Testing*, 22, 453–461.
- [41] **Yua, Y.H., Lina, C.Y., Yeha, J.M., Lin, W.H.**, 2003, Preparation and properties of poly(vinyl alcohol)–clay nanocomposite materials, *Polymer*, 44, 3553–3560.

- [42] **Xu, J., Meng, Y.Z., Li, R.K.Y., Xu, Y., Rajulu, A.V.**, 2003, Preparation and properties of poly(vinyl alcohol)–vermiculite nanocomposites, *Journal of Polymer Science, Part B: Polym Phys.*, 41, 749–755.
- [43] **Zanettia, M., Caminoa, G., Thomann, R., Mulhaupt, R.**, 2001, Synthesis and thermal behaviour of layered silicate-EVA nanocomposites, *Polymer*, 42, 4501-4507.
- [44] **Zhang, W., Chen, D., Zhao, Q., Fang, Y.**, 2003, Effects of different kinds of clay and different vinyl acetate content on the morphology and properties of EVA/clay nanocomposites, *Polymer*, 44, 7953–7961.
- [45] **Peeterbroeck, Alexandre, M., Jerome, R., Dubois, P.**, 2005, Poly(ethylene-co-vinyl acetate)/clay nanocomposites: Effect of clay nature and organic modifiers on morphology, mechanical and thermal properties, *Polymer Degradation and Stability*, 90, 288-294.
- [46] **Cabeda, L., Gimenez, E., Lagaron, J.M., Gavara, R., Saura, J.J.**, 2004, Development of EVOH-kaolinite nanocomposites, *Polymer*, 45, 5233–5238.
- [47] **Artzi, N., Nir, Y., Narkis, M., Siegmann, A.**, 2002, Melt blending of ethylene–vinyl alcohol copolymer/clay nanocomposites: effect of the clay type and processing conditions, *Journal of Polymer Science: Part B: Polymer Physics*, 40, 1741-1753.
- [48] **Artzi, N., Narkis, M., Siegmann, A.**, 2005, Review of melt-processed nanocomposites based on EVOH/organoclay, *Journal of Polymer Science: Part B: Polymer Physics*, 43, 1931-1943.
- [49] **Rhoney, I., Brown, S., Hudson, N.E., Pethrick, R.A.**, 2004, Influence of processing method on the exfoliation process for organically modified clay systems. I. Polyurethanes, *Journal of Applied Polymer Science*, 91, 1335–1343.
- [50] **Widya, T., Macosko, C.W.**, 2005, Nanoclay-modified rigid polyurethane foam, *Journal of Macromolecular Science-Physics B44* (6), 897-908.
- [51] **Oh, S.B., Kim, B.S., Kim, J.H.**, 2006, Preparation and properties of polyimide/organoclay nanocomposites from soluble polyisoimide, *Journal of Industrial and Engineering Chemistry*, 12 (2), 275-279.
- [52] **Park, C., Smith, J.G., Connell, J.W., Lowther, S.E., Working, D.C., Siochi, E.J.**, 2005, Polyimide/silica hybrid-clay nanocomposites, *Polymer*, 46 (23), 9694-9701.

- [53] **Chen, B.K., Chiu, T.M., Tsay, S.Y.**, 2004, Synthesis and characterization of polyimide/silica hybrid nanocomposites, *Journal of Applied Polymer Science*, 94, 382–393.
- [54] **Zheng, H., Zhang Y., Peng, Z., Zhang, Y.**, 2004, Influence of clay modification on the structure and mechanical properties of EPDM/montmorillonite nanocomposites, *Polymer Testing*, 23, 217–223.
- [55] **Ahmadi, S.J., Huang, Y., Li, W.**, 2005, Fabrication and physical properties of EPDM–organoclay nanocomposites, *Composites Science and Technology*, 65, 1069–1076.
- [56] **Ahmadi, S.J., Huang, Y., Li, W.**, 2004, Synthesis of EPDM/organoclay nanocomposites: effect of the clay exfoliation on structure and physical properties, *Iranian Polymer Journal*, 13 (5), 415–422.
- [57] **De Azevedo, W.M., Schwartz, M.O.E., Do Nascimento, G.C., Da Silva, E.F.**, 2004, Synthesis and characterization of polyaniline/clay nanocomposite, *Physica Status Solidi : C*, 1 (S2), S249 - S255.
- [58] **Wang, Y.Z., Li, Y.X., Yang, S.T., Zhang, G.L., An, D.M., Wang, C., Yang, Q.B., Chen, X.S., Jing, X.B., Wei, Y.**, 2006, A convenient route to polyvinyl pyrrolidone/silver nanocomposite by electrospinning, *Nanotechnology*, 17, 3304–3307.
- [59] http://www.uwplatt.edu/~sundin/114/image/11439_a.gif, 2011.
- [60] <http://en.wikipedia.org>, 2011, February
- [61] <http://en.wikipedia.org>, 2011, February
- [62] “Kirk-Othmer Encyclopedia of Chemical Technology”, 4th ed., vol. 17, John Wiley and Sons Inc., New York, 1993.
- [63] **DuBois, H., John, F.W.**, 1981. *Plastics*, 6th ed., Van Nostrand.
- [64] **Fenner, R. T.**, 1979. *Principles of Polymer Processing*; MacMillan.
- [65] Petrothene Polyolefins...a Processing Guide 5th ed., 1986. USI Chem Div., Nat'l Distillers and Chem., Quantum Chemical: Cincinnati, OH.
- [66] **Suprakas, Sinha Ray**, *Ind. Eng. Chem.*, 2006 12,. 6, 811.
- [67] **Olphen, H.**, 1979. *Data handbook for clay materials and other non-metallic minerals*, 346 p. Oxford Pergamon Pres.
- [68] **Van Oss, C.J. and Giese, R.F.**, 1995. *Clays Clay Minerals*, 43, 474 – 481,
- [69] **Quirk, I.P. and Marcelja, S.**, 1997. *Langmuir*, 13, 6241 – 6248.
- [70] **Hendricks, S.B., Jefferson, M.E.** 1938. *Am.Minerol*, 23, 863.

- [71] **Fukushima, Y.**, 1984. *Clays Clay Min.*, 32, 320 – 326.
- [72] **Meier, L.P.** 1998. *Organic Cations – Related Adsorption Behaviour of Surface Modified Smectites*, PhD Dissertation, Swiss Federal Institute of Technology, Zurich.
- [73] **Parfitt, R.L. and Greenland, D.J.**, 1970. *Clay Min* 8, 305 – 315.
- [74] **Deraj, R.N., and Guy, R.D.**, 1981. *Clays and Clay Min.*, 29, 205 – 212.
- [75] **Lagaly, G.**, 1986. *Colloids in Ullmann's Encyclopedia of Industrial Chemistry*, pp. Vol A7.
- [76] **I.V. Germashev, V.E. Derbisher, M.N. Tsapleva and E.V. Derbisher, Khim. Promyshl.** (6), 43–8 (2002).
- [77] **P. Molander, R. Trones, K. Haugland and T. Greibrokk**, *Analyst* 124,1137 41 (1999).
- [78] **Ray S. S., Okamoto M.**, 2003. "Polymer/Layered Silicate Nanocomposites: A Review from Preparation to Processing", *Prog. Polym. Sci.* Vol. 28, pp. 1539–1641.
- [79] **Gao F.**, 2004. "Clay / Polymer Composites: The Story", *Materialstoday*. Vol. 23, pp. 50-55.
- [80] **Ahmadi S. J., Huang Y. D., Li W.**, 2004. "Review: Synthetic Routes, Properties and Future Applications of Polymer-layered Silicate Nanocomposites", *Journal of Materials Science*. Vol. 39, pp. 1919-1925.
- [81] **Avella M., Errico M. E., Martelli S., Martuscelli E.**, 2001. "Preparation Methodologies of Polymer Matrix Nanocomposites", *Appl. Organometal. Chem.* Vol. 15, pp. 435-439.
- [82] **Ma J., Xu J., Ren J., Mai Y.**, 2003. "A New Approach to Polymer/Montmorillonite Nanocomposites", *Polymer*. Vol. 44, pp. 4619–4624.
- [83] **Zanetti M., Lomakina S., Camino G.**, 2000. "Polymer Layered Silicate Nanocomposites", *Macromol. Mater. Eng.* Vol. 279, pp. 1–9.
- [84] **Kornmann, X.**, *Synthesis and Characterization of Thermoset-Clay Nanocomposites*, PhD Thesis, Lulea University of Technology, 2001.
- [85] **Dennis H.R., Hunter D.L., Chang D., Kim S., White J.L., Cho J.W., Paul D.R.**, *Polymer*, 42, 9513-9522, 2001.
- [86] **Kroschwitz J.I., Mark H.F.**, "Encyclopedia of Polymer Science and Technology", 3rd Ed., Wiley Interscience, Hoboken, N.J., 2003.
- [87] **Ray S.S., Okamoto M.**, *Progress in Polymer Science*, 28, 1539-1641, 2003.
- [88] **Alexandre M., Dubois P.**, *Materials Science and Engineering*, 28, 1-63, 2000.

- [89] **Sinha R.S., Okamoto K., Okamoto M.**, *Macromolecules*, 36, 2355-2367, 2003.
- [90] **Ray, S.S, Bousmina, M.M.**, 2006, in *Polymer Nanocomposites*, Mail, Y.W.; Yu, Z.Z.; 1st ed, Woodhead Publishing, Cambridge, 2006, pp.57-129.
- [91] **Pavlidou, S., Papaspyrides, C.D.**, A review on Polymer-Layered Silicate Nanocomposites. *Progress in Polymer Science*. 2008, 33, 1119–1198.
- [92] **Paul, D.R., Robeson, L.M.**, *Polymer Nanotechnology: Nanocomposites*. *Polymer*. 2008, 49, 3187-3204.
- [93] **Ray, S. S., Bousmina, M.M.**, Biodegradable Polymers and Their Layered Silicate Nanocomposites: In *Greening The 21st Century Materials World*. *Progress in Materials Science*. 2005, 50,962–1079.
- [94] **Okamoto, M.**, 2005 in *Handbook of Biodegradable Polymeric Materials and their Applications*, Mallapragada, S.; Narasimhan, P., American Scientific Publishers, Vol.1, 2005; pp. 1-45.
- [95] **Ray, S.S., Okamoto, M.**, Polymer/Layered Silicate Nanocomposites: A review from Preparation to Processing. *Progress in Polymer Science*. 2003, 28, 1539-1641.
- [96] **Lu, C., Mai, Y.W.**, Permeability Modeling of Polymer-Layered Silicate Nanocomposites. *Composites Science and Technology*. 2007, 67, 2895-2902.
- [97] **Eitzman, D.M., Melkote, R.R., Cussler, E.L.**, Barrier Membranes with Tipped Impermeable Flakes. *AIChE Journal*. 1996, 42, 2-9.
- [98] **Sun, L., Boo, W.J., Clearfield, A., Sue, H.J., Pham, H.Q.**, Barrier Properties of Model Epoxy Nanocomposites. *Journal of Membrane Science*. 2008, 318, 128-136.
- [99] **Bharadwaj, R.K.**, Modelling the Barrier Properties of Polymer-Layered Silicate Nanocomposites. *Macromolecules*. 2001, 34, 9189-9192.
- [100] **Choudalakis, G., Gotsis, A.D.**, Permeability of Polymer/Clay Nanocomposites: A Review. *European Polymer Journal*. 2009, 45, 967-984.
- [101] **Lu, Q. W., Hoyer, T. R. and Macosko, C. W.**, *J. Polym. Sci., Part A. Polym. Chem.*, 2002,40,2310-2328.
- [102] **Zhou, M. and Han, C D.**, *Macromolecules*, 2005, 38, 9602.
- [103] **Zha, W., Choi, S., Lee, K. M. and Han, C D.**, *Macromolecules*, 2005, 38, 8418.
- [104] **Yoshioka, H.**, *Physica B*, 2000, 284-288, 1756.

- [105] **D'Souza, N. A.**, *Encycl. Nanosci. Nanotech.*, 2004, 3, 253-265.
- [106] **Ma, J., Yu, Z.-Z., Zhang, O.-X., Xie, X.-L., Mai, Y.-W. and Luck, I.**, 2004, *Chem. Mater.*, 16, 757.
- [107] **Smith, R.**, *Biodegradable Polymers for Industrial Applications*, 1st ed., CRC Press, 2005, pp. 134-176.
- [108] **Petersen, K., Nielsen, P. V., Bertelsen, G., Lawther, M., Olsen M. B., Nilsson, N. H. and Mortensen, G.**, Potential of Biobased Materials for food Packaging. *Trends in Food Science and Technology*. 1999, 10, 52-68.
- [109] **Hong, S. I., Krochta, J. M.**, Oxygen Barrier Properties of Whey Protein Isolate Coatings on Polypropylene Films. *Journal Of Food Science*. 2003, 68, 224-228.
- [110] **Fennema, O.R.** , 1975 *Principles of Food Science, Part II Physical of Food Preservation*. Marcel Dekker Inc. New York.
- [111] **Mathlouthi, M. and Leiris, J.P.** , 1990. The influence of the technology of food manufacturing on the choice of a packaging metarial. *Engineering and Food Advanced Processes*. Ed. By W.E.L.Spiess and H.Schubert, Elsevier Applied Science Publishing Co. Inc., New York U.S.A.
- [112] **Begeman, M.L. and Amstead, B.H.** , 1963. *Manufacturing Processes*. John Willey and Sons Inc., 263-288.
- [113] **Rooney, M.L.**, 1995. Overview of active food packaging, *Active Food Packaging*, Ed. By M.L.Rooney, 1-33, Chapman and Hall Inc., U.S.A.
- [114] **Kader, A.A. , Zagory, D. and Kerbel, E.L.**, 1989. Modified atmosphere packaging of fruits and vegetables. *Critical Reviews in Food Science and Nutrition*. 40 (1): 1-24.
- [115] **Labuza, T.P.**, 1990. Active food packaging technologies. *Engineering and Food Advanced Processes*, By W.E.L.Spiess and H.schubert, Elsevier Applied Science Publishing Co Inc., New York, U.S.A.
- [116] **Zagory, D.**, 1995. Ethylene removing packaging, *Active Food Packaging*, Ed. By M.L.Rooney, 38-54 Chapman and Hall Inc. U.S.A.
- [117] **Yang, S.F. and Hoffman, N.E.** , (1984) Ethylene biosynthesis and its regulation in higher plants. *Ann. Rev. Plant Physiol.*, 35, 155-89.
- [118] **Sato, M., Urushizaki, S., Nishiyama, K., Sajai, F. and Ota, Y.**, (1987) Efficient production of ethylene by *Pseudomonas syringae* pv. *Glycinea* which causes halo blight of soybeans. *Agric. Biol. Chem.*, 51, 1177-8.

- [119] **Dillworth, M.J.**, (1966) Acetylene reduction by nitrogen-fixing preparations from *Clostridium pasteurianum*. *Biochem. Biophys. Acta*, 127, 285-94.
- [120] **Fukuda, H., Fujii, T. and Ogawa, T.**, (1984) Microbial production of C₂ hydrocarbons, ethane, ethylene and acetylene. *Agric. Boil. Chem.*, 48, 1363-5. ;
Ilag, L.L. and Curtis, R.W. (1968) Production of ethylene by fungi. *Science*, 159, 1357-8.
- [121] **Owens, L.D., Lieberman, M. and Kunishi, M.**, (1971) Inhibition of ethylene production by rhizobitoxin. *Plant Physiol.*, 48, 1-4.
- [122] **Osborne, D.J.**, (1989a) The control role of ethylene in plant growth and development. In: Clijsters, H. et al (eds.). *Biochemical and Physiological Aspects of Ethylene Production in Lower and Higher Plants*. Kluwer Academic publishers. Pp. 1-11.
- [123] **Kays, S.J. and Beaudry, R.M.**, (1987) Techniques for inducing ethylene effects. *Acta Hort.*, 201, 77-116.
- [124] **Goodburn, K.E. and Halligan, A.C.**, (1987) Modified atmosphere packaging – a technology guide. Publication of the British Food Manufacturing Association, Leatherhead, UK. Pp. 1-44.
- [125] **Urushizaki, S.**, (1987a) On the Effects of Ethylene Functional Films. Autumn Meeting of Japan Society Horticultural Science. Symposium: Postharvest Ethylene and Quality of Horticultural Crops. University of Kyushu, October 8, 1987.
- [126] **Urushizaki, S.**, (1987b) Development of Ethylene Absorbable Film and its Application to Vegetable and Fruit Packaging. Autumn Meeting of Japan Society Horticultural Science. Symposium: Postharvest Ethylene and Quality of Horticultural Crops. University of Kyushu, October 8.
- [127] **Rizzolo, A., Polesello, A. and Gorini, F.**, (1987a) Laboratory screening tests of some suitable regenerable adsorbents to remove ethylene from cold room atmosphere. 1. Glycols and polyglycols. In: Third Subproject: Conservation and Processing of Foods – A Research Report (1982-1986), National Research Council of Italy, Milano. 99-100.

- [128] **Rizzolo, A., Polesello, A. and Gorini, F.,** (1987b) Laboratory screening tests of some suitable regenerable adsorbents to remove ethylene from cold room atmosphere. 1. Apolar phases. In: Third Subproject: Conservation and Processing of Foods – A Research Report (1982-1986), National Research Council of Italy, Milano. 101-2.
- [129] **Osajima, Y., Sonoda, T., Yamamoto, F., Nakashima, M., Shimoda, M. and Matsumoto, K.,** (1983) Development of ethylene absorbent and its utilization. *Nippon Nogeikagaku Kaishi*, 57, 1127-33.
- [130] **Eastwell, K.C., Bassi, P.K. and Spencer, M.E.,** (1978) Comparison and evaluation of methods for the removal of ethylene and other hydrocarbons from air for biological studies. *Plant Physiol.*, 62, 723-6.
- [131] **Holland, R.V.,** (1992) Absorbent material and uses thereof. Australian Patent Application No: PJ6333.
- [132] **Denny, F.E.,** (1924) Hastening the coloration of lemons. *H. Agr. Res.*, 27, 757-69.
- [133] **Abeles, F.B., Morgan, P.W. and Saltveit, M.E.,** (1992) *Ethylene In Plant Biology*. Academic Press, Inc., 414 pp.
- [134] **Kader, A.A.,** (1985) Postharvest biology and technology: An overview. In: A.A. Kader, R.F. Kasmire, F.G. Mitchell, M.S. Reid, N.F. Sommer and J.F. Thompson (eds), *Postharvest Technology of Horticultural Crops*. University of California, Cooperative Extension Special Publication 3311, 192 pp.
- [135] **Reid, M.S.,** (1985b) Ethylene in postharvest technology. In: A.A. Kader, R.F. Kasmire, F.G. Mitchell, M.S. Reid, N.F. Sommer and J.F. Thompson (eds), *Postharvest Technology of Horticultural Crops*. University of California, Cooperative Extension Special Publication 3311, 192 pp.
- [136] **Zhu, L., and M. Xanthos,** “Effects of Process Conditions and Mixing Protocols on Structure of Extruded Polypropylene Nanocomposites”, *J. Appl. Polym. Sci.*, Vol. **93**, pp. 1891-1899, 2004.
- [137] **Zeus Technical Whitepaper,** “Melt Extrusion: The Basic Process”, Zeus Industrial Products, Inc., 2006.
- [138] **Rauwendaal, C.,** *Polymer Extrusion*, Hanser Gardner Publications, Munich, 2001.

- [139] **Raman, V. C., Y. Jaluria, M. V. Karwe, V. Sernas**, “Transport in a Twin-Screw Extruder for the Processing of Polymers”, *Polym. Eng. Sci.*, Vol. **36**, No. 11, pp. 1531-1540, 1996.
- [140] **Prat, L., S. N’Diaye, L. Rigal, C. Gourdon**, “Solid-Liquid Transport in a Modified Corotating Twin-Screw Extruder_Dynamic Simulator and Experimental Validations”, *Chem. Eng. Process.*, Vol. **43**, pp. 881-886, 2004.
- [141] **Yoshinaga, M., S. Katsuki, M. Miyazaki, L. Liu, S. I. Kihara, K. Funatsu**, “Mixing Mechanism of Three-Tip Kneading Block in Twin Screw Extruders”, *Polym. Eng. Sci.*, Vol. **40**, No. 1, pp. 168-178, 2000.
- [142] **Silagy, D., Demay, Y., and J. F. Agassant**, *International Journal for Numerical Methods in Fluids*, 30 1-18 (1999).
- [143] http://en.wikipedia.org/wiki/Infrared_spectroscopy ,2011
- [144] **Ray, S.S, Bousmina, M.M.**, 2006, in *Polymer Nanocomposites*, Mail, Y.W.; Yu, Z.Z.; 1st ed, Woodhead Publishing, Cambridge, 2006, pp.57-129.
- [145] **Paul, D.R., Robeson, L.M.**, *Polymer Nanotechnology: Nanocomposites*. *Polymer*. 2008, 49, 3187-3204.
- [146] http://en.wikipedia.org/wiki/Infrared_spectroscopy ,2011
- [147] **Friedrich K., Ruan W.H. and Zhang M.Q.**, “Structure-Property Relationships of In-situ Crosslinking Modified Nano-silica Filled Polypropylene Composites”, *Proceeding of the 8th Polymers for Advanced Technologies International Symposium*, Budapest, Hungary, September, 2005.
- [148] <http://www.pslc.ws/mactest/dsc.htm>, 2011
- [149] <http://www.polyplastics.com/ch/support/Tecin/methods/image/mv1.gif>, 2011
- [150] <http://en.wikipedia.org>, 2011
- [151] http://hekabe.kt.dtu.dk/~vigild/2005_04_melitek/tensile_test.htm, 2011

CURRICULUM VITAE



I was born 1988 in Çorum. I started my university education at Trakya University, Chemistry department in 2005. I graduated from university in 2009. I was accepted as a master student to Istanbul Technical University, Polymer Science and Technology interdisciplinary graduate programme and I am still student. I started to work in Aksoy Plastik A.Ş. as project engineer at R&D department in 2010, May and still working there.